# The role of TIA-1 as a cellular restriction factor for tick-borne encephalitis virus infection

## Thesis

# The Role of TIA-1 as a Cellular Restriction Factor for Tick-Borne Encephalitis Virus Infection

Amelina A. Albornoz

This thesis is submitted in fulfilment of the requirements of the Open University for the degree of Doctor of Philosophy


International Centre for Genetic Engineering and Biotechnology (ICGEB)
Trieste, Italy



Director of Studies: Alessandro Marcello, PhD
External Supervisor: John McLauchlan, PhD
November, 2013

DATE of SUBMISSION: 5 SEPTEMBER 2013
DATE of AWARD: 28 JANUARY 2014

# ABSTRACT

Tick-borne encephalitis virus (TBEV) is a positive-single stranded RNA virus belonging to the *Flaviviridae* family. Flaviviruses replicate in the cytoplasm of infected cells and therefore during the different viral steps viral RNA is exposed to diverse cellular responses. The contribution of host RNA-binding proteins to flaviviral replication is an important issue under investigation. T-intracellular antigen-1 (TIA-1) is a stress-induced RNA-binding protein shown to be involved in the repression of initiation of translation of cellular mRNAs. When cells are subjected to UV radiation, heat shock, oxidative stress, as well as to certain viral infections, TIA-1 migrates from the nucleus and accumulates to form cytoplasmic foci named stress granules (SG). In this work I show that TIA-1 and TIAR knockdown by RNAi in human cells led to an increase of TBEV RNA levels as well as extracellular infectivity. Taking advantage of a TBE-luciferase replicon system developed in our lab, I could demonstrate that TIA-1 affected viral replication, more specifically at the level of the initial round of translation. I could also show by RNA immuneprecipitation of TIA-1 that the protein was interacting with viral RNA in TBEV infected cells. Moreover, during TBEV infection, cytoplasmic TIA-1 was recruited at perinuclear sites of viral replication with concomitant depletion of TIA-1 SGs. This effect was TIA-1 specific since G3BP1, another SG protein, remained in SGs and did not re-localize to sites of viral replication. In addition, heat-shock induction of TIA-1 SGs, but not G3BP1 SGs, was inhibited in TBEV infected cells. I could observe that G3BP SG contained RIG-I protein in TBEV infected cells and also I could demonstrate that RIG-I was involved in the activation of IFNβ expression upon TBEV infection. Moreover, I could show that G3BP SG were forming around the same time in which IFNβ was induced in TBEV infected cells, leading to the hypothesis of a possible cross-talk between stress pathway and immune response during TBEV infection. In conclusion, I could demonstrate that TIA-1 is recruited to sites of viral replication, binds to viral RNA and negatively regulates viral replication, possibly by inhibiting the first round of viral translation.

## TABLE OF CONTENTS

## LIST OF FIGURES

# LIST OF TABLES

## LIST OF ABBREVIATIONS

Ago2: argonaute RISC catalytic component 2

ARE: adenine-uridine rich

bp: base-pair

C: Capsid viral protein

CARD: Caspase activation and recruitment domain

CTD: Carboxi-terminal domain

Dcp-1: Deccaping mRNA 1B

DDX: DExD/H-box helicases

Denv: Dengue virus

dsRNA: double-stranded RNA

E: Envelope viral protein

EMCV: encephalomyocariditis virus

eIF2α: eukaryotic initiation of translation factor 2 α

eIF3: eukaryotic initiation of translation factor 3

ER: Endoplasmic reticulum

EGFP: enhanced green fluorescent protein

EYFP: Enhanced yellow protein

GNC2: General control non-repressed 2

G3BP: Ras-GTPase activating protein SH3 domain binding protein

HCV: Hepatitis C virus

HIV: Human immunodeficiency virus

HRI: Heme-regulated eIF2α kinase

HuR: human autoantigen R

IPS-1: mitochondrial antiviral signaling protein (also called MAVS)

IFNβ: Interferon β

IAV: influenza A virus

JEV: Japanese encephalitis virus

KDa: kilo dalton

KO: knockout

LPG2: Laboratory of genetics and physiology 2

MEF WT: mouse embryonic fibroblast wild type

MEF TIA-1: mouse embryonic fibroblast TIA-1 depleted

miRNA: microRNA

M: Membrane viral envelope

MDA5: Melanoma deficient-associated protein 5

MS2: phage MS2 capsid protein

mRNA: messenger RNA

NC: Nucleo-capsid

NF-90: Interleukin enhancer binding factor

NSP: Non-structural proteins

NTF2: Nuclear transcription factor 2

PABP: poly-(A) binding protein

PAMPs: Pathogen-associated molecular patterns

pDC: plasmacytoid dendritic cells

PERK: protein endoplasmic reticulum kinase

p-eIF2α: Phosphoryated eukaryotic initiation of translation factor

PKR: Protein kinase R

Poly IC: Polyinosinic: Polycytidylic acid

PRD: prion-like domain

prM: pre-membrane viral protein

PRRs: pattern recognition receptors

PTB: Polypirimidine tract-binding protein

RNAi: RNA interference

sfRNA: subgenomic-fragment RNA

shRNA: short hairpin RNA

SG: stress granule

SMN: Survival motor neuron protein

RD: repressor domain

RSV: Respiratory Syncytial Virus

RIG-I: Retinoic inducible gene I

RISC: RNA-induced silencing complex

siRNA: small interfering RNA

RRM: RNA recognition motif

SL: Stem loop

ssRNA: single-strand RNA

TBEV: Tick.borne encephalitis virus

TGN: Trans-golgi network

TIA-1: T-cell intracellular antigen 1

TIAR: T-cell intracellular antigen 1-related protein

TLR: Toll-like receptor

TTP: tristetraprolin

VP: Vesicle pocket

VSV: vesicular stomatitis virus

WNV: West Nile virus

YFV: Yellow fever virus

5' NCR: 5' Non coding region

3' NCR: 3' Non coding region

# 1. INTRODUCTION

## 1.1. Epidemiology and disease

Tick-borne encephalitis virus (TBEV) is the causative agent of neuroinfections of humans in Europe and Asia. In the natural environment, the virus circulates between ticks and wild vertebrate hosts (Burke and Monath, 2001). Three subtypes of TBE virus have been described based on comparative genomic sequencing (Ecker et al, 1999). The Western (European) subtype correlates with the distribution of the tick species *Ixodes ricinus* within central, eastern and northern Europe. The Far Eastern subtype correlates with the distribution of the tick species Ixodes persulcatus found in Russia, north-eastern China and parts of northern Japan. The Syberian subtype spreads westwards and has also been found in Finland (Jaaskelainen et al, 2006). Presently, global incidence of TBE ranges between 10.000 and 13.000 cases annually including 3.000 in Europe. Severe cases of TBEV infections with neurological manisfestations typically take a biphasic course (Haglund & Gunther, 2003). First phase is usually an influenza-like illness with symptoms such as fever, headache, muscle pain and malaise. Only 20-30% of the patients develop a second phase of the disease involving neurological symptoms. Among the factors influencing the manifestation of the natural TBE focus includes virus prevalence in the ticks, vector occurrence, host activity as well as socio-economic and climate changes.

## 1.2. Flaviviridae

*Flaviviridae* are a family of enveloped viruses, which cause severe disease and mortality in humans and animals. The family consists of three genera: *Flavivirus* (from latin *flavus*, "yellow"), *Pestiviruses* (from latin *pestis*, plague) and *Hepaciviruses* (from the greek *hepar, hepatos*, liver). Additionally to these genera there are two groups of unassigned viruses, GBV-A and GBV-C which await to be included in the family (Lindenbach, 2007b). The complete viral genome is between 9500-12500 nucleotides long, which encodes a polyprotein precursor. The polyprotein precursor is then cleaved and processed by cellular and viral proteases into three structural and seven non-structural proteins.

Among the members of the Pestivirus genus there are bovine viral diarrhea virus (BVDV), as well as classical swine fever virus (CSFV), and border disease virus

(BDV) of sheep, which infect animals. Hepatitis C virus (HCV) is the type member of the Hepacivirus genus, which also includes GB virus B (GBV-B). Currently, 3% of the world's population is chronically infected with HCV. From this number, 30% will develop cirrhosis which subsequently will lead to liver failure and/or hepatocellular carcinoma. Unfortunately, only half of the treated individuals respond to the current therapy (Leyssen et al, 2000).

## 1.3. Flavivirus genus

Is the largest genus of the family with seventy members, many of which are arthropod-borne. They are mainly transmitted through mosquitoes or ticks. Within the genus they can be divided in three clusters: mosquito-borne virus (MBV), tick-borne virus (TBV) and viruses with no known-vectors (NKV), which have been isolated from infected animals without a link to disease (Gubler, 2007).

Flaviviruses cause a variety of diseases in humans, which can be grouped into those that have the capacity to cause vascular leakage and hemorrhage, including Dengue virus (Denv) and Yellow Fever virus (YFV); and the ones that can cause encephalitis syndrome such us West Nile virus (WNV), Tick-Borne Encephalitis virus (TBEV) and Japanese Encephalitis virus (JEV) (Lindenbach et al, 2007a; Mukhopadhyay et al, 2005). Due to climate changes and global trade in animals, flavivirus infection is one of the biggest threats to public health worldwide (Pfeffer & Dobler, 2010). Therefore, there is a growing need to understand the molecular mechanisms involved in disease progression and pathogenesis to contribute to the development of efficient therapeutics to combat flavivirus-mediated diseases.

### 1.3.1. Flavivirus virions

Flavivirus virions are small, rounded envelope particles of about 50 nm of diameter. These particles are composed of a single strand positive polarity RNA genome that is packaged by the virus capsid protein. This nucleocapsid (NC) core is surrounded by the host-derived lipid bilayer that carries two surface proteins, the large envelope protein E and the small M protein, which derives from a larger precursor protein prM

(Lindenbach, 2007b).

**Capsid (C)** proteins are internal structural viral components whose primary function is to package viral genomic RNA into the nucleocapsids. They are highly basic proteins of approximately 12 kd. They contain N and C-terminal charged residues of which the C-terminal region may be involved with RNA association (Ma et al, 2004; Wang et al, 2002). The protein also contains a hydrophobic internal region, which mediates membrane association (Ma et al, 2004). The 20-residue hydrophobic C terminus of the precursor C protein anchors the C protein to the cytoplasmic side of endoplasmic reticulum (ER) membranes and functions as a signal sequence for translocation of the prM protein into the lumen of the ER. It has been shown that the C protein from virions lacks the C-terminal signal and is the consequence of a proteolytic cleavage by the NS2B-NS3 viral protease (Yamshchikov & Compans, 1993; Yamshchikov & Compans, 1994). The functional region for dimerization for virus assembly has been characterized and the binding to DNA or RNA induces this dimerization. (Kiermayr et al, 2004).

The **pr-M** protein is the glycoprotein precursor of the structural protein M of approximately 26 kd. The N-terminus of this protein immediately follows the signalase site from the C-terminus of the C protein. Furthermore it has been shown that the N-terminus contains from one to three N-linked glycosylation sites (Chambers et al, 1990). The C-terminal M segment, present in mature virions, contains a shortened ectodomain (approx. 41 amino acids) and retains the two potential membrane-spanning domains. The protein folds rapidly and assists the proper folding of the E protein (Konishi & Mason, 1993). The M protein is produced during maturation of the viral particle after cleavage of the prM precursor by the cellular protein furin (Stadler et al, 1997).

**Envelope (E)** is a 53 kD protein in its mature form and the major component of the virion surface. Flavivirus E protein plays an important role in virus assembly, maturation and entry (Stiasny & Heinz, 2006). This protein is composed of three domains; DI contains the N-terminus and participates in the conformational changes induced by endosomal acidification during viral entry (Bressanelli et al, 2004); DII is

involved in E dimerization and DIII is predicted to have a role in receptor binding (Rey et al, 1995) and antibody neutralization (Stiasny & Heinz, 2006). The junctions between the domains are flexible hinges which are important both in the conversion from immature to mature virions (Stiasny et al, 2009) and in the process of membrane fusion (Stiasny & Heinz, 2006).

### 1.3.2. Viral Genome

Flavivirus genomes consist of a single positive-strand RNA of approximately 11 kb with a type 1 cap (m7GpppAmp) structure at the 5' end (Cleaves & Dubin, 1979; Wengler & Gross, 1978) (Figure 1). Unlike cellular messenger RNA (mRNA), viral RNA genomes lack a 3' polyadenylate tail. Moreover, they encode a single long open reading frame (ORF) flanked by 5' and 3' non-coding regions (NCR) of 100 nucleotide (nt) and 400 to 700 nt, respectively. The 5' NCR exhibits a high degree of sequence conservation among different strains of the same virus but less conservation among the different members of the genus (Brinton & Dispoto, 1988). The region contains a Y-shaped stem loop structure (SLA) that functions as promoter for polymerase recognition and activity (Gritsun & Gould, 2007). Additionally, there is a small hairpin (SLB) located near the translation initiation codon called the 5′ upstream AUG region (5′UAR), which is complementary to the 3'NCR (3'UAR) sequence. This sequence complementarity between both ends of the RNA named cyclization sequence 5′-3′ UAR is required for replication (Alvarez et al, 2005; Kofler et al, 2006). The 3'NCR of flaviviruses is more heterogeneous in sequence and size. For example for tick-borne viruses, this region is subdivided into a variable region located downstream from the stop codon, and the core element which is the most conserved region in both structure and sequence. The most conserved domain of the 3′NCR includes a stable stem loop at the terminus (3′SL), which is required for RNA replication (Alvarez et al, 2005; Zeng et al, 1998). The 3'SL was shown to exhibit interaction with host proteins (De Nova-Ocampo et al, 2002) and viral proteins (Chen et al, 1997; Cui et al, 1998). The variable region of the 3'NCR has no decisive functional role since substitution of the entire region with an expression-cassette yield infectious virus that can be propagated in cell culture (Gehrke et al, 2005).


**Figure 1: Genomic RNA**

Consist of a positive sense single-stranded RNA of approx. 11 kb in length which is capped at the 5'-end and without a poly-A tail. It has a single open reading frame (ORF) of over 10,000 bases flanked by 5' and 3' non-coding regions (NCR)

### 1.3.3. Non-Structural proteins

**NS1** is a 46 KDa protein that contains two or three N-linked glycosylation sites and 12 conserved cysteines that form disulfide bonds (Lee et al, 1989; Mason, 1989). NS1 is found as cell-associated (Westaway, 1987), on the cell surface (Schlesinger et al, 1985), as a soluble form (Lee et al, 1989; Mason, 1989) and can also be secreted by mammalian cells. Intracellular NS1 is believed to play an important role in RNA replication possibly in negative-strand synthesis by an unknown mechanism. A large deletion in YFV NS1 abolished viral replication but can be complemented in trans by functional expression from Sindbis virus vector (Lindenbach & Rice, 1997). Mutations in the gene can lead to dramatic defects on RNA accumulation (Muylaert et al, 1997). The role of the NS1 soluble form is yet unknown. Nevertheless, correlation between high levels of the protein in serum of Denv-patients and severe disease has been found, indicating its possible role in viral pathogenesis (Avirutnan et al, 2006). Furthermore, NS1 may have a role in protective immunity since animals that have produced antibodies for this protein are protected against challenge with other flaviviruses (Bray et al, 1989).

**NS2A** is one of the small hydrophobic proteins (approx 22 KDa). The N-terminus of this protein is produced by cleavage with a host ER-resident enzyme (Falgout & Markoff, 1995). The cleavage of NS2A/NS2B is carried out by viral serine-protease. Moreover studies in YFV had shown that this protein contains an internal cleavage site for the viral protease, which produces a C-terminal truncated form that is possibly involved in virus assembly (Chambers et al, 1990; Nestorowicz et al, 1994).

**NS2B** is also a small (≈14 KDa) membrane-associated protein (Clum et al, 1997). NS2B forms a stable complex with NS3 and acts as a cofactor for the NS2B-NS3 serine protease (Falgout et al, 1991). Biochemical analysis demonstrated that NS3 protease activity is dependent upon association with the hydrophilic domain within NS2B (Chambers et al, 1990; Preugschat et al, 1990). The remainder of NS2B protein encodes three hydrophobic membrane domains, which are known to facilitate the association of the protease with membranes within the replication complex (RC) (Brinkworth et al, 1999; Droll et al, 2000). Mutagenesis experiments have identified specific residues within the protein, which are essential for the interaction with NS3 (Droll et al, 2000). This information could be exploited for the design of allosteric inhibitors able to block the interaction between NS2B and NS3.

**NS3** is the second largest viral protein of about 70 KDa. It is a multifunctional protein, at the N-terminus contains a trypsin-like protease domain (NS3pro) that has a highly specific substrate recognition sequence conserved among flaviviruses (Mandl et al, 1989). The C-terminus portion (NS3hel) exhibits different activities such as nucleoside triphosphatase (NTPase), RNA triphosphatase (RTPase) and helicase activities (Lindenbach et al, 2007b). NS3 helicase activity is thought to be involved in initiation of RNA synthesis by unwinding RNA secondary structures in the 3'UTR of the genome, to facilitate polymerase processivity during elongation or to separate double-stranded RNA (dsRNA) intermediates generated during viral replication (Lindenbach et al, 2007b). The NS3 RTPase activity is involved, together with the NS5 methyltransferase (MTase) domain in capping of the viral RNA (Wengler, 1993).

**NS4A** is a small hydrophobic protein of about 16 KDa. NS4A localizes within cytoplasmic replicative vesicles (Welsch et al, 2009) and its interaction with the NS1 protein is required for efficient RNA amplification (Lindenbach & Rice, 1999). Over-expression studies demonstrated that regulated cleavages of the NS4A/2K/NS4B junctions play an essential role in the induction of membrane rearrangements that form the scaffold for the viral RCs (Roosendaal et al, 2006).

**NS4B** is an hydrophobic protein, which localizes in ER membranes. Yeast two-hybrid assays and immunoprecipitation studies have shown the association between NS4B and the NS3-NS5 complex. Full length NS4B interacts with the C-terminal region of NS3. This observation suggested a role for NS4B in viral replication by helping the dissociation of the NS3 helicase from the RNA, and allowing binding of another duplex. Alternatively, NS4B might hold the separated RNA strand apart as the replication complex moves along the duplex (Umareddy et al, 2006). Furthermore, together with NS4A and NS2A, NS4B has also been suggested to take part in IFN antagonism (Munoz-Jordan et al, 2005)

**NS5** is located at the C terminus of the viral polyprotein and is the largest and most highly conserved flaviviral protein (around 103 KDa). It has two distinct enzymatic activities; the N-terminal is a methyl-transferase (MTase) involved in the capping of viral RNA, separated by an inter-domain region and the C-terminus contains the RNA-dependent RNA polymerase (RdRp) domain. Consistently with the presence of a nuclear localization signal between the MTase and polymerase domains, NS5 has been detected in both the cytoplasm and the nucleus of infected cells (Buckley et al, 1992; Uchil et al, 2006) suggesting that the host cell nucleus can provide an additional site for viral replication. In addition, studies on TBEV and Denv demonstrated that NS5 antagonizes IFN signalling by inhibiting the JAK-STAT (Janus kinase - signal transducer and activator of transcription) signal transduction pathway (Ashour et al, 2009; Best et al, 2005; Mazzon et al, 2009; Werme et al, 2008). Therefore, NS5 may be a common IFN antagonist that plays a crucial role in flavivirus pathogenesis in addition to its central function in viral RNA replication.

### 1.3.4. Flavivirus life cycle

Viral Entry

Virus entry to the cell is accomplished when the mature virion attaches to the cell surface through the Envelope (E) protein and cellular receptors. Subsequently, the virus is internalized into the host cell through clathrin-mediated endocytosis. After the entry, the virus is delivered to endosomes where the acidic environment will trigger a

change in the conformation of the structural viral protein envelope (E) leading to the fusion of the host and viral membranes (Krishnan et al, 2007; Stiasny et al, 2009). The viral genome is then released into the cytosol where it is translated into a single polyprotein by the host cell machinery.

Translation and protein processing

The flaviviral genome is translated into a single large polyprotein that is co- and post-translationally processed by host and viral proteases into ten proteins. The three structural proteins named capsid (C), pre-membrane (prM) and envelope (E) constitute the virion particle while the non-structural proteins (NS1, NS2A, NS2B, NS3, NS4A, NS4B, and NS5) are involved in viral replication, virus assembly and immune response evasion (Lindenbach et. al. 2007) (figure 2).

Processing of the polyprotein occurs before the translation is completed and is carried out by both host proteases and the viral protease NS3 together with its cofactor NS2B in the lumen of the ER. Between C/prM, prM/E, E/NS1 and between NS4A/NS4B, the proteolytic cleavage is mediated by the host enzyme signal peptidases, while the serine protease domain of NS3 cleaves the polyprotein between NS2A/NS2B, NS2B/NS3, NS3/NS4A, NS4B/NS5 and some other residues within its own C-terminus domain (Randall et al, 2007).

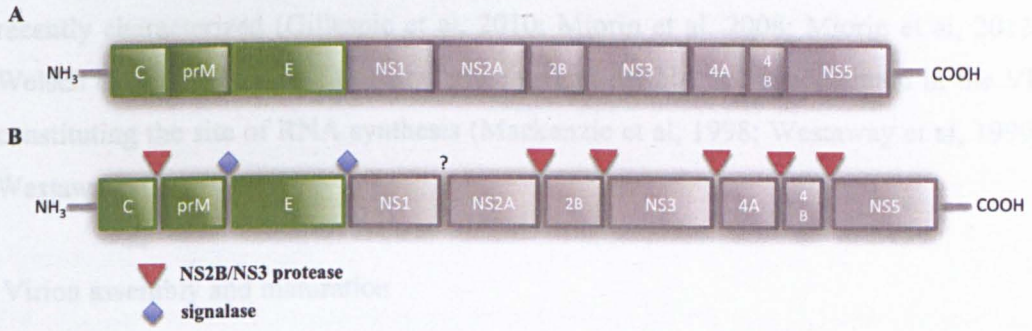


**Figure 2: Viral polyprotein organization**

A) From the N-terminal end the order of the encoded proteins in the long ORF is 5'-C-prM(M)-E-NS1-NS2A-2B-NS3-NS4A-4B-NS5-3'. The structural proteins (C) Capsid, M (Membrane whose precursor is prM) and E (Envelope) are located in the 5' quarter of the genome and genes for non-structural proteins are positioned in the remainder. B) Sites of polyprotein cleavage mediated by the viral

NS2BNS3 and by host signalase and furin are shown, and the enzymatic activities of NS3 and NS5 are also indicated (Sampath & Padmanabhan, 2009).

## Viral Replication

After the first round of translation viral replication is initiated. Viral RNA-dependent-RNA polymerase, begins with the synthesis of the negative-sense RNA that will serve as a template for the generation of newly synthesized genomic RNA. Viral RNA synthesis seems to be asymmetric, with an excess of the plus-sense RNA synthesized over the minus-sense RNA (Cleaves et al, 1981; Westaway et al, 1999) (Wengler & Gross, 1978). The newly synthesized plus-sense RNA is subsequently used for translation of additional viral proteins or synthesis of other negative-sense RNA, or it becomes incorporated into new viral particles. Thus, the genomic RNA has at least three different functions (translation, replication, and association with nascent viral particles), which need to be tightly regulated and coordinated during the viral replication cycle.

Viral replication occurs in the rough endoplasmic reticulum (ER) and in the Golgi-derived membranes called vesicle pockets (VP) (den Boon et al, 2010; Mackenzie, 2005). Such membranes may serve as a scaffold for anchoring the viral replication complexes as well as may be exploited by the virus to shield replication intermediates from host defences (Miorin et al, 2012; Miorin et al, 2013; Overby et al, 2010). The composition and three-dimensional organization of these compartments have been recently characterized (Gillespie et al, 2010; Miorin et al, 2008; Miorin et al, 2013; Welsch et al, 2009). Non-Structural proteins and dsRNA are concentrated in the VP constituting the site of RNA synthesis (Mackenzie et al, 1998; Westaway et al, 1999; Westaway et al, 1997).

## Virion assembly and maturation

Assembly of the virion particles occurs in the lumen of the ER. One of the earliest steps during flaviviral assembly is the formation of the NC, which consists of one copy of genomic RNA and multiple copies of capsid protein (Khromykh & Westaway, 1996). Subsequently, E and PrM proteins hetero-dimerize and envelope the NC forming an immature virus particle that buds from the ER lumen into the Golgi (Mackenzie & Westaway, 2001). Maturation of virus particles occurs in the

trans-Golgi network, where prM is cleaved to M by furin, resulting in a conformational rearrangement of E (Li et al, 2008; Mukhopadhyay et al, 2005; Yu et al, 2008). The maturate virion exits the cell through exocytosis.

Sub-viral particles have been routinely observed during flaviviral infection. These particles have a diameter of around 31 nm. They are assembled in the ER and undergo the same posttranslational modifications as infectious particles before they are released from the host cell. One important feature of these particles is that they only contain M and E proteins and a lipid membrane. A schematic picture of the entire viral cycle is shown in figure 3.

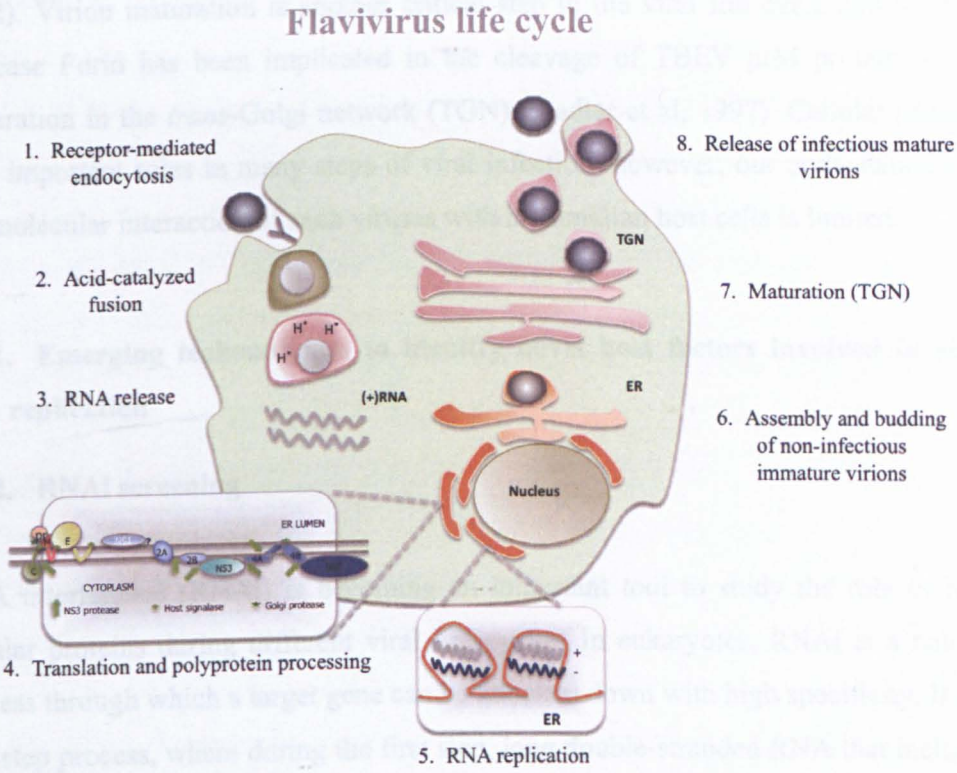


**Figure 3: Flavivirus life cycle**

The virus enters to the cell through receptor-mediated endocytosis, and after the fusion of the host and virus membranes, the positive-strand RNA is released into the cytosol to be translated by the host cellular machinery. The non-structural proteins will form the replication complexes surrounded by ER-membranes. During viral replication, the negative-strand RNA is synthesized and used as a template for the production of genomic RNA. The virions are assembled in the ER and their maturation occurs in the trans-Golgi (TGN). Then they exit the cell through exocytosis.

## 1.4. Host Proteins-Pathogen Interactions

Since flaviviruses only encode ten proteins, it is important for them to exploit the host cellular machinery in order to complete their life cycle. Several cellular pathways and host factors have been involved in flaviviral replication but the biological relevance of these interactions is not yet understood. For example, Heat Shock proteins 90 and 70 have been identified to be part of a receptor complex involved in DENV entry (Reyes-Del Valle et al, 2005). Additionally, during WNV replication host factors such as T-cell-restricted intracellular antigen-1 (TIA-1) and TIA-1 related protein (TIAR) have been reported to be involved in the synthesis of negative strand RNA (Li et al, 2002). Virion maturation is another critical step in the viral life cycle and the host protease Furin has been implicated in the cleavage of TBEV prM protein during maturation in the *trans*-Golgi network (TGN) (Stadler et al, 1997). Cellular proteins play important roles in many steps of viral infection; however, our understanding of the molecular interaction of such viruses with mammalian host cells is limited.

### 1.4.1. Emerging techonologies to identify novel host factors involved in viral replication

### 1.4.2. RNAi screening

RNA interference (RNAi) is becoming an important tool to study the role of host cellular proteins during different viral life cycles. In eukaryotes, RNAi is a natural process through which a target gene can be knocked down with high specificity. It is a two-step process, where during the first step, long double-stranded RNA that includes a hair pin structure, is synthesized in the nucleus and processed by Drosha into a miRNA precursor (Lee et al, 2002). It is then exported to the cytoplasm through the exportin-5 complex (Bohnsack et al, 2004). Once in the cytoplasm, the double-stranded RNA precursor is processed by Dicer, which produces a dsRNA of about 20-25 base pairs long with a 5' and 3' two base over-hang (Elbashir et al, 2001; Shan, 2010).

The siRNA and miRNA produced are then loaded into the RNA-induced silencing complex (RISC), where the strands are separated into a single strand, the sense strand

hybridizes the homologous cellular mRNA and the other strand is degraded (Tuschl et al, 1999). RISC catalyzes the cleavage to the target RNA in an ATP-independent manner (Nykanen et al, 2001; Pham et al, 2004). A schematic representation of the siRNA and miRNA pathway is shown in figure 4. In animals, unlike siRNA, which has high specificity for its target mRNA, it has been shown that the binding of miRNA to target mRNA is not very efficient due to incomplete complementarity and this leads to the repression of translation rather than mRNA cleavage (Lim et al, 2005).

In cultured cells, silencing of specific cellular genes can be carried out by transfection of synthesized small-interfering RNA molecules (siRNAs) or plasmid-based short hairpin RNAs (shRNAs) that are subsequently processed to siRNAs inside the cell. shRNA constructs can be delivered by lentiviral vectors which integrate the construct into the cellular genome to obtain long-term gene suppression (Brummelkamp et al, 2002; Paddison et al, 2002). The availability of highly specific methods for gene inactivation now allows a systematic examination of the roles of individual human genes in the viral life cycle and the identification of new potential drug targets. Concerning to this, Genome-wide RNA interference screenings have been made with flaviviruses such us WNV and Denv (Chu & Yang, 2007; Krishnan et al, 2008; Tai et al, 2009). From WNV screen, they found 305 host factors affecting viral replication. Interestingly, they performed the same screen for Dengue virus, but only 36 percent of the hits down-regulating WNV replication were reducing Denv replication. Moreover, 22 hits that were up-regulating WNV replication were affecting in the reverse way to Denv, demonstrating host-pathogen specific interactions. By this approach several previously unknown host factors, affecting viral replication, have been identified. These proteins are involved in different cellular processes such as intracellular protein trafficking, signal transduction, nucleic acid, protein and lipid metabolism, among others. However, very few host genes are overlapping between the screenings. This variability is due to the use of different RNAi libraries, cells, replicons versus infections and also statistical parameters. Therefore there is a growing need for the validation of these host proteins as well as for the understanding of the biological relevance of these interactions.

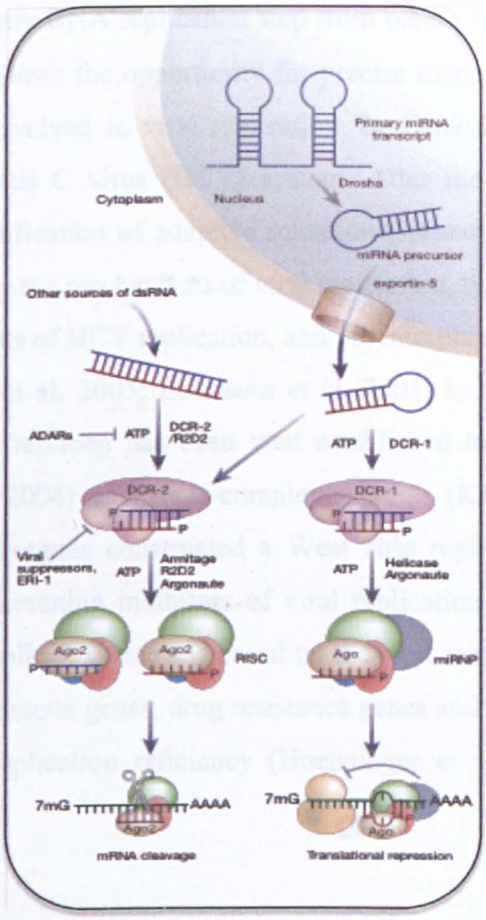


**Figure 4: Schematic model of siRNA and miRNA processing**

Primary miRNA transcript is processed in the nucleus by Drosha. miRNA precursor is exported to the cytosol through exportin 5. In the cytoplasm, miRNA precursor or long dsRNA from different sources are processed by Dicer producing dsRNA of 20-25 pb. This dsRNA is loaded in the RISC complex where the sense strand of the RNA will hybridize to the complementary mRNA and the RISC complex will catalize the cleavage of the RNA. When the complementarity of the sense RNA is not complete like in the case of miRNAs, instead of a cleavage of the RNA, there is a translational repression of the mRNA (Meister & Tuschl, 2004).

### 1.4.3. Sub-genomic Replicons

The utilization of flaviviral subgenomic replicons has become a very important tool for the study of viral replication. They are self-replicating RNA that contain all of the genetic elements needed for amplification in susceptible hosts but lack the major part of the genes encoding the structural proteins. Consequently, the RNA replicates but is not packaged into viral particles. The advantage of using these systems is that they

permit to study separately RNA replication step from others such as virion assembly and maturation. This allows the opportunity for precise mapping of proteins, motifs and RNA sequences involved in viral replication. In *Flaviviridae*, one of the best characterized is Hepatitis C virus (HCV) system. After the introduction of HCV replicons and the identification of adaptive mutations, researchers have utilized the replicon system to study the mechanisms of viral replication, the identification of viral and cellular determinants of HCV replication, and the interplay between virus and the Huh-7 cell (Lohmann et al, 2003; Lohmann et al, 2001; Lohmann et al, 1999). In *Flavivirus*, the Kunjin replicon has been well established to characterize adaptive mutations (Liu et al, 2004) and trans-complementation (Khromykh et al, 2000). Moreover, Lo and colleagues constructed a West Nile replicon to use in a high-throughput assay for screening inhibitors of viral replication (Lo et al, 2003). The particularity of these replicon systems is based on the replacement of the deleted viral parts with expression cassette genes, drug resistance genes and reporter genes that still allow monitoring of replication efficiency (Hoenninger et al, 2008; Miorin et al, 2008).

### 1.4.4. Reporter genes

With the development of transient RNA replication assays that allow faster and direct analysis of relative replication efficiencies, the study of the viral life cycle in cultured cells became more practical. Different reporter genes had been used such as luciferase and β-lactamase, as well as transactivator inducing secreted alkaline phosphatase (SEAP). For example, firefly luciferase gene has successfully been inserted in TBEV replicon where the region of the structural proteins is deleted (Hoenninger et al, 2008), conserving high rates of replication, thus enabling viral replication to be followed at different time points after transfection by measuring luciferase activity. Moreover, TBEV bicistronic replicons had been made containing two different reporter genes: from the 5' end, the first 17 aminoacids of C protein is fused to luciferase gene followed by non-structural proteins under the control of cap-dependent translation and a GFP reporter gene under the control of an internal ribosomal entry-site (IRES) at the variable region of the 3' end (Hoenninger et al, 2008). The advantage of using replicon reporter genes that allows for a rapid

determination of replicative ability is that they can be adapted to high-throughput analysis. For example, β-lactamase reporter gene has successfully been used for the screening of HCV replication inhibitors (Zuck et al, 2004). The use of β-lactamase as a reporter, coupled to the use of a cell-permeable FRET β-lactamase substrate, enabled the measurement of biological responses in live cells without the need of a cell lysis step. On the other hand, Zuck and co-workers had to face several optimizations of the system in order to obtain robust results.

### 1.4.5. MS2-based tagging system

Different techniques had been used for the visualization of nucleic acids to study host-pathogen interactions. The most widely used for this purpose has been fluorescence *in situ* hybridization (FISH) that depends on the fixation of the samples (Chu & Ng, 2004; Grief et al, 1997). Moreover, double-stranded RNA which is the viral replication intermediary has been detected by using a specific antibody (Mackenzie et al, 1998; Westaway et al, 1999). Few years later, researchers had improved this technique by tagging viral DNA or RNA in live cells using different methods like hybridization with molecular beacons (Cui et al, 2005) and the incorporation of fluorescent dyes to monitor Poliovirus genome (Brandenburg et al, 2007). Interestingly, herpes simplex virus and adeno-associated virus DNA were engineered by inserting specific sequences that were binding fluorescent protein like the Lac operator/repressor system (Bertrand et al, 1998; Fraefel et al, 2004; Sourvinos & Everett, 2002).

The MS2-based method allows the monitoring of RNA dynamics in living cells (figure 5). The system consists of the delivery of fluorescent molecules to the target RNA, which involves the non-covalent binding to a cognate tag region located in the RNA.

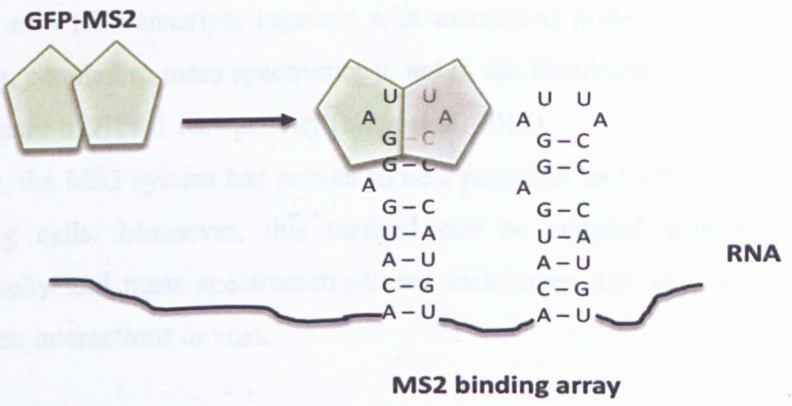


**Figure 5: RNA detection using the MS2 system**

RNA molecules are detected using a fusion protein that comprises a fluorescent tag, such as the green fluorescent protein (GFP) and the MS2 bacteriophage coat protein. MS2 has an extremely high affinity for a 19 nt RNA-recognition motif that is derived from the phage genome.

Bertrand and co-workers exploited an RNA-protein interaction discovered in the MS2 phage as the basis for their labelling strategy. The bacteriophage MS2 protein binds to a short RNA hairpin secondary structure, which was inserted into the 3'UTR of an mRNA while the MS2 protein was genetically fused to GFP. Expression of the mRNA and the GFP-MS2 fusion protein resulted in delivery of GFP to the RNA deriving in a successful visualization (Bertrand et al, 1998). Furthermore, this system was efficiently used for tracking viral RNA synthesis in living cells. Miorin and collaborators developed a TBEV replicon system, which contains an array of binding sites for YFP- MS2 fusion protein. By performing FRAP analysis, to study the mobility of viral RNA in the replication complexes they observed a delay of the recovery of fluorescence after photobleaching within the regions of EYFP-MS2 accumulation. This evidence was suggesting an impaired movement of the genomic RNA inside the replication complexes (Miorin et al, 2013).

Alternatively, the MS2 system can be used as a tool for affinity purification coupled with proteomic studies. MS2 fused to the maltose binding protein (MBP) has been utilized to purify the spliceosome by affinity chromatography of cellular extracts (Zhou et al, 2002). Using this approach more than 100 distinct spliceosomal proteins were identified. Furthermore, this tagging system has been also exploited to identify

novel host factors associated with HIV-1 RNA (Maiuri et al, 2011). Affinity purification of viral transcripts together with associated proteins via a flag-tagged MS2 protein, coupled to mass spectrometry, led to the identification of Matrin 3 as a cellular cofactor of HIV-1 Rev activity (Kula et al, 2011).

In summary, the MS2 system has proven to be a powerful tool for RNA detection in single living cells. Moreover, this method can be coupled with high affinity chromatography and mass spectrometry-based techniques that allows the study of host-pathogen interactions *in vivo*.

## 1.5. Stress Response: stress granules

Stress Granules (SGs) were first observed as phase-dense cytoplasmic granules in cultures of Peruvian tomato cells exposed to heat shock (Nover et al, 1983). A few years later, through immunofluorescence analysis SGs also were observed in the cytoplasm of mammalian cells subjected to heat shock (Arrigo et al, 1988). Plant SGs were shown to contain RNA in addition to Heat-Shock Proteins (HSPs). The RNA content of plant heat-shock SGs was specific to housekeeping genes but the newly synthesized heat-shock mRNA was excluded (Nover et al, 1989). The inactive RNA present in the SGs could be translated *in vitro* and also when the cells had recovered from the stress, therefore it was proposed that the SGs were sites of RNA storage during stress.

### 1.5.1. Stress granules proteins

TIA-1

T-Cell intracellular antigen 1 (TIA-1) is a 40 KDa protein and is a member of the RNA recognition motif (RRM) family of RNA-binding protein (Beck et al, 1996; Dember et al, 1996; Kawakami et al, 1992; Kawakami et al, 1994; Tian et al, 1991). TIA-1 has two isoforms, i) 42 KDa TIA-1a, ii) 40 KDa TIA-1b that differ from each other by an 11 amino-acid deletion. These isoforms are usually found in cells in a 1:1 ratio (Beck et al, 1996). The cellular localization of this protein is mainly nuclear and shuttles between the nucleus and the cytoplasm and it has been implicated in RNA

metabolism such us pre-mRNA splicing and mRNA translation, respectively. At the amino terminal domain contains three RNA binding domains from which the first RRM1 does not present RNA binding activity, the RRM2 contains a AU-rich sequence specific RNA binding activity and the third RRM3, presents a general RNA binding activity (Dember et al, 1996). These features allow the protein to bind either uridine-rich sequences with high affinity and also to bind heterogenous mRNAs without sequence specificity (Dember et al, 1996). Therefore the sequence non-specific binding could allow the protein to recruit the untranslated mRNA to stress granules (SG), and the sequence–specific binding to regulate the translation of cellular transcripts such us TNF-α (Piecyk et al, 2000). Interestingly, biochemical studies demonstrated that TIA-1 as well as its paralog TIAR was binding WNV negative-strand 3'-end SL RNA (Li et al, 2002) through its sequence-specific binding domain RRM2. Moreover, in the same studies they used TIA-1 and TIAR knock-out MEF cells to analyze the functional relevance of these proteins in WNV replication. They found no change in WNV replication in TIA-1 KO MEF cells and down-regulation of replication in TIAR KO cells. However, the function of these cellular proteins binding to viral RNA in the virus life cycle has not yet been elucidated.
Furthermore, TIA-1 protein also contains a glutamine-rich region at the carboxi-terminal end called prion-like domain (PRD), which shares structural and functional aggregation features with mammalian and yeast proteins (Gilks et al, 2004). PRD is capable of self-aggregation (Gilks et al, 2004) and is essential for the formation of SGs (Kedersha et al, 2000).

TIAR

TIA1 cytotoxic granule-associated RNA binding protein-like 1 (TIAR) is structurally and functionally related to TIA-1. TIAR has two isoforms, i) 42 KDa TIARa, ii) 40 KDa TIARb, that differ from each other by a 17 amino-acid deletion. TIARb is generally more abundant than TIARa in cells (Beck et al, 1996). Like TIA-1, TIAR possesses three N-terminal RRMs and a C-terminal PRD. TIAR and TIA-1 share 90% of amino acid identity in their RRMs and a 50% identity within C-terminal PRD. Due to the sequence homology with TIA-1, TIAR cellular localization is mostly nuclear and it has been involved in cellular processes such as translation, splicing and apoptosis (Gueydan et al, 1999; Izquierdo et al, 2005; Kawakami et al, 1992).

Moreover, its participation during SG formation has been shown (Kedersha et al, 1999).

G3BP

Ras-GTPase activating protein SH3 domain binding protein (G3BP) is a 68 KDa protein that contains RNA binding motifs at the C-terminal domain. Different genes on human chromosomes 5 and 4 encode G3BP1 and G3BP2, respectively (Kennedy et al, 2001). Its cellular localization is primarily cytoplasmic but may have the capacity to enter to the nucleus (Parker et al, 1996; Tourriere et al, 2001). Despite the absence of any identifiable ribonuclease domain, this protein was shown to be involved in the degradation of *c-myc* transcript *in vitro* (Gallouzi et al, 1998). Moreover, Gallouzi and colleagues showed that this protein is heavily phosphorylated in quiescent cells and dephosphorylated in growth-stimulated cells suggesting a role in cell cycle regulation (Gallouzi et al, 1998). In this work they postulated that G3BP acts as a growth factor sensor allowing the accumulation of transcripts involved in cell cycle regulation such as *c-myc* in stimulated cells but facilitating their degradation in resting cells. Interestingly, Tourriere and co-workers showed that G3BP was very efficiently recruited to SGs (Tourriere et al, 2003). Additionally, over-expression of this protein could efficiently trigger assembly of SGs indicating its role as a SG nucleation protein like TIA-1 and TIAR (Kedersha et al, 1999). Due to its role as a ribonuclease, the authors suggested that the RNA present in G3BP positive granules is possibly been degraded. On the figure 6, a schematic representation of TIA-1, TIAR and G3BP proteins is shown.

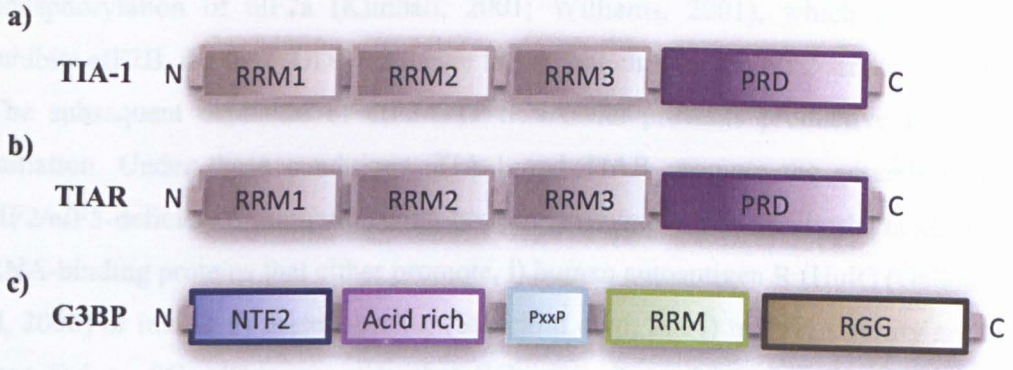


**Figure 6: Schematic representation of stress response proteins**

a) and b) TIA-1 and TIAR protein domains. Each protein contains from the N-terminal domain three RNA Recognition Motifs (RRM), which had been shown RRM2 to bind AU-rich sequences and RRM3 binds to RNA not in a sequence specific manner. At the C-terminal domain presents a glutamine-rich domain called prion-like domain (PRD) wich gives to the protein the capacity to perform self-aggregation. c) G3BP protein domains. The protein contains at the N-terminal domain an NTF2-like domain which may give a role in nuclear transport. In the central region there is an acid domain and a PxxP motif for SH3 binding domain. Whereas the C-terminal region contains RRM and RGG which are RNA biding motifs.

### 1.5.2. Stress Granules assembly

After years of research, Kedersha and colleagues identified the protein components of mammalian SGs. TIA-1 and TIAR were found to be robust markers of these cytoplasmic foci (Kedersha et al, 2000). As mentioned before, these proteins shuttle between nucleus and cytoplasm, but under stress conditions the proteins accumulate in the cytoplasm, where they bind the 48S complex instead of the ternary complex, promoting polysome disassembly and the subsequent routing of the mRNA into SGs (figure 7).

Translation is normally initiated when the small ribosomal subunit and its associated initiation factors are recruited to a capped mRNA transcript to form a 48S complex. Hydrolysis of eIF2- associated GTP by eIF5 displaces the early initiation factors, allowing the binding of the large ribosomal subunit. Repeated cycles of successful initiation convert an mRNA into a polysome. In stressed cells, activation of one or

more eIF2a kinases (e.g. PKR, PERK/PEK, GCN2, HRI) results in the phosphorylation of eIF2a (Kimball, 2001; Williams, 2001), which consequently inhibits eIF2B, the GTP/GDP exchange factor that charges the eIF2 ternary complex. The subsequent depletion of eIF2-GTP-tRNAiMet prevents productive translation initiation. Under these conditions, TIA-1 and TIAR promote the assembly of an eIF2/eIF5-deficient preinitiation complex that is routed to SGs (Kedersha et al, 2002). RNA-binding proteins that either promote, i) human autoantigen R (HuR) (Gallouzi et al, 2000) or inhibit ii) tristetraprolin; (Stoecklin et al, 2004) mRNA stability are also recruited to SGs. This suggests that SGs are sites where the fates of specific transcripts are determined by the activity of different RNA-binding proteins. Whether the SG is also a site of mRNA processing (e.g. through degradation by exosomes) remains to be determined.

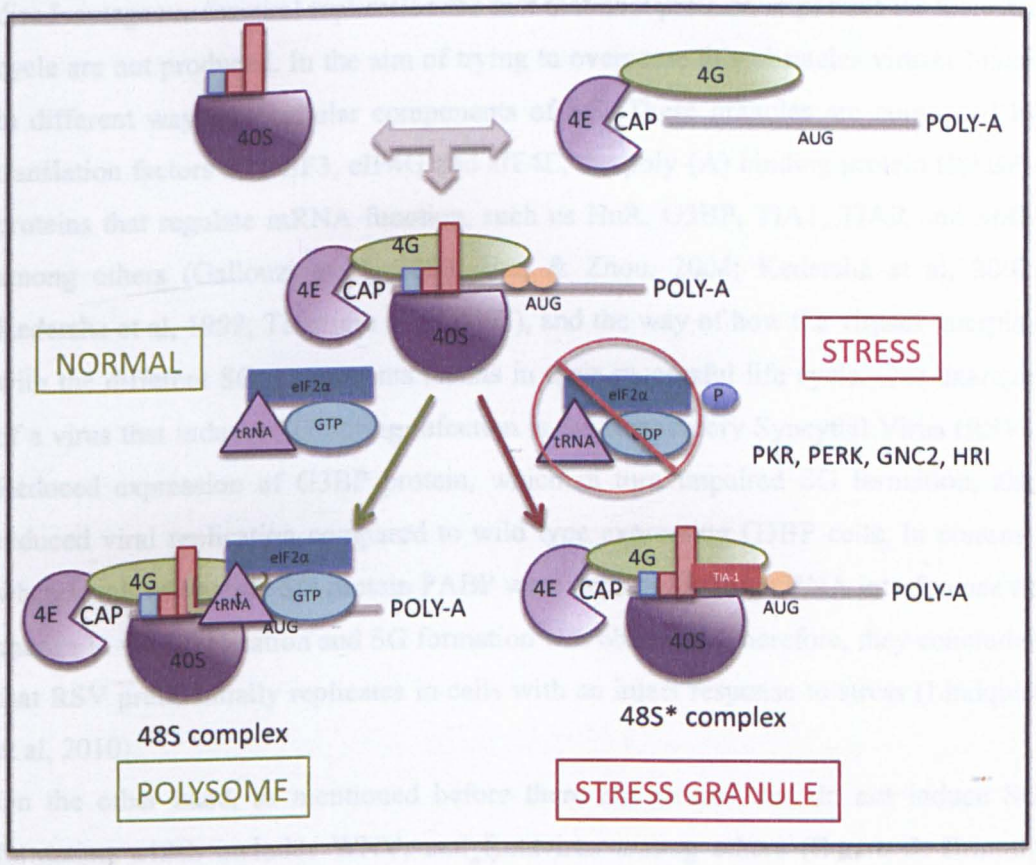


**Figure 7: Stress granules assembly**

Translation initiation starts when eIF2α together with initiation factors binds to the capped mRNA to form 48S complex. Hydrolysis of eIF2α-associated GTP by eIF5 displaces the early initiation factors,

allowing the binding of the large ribosomal subunit. Repeated cycles of successful initiation convert mRNA into a Polysome. In stressed cells, there is activation of eIF2α kinases (PKR, PERK, GNC2 and HRI), which in turn phosphorylate eIF2α (Kimball, 2001) and this process leads to the inhibition of the formation of the ternary complex eIF2α-GTP-Met. Therefore TIA-1 promotes the assembly of an eIF2α-GTP-Met deficient preinitiation complex denoted 48S* that routes mRNA to SG. Adapted from (Anderson & Kedersha, 2002)

### 1.5.3. Stress granules during viral replication

Different kind of stresses have been described to induce SG formation in eukaryotic cells such us heat shock, oxidative stress and virus infections (Kedersha et al, 2002). Several viruses can cause a translational shutoff of cellular proteins to benefit the viral translation. This process gives the advantage to the virus to replicate faster and to avoid the production of antiviral cellular proteins, but at the same time could be disadvantageous for viral replication the fact that host proteins important for their life cycle are not produced. In the aim of trying to overcome this obstacles viruses hijack in different ways the cellular components of SG. These granules are composed by translation factors like eIF3, eIF4G and eIF4E, the poly-(A) binding protein (PABP), proteins that regulate mRNA function, such us HuR, G3BP, TIA1, TIAR and SMN among others (Gallouzi et al, 2000; Hua & Zhou, 2004; Kedersha et al, 2002; Kedersha et al, 1999; Tourriere et al, 2003), and the way of how the viruses interplay with the different SG components results in their successful life cycle. One example of a virus that induces SG during infection is the Respiratory Syncytial Virus (RSV). Reduced expression of G3BP protein, which in turn impaired SG formation, also reduced viral replication compared to wild type expressing G3BP cells. In contrast, when levels of another SG protein PABP were depleted through RNA interference no change in viral replication and SG formation was observed. Therefore, they concluded that RSV preferentially replicates in cells with an intact response to stress (Lindquist et al, 2010).

On the other hand, as mentioned before there are viruses that do not induce SG formation which includes WNV, and Rotavirus among others (Emara & Brinton, 2007; Lindquist et al, 2010). For Rotavirus it has been observed a translational shutoff after infection shown by the presence of phosphorylated eIF2α without SG formation. Through immuno-fluorescence analysis it was observed a change in intracellular localization of the SG component protein PABP and this effect was

dependent on the viral protease NSP3 (Montero et al, 2006). In addition, studies from Emara and colleagues demonstrated that SG assembly was reduced in cells infected with WNV compared to mock cells upon arsenite treatment a well-known SG inducer (Emara & Brinton, 2007). They also observed that SG markers TIA-1 and TIAR were recruited, at different time points post-infection, to WNV and Denv replication sites (Emara & Brinton, 2007). This evidence indicated that infection by these viruses interferes with SG assembly by hijacking the cellular localization of SG proteins. The relevance of these interactions is a current topic of research.

## 1.6. Immune response

Mammalian cells have evolved a variety of defence mechanisms to detect, contain and clear viral infections. There are two fundamentally different types of responses to invading pathogens: the innate and the adaptive immune response. The innate immune response offers the first early protection against foreign invaders and is mediated by a limited number of germline-encoded pattern-recognition receptors (PRRs). In contrast, adaptive immunity is implicated in pathogen clearance during the late phase of the infection and involves lymphocytes (T and B cells) clonally expressing a big range of rearranged antigen-specific receptors.

Pathogen-associated molecular patterns (PAMPs) are molecular structures such as glycoproteins, proteoglycans, lipopolysaccharides and nucleic acid motifs that are shared by different microorganisms and are essential to the survival or infectivity of the microbe. Germ-line encoded pattern recognition receptors (PRRs) are the proteins responsible for sensing microbial invasion. The strategies of employing multiple families of PRRs afford the advantage to the host of sensing and immediately responding to a diverse range of pathogens (Akira et al, 2006).

The sensing of PAMPs by PRRs, upregulates the transcription of genes involved in the inflammatory responses such as cytokines and type I interferons (IFN). Production of IFN ($\alpha/\beta$) plays an important role in the induction of antiviral responses by triggering the transcription of many interferon inducible genes that influence protein synthesis, cellular growth and apoptosis. Type I interferons also enhance the maturation of dendritic cells (DC), cytotoxicity of natural killer (NK) cells and

differentiation of virus-specific T lymphocytes, providing a link between innate and adaptive immune response (Honda et al, 2005).

To date, two distinct families of sensors have been characterized as key players in sensing RNA viruses: the Toll-like receptor (TLR) and the RIG-I (retinoic acid inducible gene-I)-like receptor (RLR) families.

### 1.6.1. Toll-like receptor family

Toll-like receptors (TLRs) are transmembrane glycoprotein receptors with an N-terminal extracellular PAMP-binding region and a C-terminal intracellular signalling region. The C-terminal region mediates downstream signalling events upon activation of the receptor (Akira & Takeda, 2004). Upon extracellular ligand recognition, TLR dimerization is thought to occur, bringing together the cytoplasmic domain and subsequently initiating the signalling process (Akira et al, 2006). The human TLR family comprises 10 members of which TLR2, 3, 4, 7 and 8 are important in the recognition of structural components of viruses, including viral double-stranded RNA (dsRNA), single-stranded RNA (ssRNA) and surface glycoproteins. Among these receptors, TLR3, 7 and 8 recognize nucleic acid motifs and are preferentially located to intracellular compartments, such as the endoplasmic reticulum (ER), lysosomes, and endosomes rather than being expressed in the cell surface (Akira et al, 2006).

TLR3 was the first characterized receptor involved in dsRNA recognition. As mentioned before, dsRNA agonists can be generated during viral infection as a replication intermediate for single stranded RNA (ssRNA) viruses. The role of TLR3 in the generation of effective antiviral immune responses is still controversial. Experiments performed in TLR3 knockout mice infected with multiple RNA viruses failed to show increased mortality or altered viral burden phenotypes (Edelmann et al, 2004). Conversely, Wang and colleagues showed that WNV virulence was attenuated in TLR3 knockout mice, most likely because of a decreased inflammatory response that diminished blood-brain barrier permeability and viral entry to the brain (Wang et al, 2004).

TLR7 and 8 sense ssRNA containing guanosine and uridine-rich sequences from RNA viruses. The subcellular localization of these receptors in endosomal compartments of plasmacytoid dendritic cells (pDCs) supports the idea that they are

activated by viruses that enter the cell through endosomes. Alternatively, they can also be activated by viral RNA uptake from the cytoplasm of infected cells. TLR7 is known to recognize influenza A virus (IAV), vesicular stomatitis virus (VSV), and Denv among others (Diebold et al, 2004; Lee et al, 2007; Wang et al, 2006).

### 1.6.2. RIG-I like receptors

The RIG-I like receptors (RLRs) (Figure 8) are cytosolic proteins that recognize viral RNA species and they are expressed by most cells of the human organism. RLRs belong to the family of DExD/H-box helicases and include three members: the retinoic acid-inducible gene I product RIG-I, melanoma differentiation-associated antigen 5 (MDA-5) and laboratory of genetics and physiology 2 (LPG2) (Kang et al, 2002; Yoneyama et al, 2005). RLRs are critical sensors of viral infection in most cell types except pDCs, which preferentially employ TLRs for detection of RNA virus infection (Kato et al, 2005).

Retinoic acid-inducible gene I (RIG-I) contains an ssRNA/dsRNA (ss/dsRNA)-binding C-terminal domain (CTD) that when unbound, functions as a repressor domain (RD) (Saito et al, 2007). Upon binding to viral RNA structures produced during viral replication, the CARD-like domain is exposed, and subsequently able to interact with other CARD-containing proteins to trigger downstream signalling events. In the inactive state RIG-I adopts a closed structure with unexposed CARD. The RD specifically recognizes virus-associated RNA species, including dsRNA and 5'-triphosphate ssRNA (Kato et al, 2006). RIG-I is important in recognizing a wide range of viruses from many different families, including *Flaviviridae* (Fredericksen et al, 2008; Kato et al, 2006) and *Paramyxoviridae* (Habjan et al, 2008; Kato et al, 2005) among others.

Melanoma differentiation-associated antigen 5 (MDA5) is very similar to RIG-I and exhibits the same overall domains. Upon binding to long dsRNA fragments, MDA5 exposes a CARD domain and initiates cytokine and type I IFN production via IPS-1 similarly to RIG-I (Kang et al, 2002). MDA5 is crucial for triggering a cytokine response to an invasion with picornaviruses, such as encephalomyocariditis virus (EMCV), and in cooperation with RIG-I, for WNV and Dengue virus (Fredericksen et al, 2008; Gitlin et al, 2010; Loo et al, 2008).

Laboratory of genetics and physiology 2 (LPG2) is the third member of RLRs and is less well-characterized. LPG2 gene lacks the region-encoding CARD in RIG-I and MDA5. Since this region is responsible for the interaction with IPS-1 to activate the signaling cascade, LPG2 is thought to be a negative regulator of RLR signalling via association between the RD of LPG2 and RIG-I (Rothenfusser et al, 2005). Studies performed in mice lacking LPG2, have observed an increased antiviral response with VSV (Venkataraman et al, 2007). As mentioned before, VSV is recognized by RIG-I rather than MDA5. On the other hand, evidence suggests that LPG2 deficiency reduces the reponse to infection with EMCV, which is known to be recognized by MDA5 (Venkataraman et al, 2007). Therefore it is thought that LPG2 could be a modulator of the innate immune response to a viral infection and not a sensor of PAMPs in that LPG2 does not initiate antiviral gene expression.

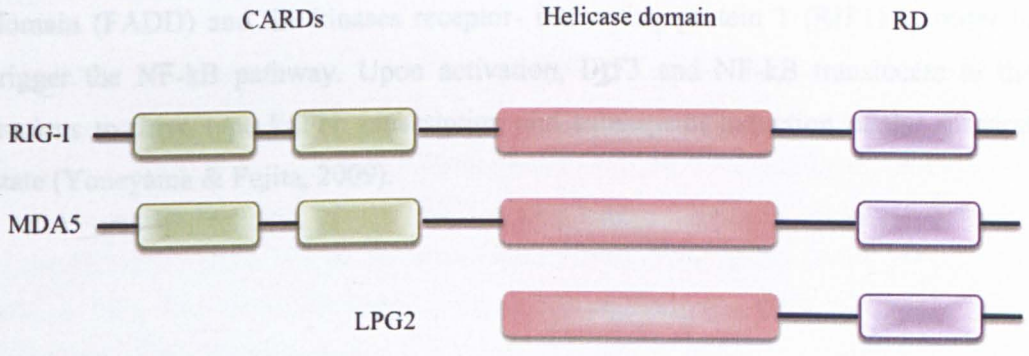


**Figure 8: Schematic representation of RLRs proteins**

(1) The N-terminal CARD domain composed of two tandem CARDs. (2) The central helicase domain, belonging to the DExD/H family of RNA helicases. (3) The unique C-terminal domain containing multiple regulatory functions (RD). The CARD domain, present in RIG-I and MDA5 but absent in LGP2, is required for interaction with MAVS and downstream signaling. CARD is involved in physical interaction with the CARD domain of MAVS The helicase domain contains six conserved DExD/H helicase motifs and is involved in translocation/unwinding of RNA and ATP hydrolysis required for RLR function. The helicase domain is also implicated in RNA binding for all three RLR members. The RD is required for recognition and binding of RNA substrates. This domain provides specificity for either 5'ppp containing RNA (RIG-I) or dsRNA (MDA5, LGP2).

### 1.6.3. RLR signalling pathway

The binding of viral RNA to the RLRs C-terminal domain induces an ATP-dependent conformational change of the receptor that results in the exposure of CARDs and initiation of downstream signalling cascade (Yoneyama & Fujita, 2009) (Figure 9). Upon RIG-I and MDA5 activation they may interact with the adaptor IPS-1 through the CARD repeats. IPS-1 itself is probably not directly involved in the signalling process but serves as a platform to orchestrate the molecular interactions, which will lead to the activation of IRF3 and NF-κB (Yoneyama et al, 2004). CARD proteins interaction trigger the recruitment of downstream signalling molecules that are involved in induction of type I IFN expression. In particular, IPS-1 associates with tumor necrosis factor (TNF) receptor-associated factor (TRAF) 3 leading to TBK1 and inhibitor of kB kinase (IkB) ε (IKKε) activation and subsequent IRF3 phosphorylation. Alternatively, IPS-1 recruits the adaptor Fas-associated death domain (FADD) and the kinases receptor- interacting protein 1 (RIP1) in order to trigger the NF-kB pathway. Upon activation, IRF3 and NF-kB translocate to the nucleus to drive type I IFN transcription and subsequent induction of the antiviral state (Yoneyama & Fujita, 2009).

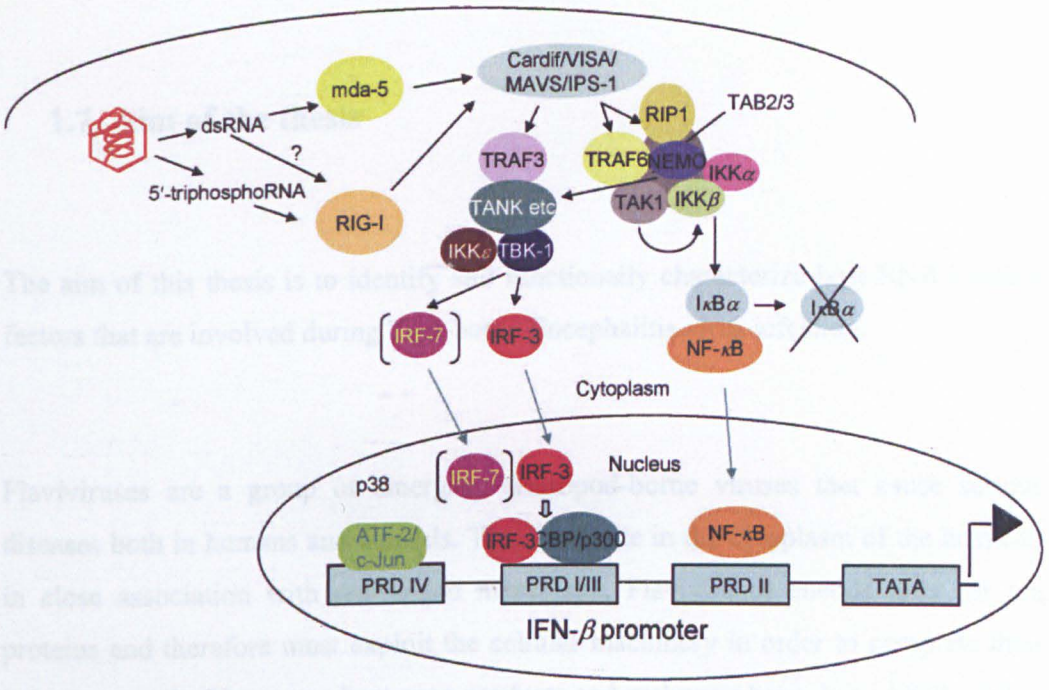


Figure 9: Signaling pathways activated by cytoplasmic helicases

Viral dsRNA in the cytoplasm is detected by one of two cytoplasmic helicases, MDA5 or RIG-I. RIG-I also detects 5′-triphosphate single-stranded RNA (ssRNA). IFNβ promoter stimulator 1 (IPS-1; also known as mitochondrial antiviral signalling protein (MAVs), virus-induced signalling adaptor (VISA) or caspase-recruitment domain (CARD) adaptor inducing IFNβ (CARDIF)) is a central target of both MDA5 and RIG-I. Through the recruitment of TRAF3, IPS-1 together with TANK and TBK1 activates IRF3. After IRF-3 activation, it translocate to the nucleus to act as transcription factor. Alternatively, during NF-κB activation, IPS-1 recruits RIP complex that phosphorylates IκB which in turn will be ubiquitinated and subsequently degraded. Active NF-κB translocates to the nucleus to act as transcription factor for the expression of IFNβ (Randall & Goodbourn, 2008)

## 1.7. Aim of the thesis

The aim of this thesis is to identify and functionally characterize host RNA binding factors that are involved during Tick-borne Encephalitis virus infection.

Flaviviruses are a group of emerging arthropod-borne viruses that cause serious diseases both in humans and animals. They replicate in the cytoplasm of the host cell in close association with rearranged membrane. Flaviviruses encode only for ten proteins and therefore must exploit the cellular machinery in order to complete their infectious cycle. Numerous host gene products and pathways have been implicated in the replicative cycle of flaviviruses but the biological relevance of many of these interactions is not yet clear.

In order to better understand host-TBEV interactions, I followed two approaches i) to functionally characterize RNA binding factors already identified in different contexts. ii) to design a sub-library of host genes that have been identified by RNAi screenings to conduct an RNAi screen using cell lines that recapitulate viral replication. The model flavivirus that will be exploited is TBEV for which a replicon-based visualization system has been developed in our laboratory (Miorin, 2008).

# 2. MATERIALS AND METHODS

## 2.1. Materials

### 2.1.1. Cells

Bacteria

- **Max Efficiency DH10B Competent Cells** (Invitrogen).
  Genotype: F- *mcr*A Δ(*mrr-hsd*RMS-*mcr*BC) φ80*lac*ZΔM15 Δ*lac*X74 *rec*A1 *end*A1 *ara*D139 Δ (*ara*, *leu*)7697 *gal*U *gal*K λ- *rps*L *nup*G /pMON14272 / pMON7124.
- **XL10-Gold Ultracompetent Cells** (Stratagene).
  Genotype: Tetr Δ(mcrA)183 Δ(mcrCB-hsdSMR-mrr)173 endA1 supE44 thi-1 recA1 gyrA96 relA1 lac Hte [F′ proAB lacIqZΔM15 Tn10 (Tetr) Tn5 (Kanr) Amy].

Mammalian Cells

- **BHK-21 (clone 13):** Baby hamster kidney cell line (ECACC No. 85011433).
- **U2OS:** Human osteosarcoma cell line (ECACC No. 92022711)
- **Vero:** African green monkey kidney (ECACC No. 84113001)
- **MEF WT:** Mouse embryonic fibroblast cells (Anderson laboratory, (Gilks et al, 2004)
- **MEF TIA-1** $^{-/-}$ : Mouse embryonic fibroblast cells TIA-1 depleted (Anderson laboratory, (Gilks et al, 2004)

### 2.1.2. Media

Bacteria

- **Luria-Bertani (LB) Medium:** 10 g bacto-trypton, 5 g bacto-yeast extract, 10 g NaCl per 1 liter medium. Ampicillin was added at a concentration of 50-100 μg/ml. For hardening 1.5 % agar-agar was added to the liquid medium.
- **SOC Medium:** is identical to Super Optimal Broth (SOB) medium (20 g bacto-trypton, 5 g bacto-yeast extract, 0.5 g NaCl per 1 liter medium), except that it contains 20 mM glucose.

- Mammalian Cells
- **DMEM complete medium:** Dulbecco's modified minimal essential medium (Gibco-Invotrogen) supplemented with antibiotic-antimycotic solution (Gibco-Invitrogen) and 10 % fetal calf serum (FCS, Gibco-Invitrogen). For selection G418 (Invitrogen) was added at a concentration of 0,8 mg/ml.
- **OptiMEM:** defined medium formulation with reduced serum (Gibco-Invitrogen)
- **Cryo medium:** for long-term storage, cells were frozen in liquid nitrogen in 90% FCS, 10 % DMSO.

### 2.1.3. Antibodies and antisera

Primary antibodies:

**Table 1: Primary antibodies used in this study**

| Reactivity | Species | Subtype | Source | Comments |
|---|---|---|---|---|
| TBEV-NS1 | Mouse | IgG Monoclonal | Dr. Connie Schmaljohn (Iacono-Connors et al, 1996) | 1:1000 WB |
| TBEV-polyprotein | Rabbit | Polyclonal | Dr. C.W. Mandl (Orlinger et al, 2006) | 1:100, IF |
| dsRNA J2 | Mouse | IgG Monoclonal | English & Scientific Consulting | 1:200, IF |
| TBEV-prM | Rabbit | Polyclonal | Kindly provided by Dr. Heinz, Medicine University, Vienna | 1:1000 WB |
| Human TIA-1 | Goat | Polyclonal | Santa Cruz | 1:200 IF 1:1000 WB |
| Human TIAR | Goat | Polyclonal | Santa Cruz | 1:200 IF 1:1000 WB |
| Human G3BP | Mouse | IgG Monoclonal | BD transduction laboratories | 1:100 IF |
| Human eIF2α | Rabbit | Polyclonal | Santa Cruz | 1:1000 WB |
| Human phospho-eIF2α(Ser51) | Rabbit | Polyclonal | Cell Signalling | 1:500 WB |
| GFP | Rabbit | Polyclonal | Molecular Probes, Invitrogen | 1:1000, WB |

| | | | | |
|---|---|---|---|---|
| Human RIG-I | Rabbit | Polyclonal | Kindly provided by Dr. Takashi Fujita, Kyoto University | 1:100 IF |

Secondary antibodies:

- Donkey anti-rabbit IgG, Alexa Fluor 594 (Molecular Probes); 1:500 for IF.
- Donkey anti-mouse IgG, Alexa Fluor 594 (Molecular Probes); 1:500 for IF.
- Donkey, anti-rabbit IgG, Alexa Fluor 488 (Molecular Probes); 1:500 for IF.
- Donkey, anti-goat IgG, Alexa Fluor 594 (Molecular Probes); 1:500 for IF.
- Goat polyclonal, anti-rabbit immunoglobulins/HRP (DakoCytomation); 1:10000 for WB.
- Rabbit polyclonal, anti-goat immunoglobulins/HRP (DakoCytomation); 1:10000 for WB.
- Rabbit polyclonal, anti-mouse immunoglobulins/HRP (DakoCytomation); 1:10000 for WB.
- Monoclonal Actin-HRP (Sigma) from dilution 1:50, use 1:1000

### 2.1.4. Vectors

**Table 2: Vectors used in this study**

| Plasmid | Relevant characteristics | Reference |
|---|---|---|
| pTNd/ΔME_EGFP | NS proteins,<br>IRES-EGFP | (Gehrke et al, 2005)<br>Figure 10 |
| 24xMS2 | Firefly luciferase,<br>NS proteins,<br>24xMS2 repeats | (Hoenninger et al, 2008)<br>Figure 10 |
| pTNd/ΔME_24xMS2 | NS proteins,<br>24xMS2 repeats | (Miorin et al, 2008)<br>Figure 15 |
| TBEV-LUC_NEO-EGFP | Firefly luciferase,<br>NS proteins,<br>Neomycin,<br>IRES-EGFP | Produced in this thesis<br>Figure 10 |
| pTNd/ΔME_GAA | NS proteins,<br>24xMS2 repeats,<br>NS5 mutated | (Miorin et al, 2008) |
| pCherry-MS2nls | $Amp^r$ | (Boireau et al, 2007) |
| pcDNA-MS2-EYFPnls | $Amp^r$ | (Boireau et al, 2007) |
| pEGFP-C1 | $Kan^r$ | Promega |
| pRL-CMV | $Amp^r$ | Promega |
| EGFP-TIA-1a | $Kana^r$ | (Izquierdo & Valcarcel, 2007) |

### 2.1.5. Oligonucleotides

**Table 3: Sequences of oligonucleotides used in this study**

The restriction sites contained in the primer sequence are underlined.

| Name | Sequence (5' to 3') |
|---|---|
| 5'NCRA1fw | GCGTTTGCTTCGGA |
| 5'NCRA1rv | CTCTTTCGACACTCGTCGAGG |
| 3'NCR-fw | TTGGCAGCTCTCTTCAGATTT |
| 3'NCR-rv | AGCGGGTGTTTTTCCGAGTC |
| BA1 | CATGTGCAAGGCCGGCTTCG |
| BA4 | GAAGGTGTGGTGCCAGATTT |
| IFNβ-fw | AGGACAGGATGAACTTTGAC |
| IFNβ-rv | TGATAGACATTAGCCAGGAG |
| MDA5-fw | GATTCAGGCACCATGGGAAGT |
| MDA5-rv | AGGCCTGAGCTGGAGTTCTG |
| RIG-I-fw | GACTGGACGTGGCAAAACAA |
| RIG-I-rv | TTGAATGCATCCAATATACACTTCTG |
| Neo-NotI-fw | CGAATGCGGCCGCTTATTGAACAAGATGGATTGC |
| Neo-NotI-rv | GTTTAGCGGCCGCAAGAAGAACTCGTCAAGAAGG |
| NotI-del-fw | GGAAAATCCCGGGCCCCGGCCGCTTGGAAGACG |
| NotI-del-rv | CGTCTTCCAAGCGGCCGGGGCCCGGGATTTTCC |
| U6-fw | GCTTCGGCAGGACATATACTAAAAT |
| U6-rv | CGCTTCACGAAT TTGCGTGTCAT |

### 2.1.6. RNAi experiment

**Table 4: siRNA oligos used in this study**

| siRNA name | siRNA sequence |
|---|---|
| ON-TARGET plus SmartPool DDX58 (RIG-I) | GCACAGAAGUGUAUAUUGG, CCACAACACUAGUAAACAA, CGGAUUAGCGACAAAUUUA, UCGAUGAGAUUGAGCAAGA |
| ON-TARGET plus SmartPool MDA5 | GAAUAACCCAUCACUAAUA, GCACGAGGAAUAAUCUUUA, UGACACAAUUCGAAUGAUA, CAAUGAGGCCCUACAAAUU |
| ON-TARGET plus SmartPool TIA-1 | UAUGAUAAAUCCCGUGCAA, CAACAAAUUGGCCAGUAUA, GACGGAAGAUAAUGGGUAA, GAUCUCAGCCCACAAAUUAA |
| ON-TARGET plus SmartPool TIAR | GGUGAACGGUACUACGAUU, CCAAUUGGGCCACUCGUAA, GAUAUGGUAUGGCAAGUUA, GGAAUUGCGUCUGGUUAA |

## 2.2.General Procedures

### 2.2.1. Cell culture

Monolayers of cells were grown at 37°C, 5 % $CO_2$ in DMEM complete medium. Cells were passaged after treatment with 0.05 % Trypsin – 0.02 % EDTA and seeded at the appropriate dilution. Upon electroporation cells were washed and seeded in medium without addition of antibiotic-antimycotic solution.

### 2.2.2. Plasmid construction

All plasmid constructs containing the cDNA of TBE Western subtype prototypic strain Neudoerfl were derived from pTNd/ΔME-EGFP (Gehrke et al, 2005).

The construct TBE-LUC-NEO_EGFP was generated in two steps i) adding the neomycin gene in frame with luciferase reporter gene from 24xMS (Hoenninger et al, 2008) and ii) transferring the luciferase-neomycin fusion genes into pTNd/ΔME-EGFP (Gehrke et al, 2005). The first step was achieved by performing a site directed mutagenesis in order to eliminate the second NotI site that was flanking TaV2A site in 24xMS consrtuct. For this purpose, the fragment SalI-ClaI from 24xMS was sub-cloned in pBluescript II KS+. The primers used for the mutagenesis of the second NotI by PCR are listed in table 3, Not-del primers. The approach was to insert the neomycin gene in the first NotI site between luciferase and Tav2A sequences. For this, the neomycin gene was amplified with specific primers with the NotI digestion sites flanking the gene (Neo-NotI primers in table 3) from pcDNA3.1 plasmid. The PCR fragments were digested with NotI. After confirmation by sequencing of the second NotI site mutated, the plasmid was linearized with NotI and ligated with NotI-neomycin-NotI. Next, the fragment was recovered through SalI-ClaI digestion and replaced into the SalI-ClaI digested pTNd/ΔME-EGFP to produce the final TBE-LUC-NEO_EGFP.

### 2.2.3. *In vitro* RNA transcription

Template DNA for *in vitro* transcription was prepared from large-scale preparations of plasmid DNA performed using QIAfilter Plasmid Maxi kit (Qiagen) according to the manufacturer's protocol. All the pTNd/ΔME-EGFP derivative plasmids were

linearized by digestion with NheI. After phenol-chloroform extraction and ethanol precipitation, the 5'-overhang was partially filled-in using Klenow polymerase (New England Biolabs) in the presence of 12.5 μM dCTP and dTTP at 25°C for 30 minutes. Linearized DNAs were again purified by phenol-chloroform extraction, precipitated with ethanol and washed with 70 % ethanol. The pellet was then resuspended with RNase-free water and 500 ng of template were transcribed using the T7 MEGAscript kit (Ambion). The transcription reaction contained 7.5 mM each of ATP, CTP and UTP, 1.5 mM GTP and 1 mM cap analogue ($m^7G(5')ppp(5')G$; Ambion). The reaction mixture (20 μl) was incubated for 3 hours at 37°C. At the end of the reaction, 2U of TURBO DNase (Ambion) were added and the mix was incubated for 15 minutes at 37°C to remove the template DNA. RNA was purified using the RNeasy Mini kit (Qiagen). The RNA was eluted in RNase free water and the integrity of the *in vitro* transcripts was confirmed by denaturing agarose gel electrophoresis. The yield of RNA was determined by absorbance at 260 nm.

### 2.2.4. RNA transfection by electroporation

Single cell suspensions were prepared by trypsinization of monolayers and subsequent resuspension with DMEM complete medium. Cells were then washed in ice-cold PBS and counted. Aliquots of 5 x $10^6$ cells were resuspended in 500 μl ice-cold phosphate buffered saline (PBS) and were mixed in a 0.4 cm Gene Pulser cuvette with 10 μg of RNA and 5-10 μg of plasmid DNA when required. Cells were electroporated with a Bio-Rad Gene Pulser apparatus applying either two subsequent pulses at 0.25 KV, 500 μF (for BHK-21 cells) or one single pulse at 0.25 KV, 960 μF (for U2OS cells, MEF WT and MEF TIA-1 cells). After electroporation cells were washed three times in DMEM complete without antibiotic-antimycotic solution and seeded in the same medium.

### 2.2.5. Indirect Immunofluorescence analysis

Expression of viral proteins was determined by immunofluorescence (IF) staining with a polyclonal rabbit anti-TBEV serum that can be used for both structural and non-structural protein detection (Orlinger et al, 2006). The J2 mouse monoclonal anti-dsRNA antibody (English & Scientific Consulting, Szirak, Hungary) was used to detect the replication complexes.

In general, cells were seeded into 6-wells plates containing microscope coverslips and supplied with complete growth medium to be confluent at the time of fixation. For IF analysis cells were washed three times with PBS and fixed in 3.7 % paraformaldehyde (PFA) solution for 15 minutes at room temperature (RT). Thereafter, cells were again washed three times with PBS and incubated 5 minutes with 100 mM glycine in order to saturate excesses of PFA and to stop the fixation reaction. For permeabilization, cells were incubated for 5 minutes with 0.1 % Triton X-100 in PBS and washed three times. Before incubation with antibodies, a blocking step was performed at 37°C for 30 minutes with PBS, 1 % bovine serum albumin (BSA) and 0.1 % Tween 20 (blocking solution). Primary antibodies were diluted to the desired concentration in blocking solution to prevent aspecific binding of the antibodies. After one hour incubation at 37°C, or overnight (O/N) incubation at 4°C, coverslips were rinsed three times with PBS 0.1 % Tween 20 (washing solution) and incubated with secondary antibodies for 45 minutes at 37°C. Coverslips were finally washed three times with washing solution and mounted on slides using Vectashield mounting medium with addition of DAPI (Vector Laboratories).

In order to detect endogenous RIG-I intracellular localization, U2OS cells were fixed and permeabilized as previously described. The blocking was instead performed at 37°C for 1 hour with PBS, 0.5 % BSA and 0.04 % Tween 20 following Dr. Takashi Fujita protocol (Onomoto et al, 2012). Cells were next incubated O/N at 4°C with the anti RIG-I antibody diluted in the blocking solution described above, washed twice for 20 minutes at RT with PBS 0.04 % Tween 20 and finally incubated with the secondary antibody for 45 minutes at 37°C with the same blocking solution used before. After two washes at RT for 20 minutes, coverslips were mounted on slides as already described.

### 2.2.6. Flow cytometry analysis

For the analysis of MS2-EYFP expression, 24 hours after transfection, cell monolayers were treated with 0.05 % Trypsin – 0.02 % EDTA to prepare single cell suspensions. Cells were then washed twice with PBS, were resuspended with 300 - 500 µl PBS and analyzed immediately by flow cytometry using a FACSCalibur apparatus (Becton Dickinson) and the Cell Quest Pro software. The same procedure was performed to analyze EGFP-TIA cell line.

### 2.2.7. Transfection of U2OS cells with Lipofectamine LTX

Plasmid DNAs, Poly(I:C) (InvivoGen) were delivered into U2OS cells using Lipofectamine LTX (Invitrogen) according to the manufacturer's instructions.

### 2.2.8. Luciferase assay

In order to assess the effect of TIA-1 depletion on TBEV translation and replication, a Beetle-Juice and Renilla-Juice (p.j.k.) was used according to the manufacturer's instructions to simultaneously measure both firefly and Renilla luciferase activity. After electroporation of MEF WT and MEF TIA-1 KO cells with RNA and/or DNA, cells were washed once with growth medium without phenol red and counted. A maximum of 60,000 cells were seeded onto 96-well plates (Perkin Elmer), and triplicate wells were lysed at individual time points, followed by measurement with the Envision Multimode Plate Reader (Perkin Elmer). The primary data are given in relative light units (RLUs). For normalization of the firefly luciferase values, replicon RNA containing the firefly luciferase gene was cotransfected with either 3 μg of RNA that had been transcribed *in vitro* from phRL-CMV (encoding Renilla luciferase) as a standard for the early time points (4 hours), or 5 μg of phRL-CMV DNA for later time points (13-48 hours). In addition, a separate "control standard" consisting of MEF cells transfected with the control nucleic acid alone was included in each experiment, and the mean value of the Renilla luciferase activity of these cells was determined at each time point. The ratio of the uncorrected luciferase activity measured for the RNA versus the DNA controls differed less than two-fold between individual transfection experiments indicating that only little variability was introduced due to the usage of two different controls within a single time course experiment. The same electroporation conditions were used for DNA and RNA samples and yielded consistently high efficiencies between 50 and almost 100 % of the transfected cells as determined by immunofluorescence or flow cytometry. To calculate the normalized firefly luciferase activity, the measured Renilla luciferase activity from each cotransfected sample was divided by the corresponding control standard value to obtain a normalization factor by which the measured firefly luciferase value of that well was divided. To correct for variability between different plates, the control standards from each plate were normalized to a single standard to

obtain a factor by which the firefly luciferase values for that plate were then multiplied. In this way, corrections could be made for differences in transfection efficiency as well as total cell count at different time points. The corrected data are presented as "normalized RLUs" (Hoenninger et al, 2008).

To monitor TBE-LUC-NEO_EGFP replication over 7 days, U2OS and BHK-21 cells were seeded on 6-well plates, grown and lysed at individual time points, followed by measurement with the Envision Multimode Plate Reader (Perkin Elmer). For normalization, replicon was cotransfected with 5 μg of phRL-CMV DNA as described above.

### 2.2.9. RNA Interference

Pools of siRNAs were obtained from Dharmacon: DDX58, MDA5, TIAR, TIA-1 and siGENOME Non-Targeting siRNA Pool #3. Human U2OS cells were transfected with siRNAs at the concentration of 100nM and with HiPerFect Transfection Reagent (Qiagen) according to manufacturer's instructions. After siRNA transfection cells were incubated at 37°C for 48 h, and then infected with Hypr TBEV at a MOI of 2. According to the different experiments, total RNA was collected at different time points after transfection for further analysis.

### 2.2.10 Real-time quantitative reverse transcription PCR (qRT-PCR)

Total cellular RNA was extracted by using Trizol (Invitrogen) according to the manufacturer's instructions, treated with DNase I (Invitrogen) and then quantified. Aliquots of 600 ng were used as a template to synthesize cDNA using random primers (Invitrogen) and M-MLV Reverse Transcriptase (Invitrogen) according to manufacturer's protocol. Real-time quantitative PCR using iQ SYBR Green Supermix (Bio-Rad) was performed from cDNA samples. Signals of inducible cellular mRNAs or viral RNAs were normalized to the β-actin mRNA signal.

The sequences of oligonucleotides used for this analysis are reported in table 3. Amplification and detection were carried out on a CFX96 Real Time System (Bio-Rad).

### 2.2.11 RNA-TIA-1 co-immunoprecipitation assay

Immunoprecipitations (IPs) were performed using the TIA-1 antibody (Santa Cruz, sc: 1751). Briefly, U2OS cells were lysed with RIPA buffer (50 mM Tris pH 7.4, 150 mM NaCl, 1% NP-40, 0.1% SDS, 1 mM EDTA, RNAse inhibitor, protease inhibitor) and the cellular extracts were incubated for 4 hours with the TIA-1 antibody coupled to A/G PLUS agarose beads (Santa Cruz, sc-2003) at 4°C under rotation. IPs were spun down and washed six times in PBS for 5 minutes at 4°C. Subsequently the beads were resuspended in buffer (50 mM Tris pH 7.5, 5 mM EDTA, 10 mM DTT, 1% SDS) for further analysis of RNA extraction and western blot.

### 2.2.12 Western blot analysis

Whole cell lysates were resolved by SDS–polyacrylamide gel electrophoresis (SDS-PAGE). For Western blotting, nitrocellulose membrane (Reinforced NC, Whatman) was used and membranes were blocked for 1 hour in 4% milk followed by incubation with the appropriate primary antibodies diluted in 4% milk / 0,5% Tween-20 at 4°C O/N. After three washing with TBS 0.5% Tween-20 secondary antibodies conjugated with HRP (DakoCytomation) were diluted in 4% milk / 0,5% Tween-20 and incubated for 1 hour. Blots were developed using Immobilon Western Chemiluminescent HRP Substrate (Millipore) according to manufacturer's instructions.

## 2.3 Working with viruses

### 2.3.1 Preparation of TBEV stocks

Viral stocks were prepared by infection of Vero cells at a low multiplicity. The TBEV strain Hypr was used for these studies. After cytopathic effect (CPE) was observed, cell culture supernatant was collected, clarified by centrifugation, supplemented with 20 % FBS, and stored in aliquots at -80°C. Viral titres were determined by using a plaque-forming assay. Vero cells were seeded into 24-well dishes till monolayer was formed and infected with a 10-fold serial dilution of TBEV in a total volume of 200 µl of serum-free medium. After 1 hour incubation at 37°C with 5 % $CO_2$, the inoculum was removed and a 500 µl overlay containing 1 volume of 6%

carboxymethyl cellulose (CMC) to 1 volume of maintenance medium (DMEM supplemented with 4 % FCS) was added. The plates were incubated for 5 days before fixation with 4 % PFA dissolved in PBS. Infected cells were stained adding 300 µl of crystal violet solution in 80 % methanol / 20 % PBS. After 30 minutes the staining solution was removed and cells were washed 3-4 times with water. The titre of the virus was determined by counting the number of plaques produced at each dilution.

### 2.3.2 TBEV infection of cells

For standard infection assays, U2OS cells were seeded at a density of 1.3 x $10^5$ per well of a 12-well plate. 24 hours after, cells were infected at the appropriate MOI by adding 500 µl of virus stock properly diluted in serum-free medium. After 1 hour incubation at 37°C with 5 % $CO_2$, the inoculum was replaced with maintenance medium (DMEM supplemented with 4 % FCS). Cells were then harvested at the appropriate time point.

### 2.3.3 Measurement of Virus titre

In order to address the virus titre from TIA-1/TIAR depletion experiments, 10-fold serial dilutions of the supernatants collected from each time point were performed. Monolayer of Vero cells were seeded in a 24-well plate and infected with the different dilutions. The rest of the protocol is as described in section 2.3.1

## 2.4 Microscopy and image acquisition.

### 2.4.1 Imaging of fixed cells

Fluorescent images of fixed cells were captured with the LSM 510 META confocal microscope (Carl Zeiss Microimaging, Inc.).

The LSM 510 META confocal microscope was equipped with a 63× NA 1.4 Plan-Apochromat oil objective. The pinhole of the microscope was adjusted to get an optical slice of less than 1.0 µm for any wavelength acquired. MS2-EYFP was excited with the 488 nm line of the Ar laser and its emission was monitored using a custom-made Meta band pass filter between 510 and 563 nm. The Alexa594 (Molecular Probes) and Cy3 (Molecular Probes) fluorophores as well as the Cherry variant of the MS2 tagged protein were excited with the 543 nm HeNe laser and their emission

collected using a custom-made Meta band pass filter between 552 and 670 nm. Online emission fingerprinting was performed for the simultaneous acquisition of MS2-EYFP and EGFP. Previously acquired emission spectra of cells transfected only with EGFP or MS2-EYFP, both excited with the 488 nm laser line, were used as standards for the linear unmixing algoritm of the LSM510 META software.

# 3. RESULTS

## 3.1. Development of a robust cell line that recapitulates specific steps of TBEV RNA biogenesis for screening

### 3.1.1 Generation of a TBEV replicon suitable for obtaining a stable cell line

RNAi screening is a valuable tool for identifying host factors involved in the flaviviral life cycle. A number of siRNA screenings for flaviviruses has been performed. In these studies different viral systems have been used such as infectious viruses and sub-genomic replicon cell lines. Although the results obtained working with infectious viruses can be translated to physiological conditions it is more difficult to discriminate which step of the viral life cycle is affected. On the other hand, sub-genomic replicon cell lines are suitable for the study of specific steps of the viral life cycle. In order to obtain a robust and reproducible cell line that recapitulates viral replication I took advantage of a well-characterized TBEV subgenomic replicon previously described by Mandl and co-workers as well as our laboratory (Hoenninger et al, 2008; Miorin et al, 2008). Using as template two different constructs I generated a bi-cistronic replicon system, which contains the firefly luciferase reporter gene in-frame with the neomycin resistance gene for drug selection generating a fusion protein that has been shown to be successful for these type of studies (Tai et al, 2009). An IRES-GFP cassette was located at the 3'NCR of the replicon. The replicon is based on the Neudoerfl TBEV strain where the regions encoding for capsid, prM/M and envelope structural proteins were deleted. TBEV-24xMS2 is the replicon that I used to insert the neomycin gene. The construct is formed by the natural translation initiation site of the viral polyprotein together with the first 17 aminoacids of a capsid protein fused to the firefly luciferase reporter gene. Moreover, this replicon contains the elements needed for RNA replication: 5'NCR, non-structural proteins and a modified 3'NCR in which the variable region carries an array of 24 MS2 binding sites (Hoenninger et al, 2008). After inserting the neomycin gene in-frame with the firefly luciferase gene the 5'NCR-f-luciferase-neomycin fragment was removed and inserted in a second TBEV-based pTNd/ΔME-EGFP expression vector (Gehrke et al, 2005). Figure 10 shows a schematic representation of constructs mentioned before.

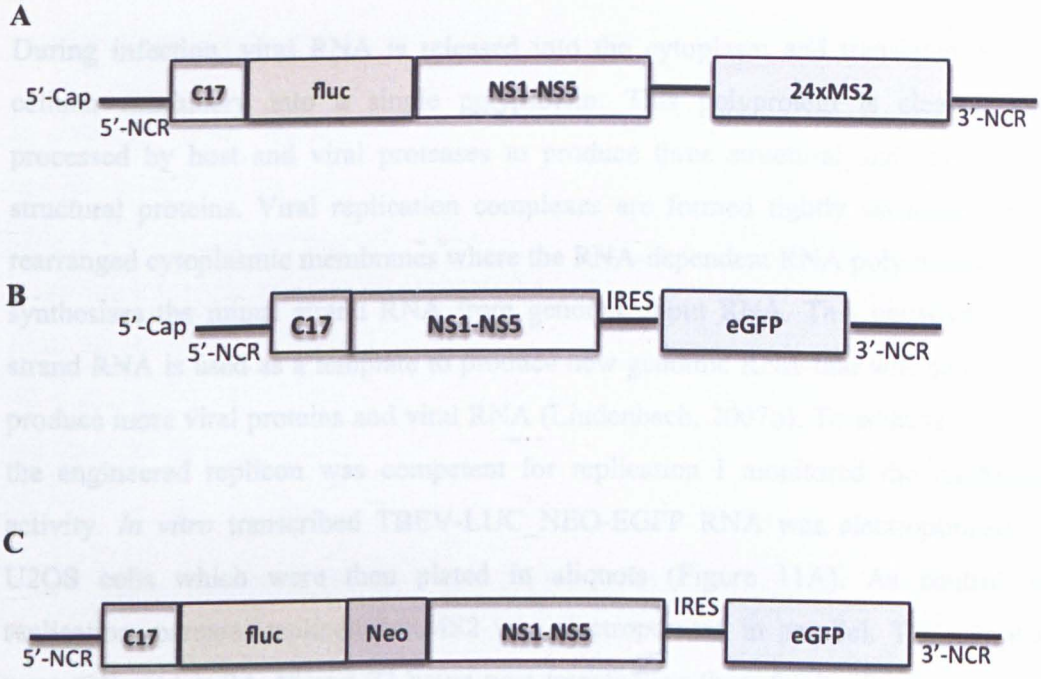


**Figure 10: Schematic representation of TBEV constructs**

The rectangles show the main parts of the replicon. A) The *in vitro* transcribed RNA is 5' capped, contains the first seventeen aminoacids of capsid protein (C) whereas the rest of the structural proteins have been deleted and replaced by the firefly luciferase reporter gene. In the variable region of 3'NCR an array of biding sites for bacteriophage MS2 coat protein (24xMS2) is localized (Hoenninger et al, 2008). B) The second construct used for cloning consists of the first seventeen aminoacids of capsid protein (Gehrke et al, 2005) (C) and the structural proteins have been deleted. In the variable region of the 3'NCR, there is an EMCV IRES-eGFP reporter expression cassette. C) TBEV-LUC_NEO-EGFP replicon. It contains the first seventeen aminoacids of capsid protein (C) followed by firefly luciferase reporter gene in frame with selectable marker neomycin gene. In the variable region of 3'NCR there is an IRES-eGFP expression reporter cassette.

### 3.1.1. Characterization of TBE-Neo replicon in human cells

Luciferase reporter gene

During infection, viral RNA is released into the cytoplasm and translated by the cellular machinery into a single polyprotein. This polyprotein is cleaved and processed by host and viral proteases to produce three structural and seven non-structural proteins. Viral replication complexes are formed tightly associated with rearranged cytoplasmic membranes where the RNA-dependent RNA polymerase NS5 synthesises the minus strand RNA from genomic input RNA. This negative sense strand RNA is used as a template to produce new genomic RNA that will be used to produce more viral proteins and viral RNA (Lindenbach, 2007b). To address whether the engineered replicon was competent for replication I monitored the luciferase activity. *In vitro* transcribed TBEV-LUC_NEO-EGFP RNA was electroporated in U2OS cells which were then plated in aliquots (Figure 11A). As control of replication, parental replicon 24xMS2 was electroporated in parallel. The samples were collected at 24, 48 and 72 hours post transfection (hpt) for luciferase analysis. As shown in figure 11B, enzyme activity derived from TBE-LUC_NEO-EGFP was increased with time. Renilla luciferase plasmid was co-transfected as internal control in order to normalize firefly luciferase values. This data indicates that TBE-LUC_NEO-EGFP is replicating efficiently in human U2OS cells.

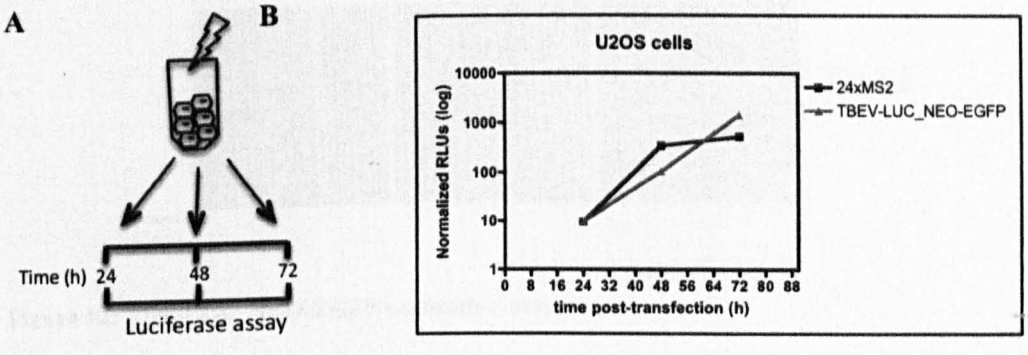


**Figure 11: Time course of TBEV RNA replication**

**A)** Schematic diagram of the experimental design. After electroporation of U2OS cells with TBEV-LUC_NEO-EGFP and renilla luciferace control plasmid, equal amount of cells were seeded into dishes. The same procedure was done in parallel with the 24xMS2 replicon as postive control of

replication. Transfected cells were harvested at the indicated time points. **B)** Kinetics of luciferase reporter expression in U2OS cells transfected with TBEV-LUC_NEO-EGFP replicon RNA (grey curve) and parental replicon 24xMS2 (black curve), shown in logarithmic scale.

## Non-structural viral proteins and EGFP expression

In order to further characterize the TBE-LUC_NEO-EGFP replicon, expression of non-structural proteins was assessed by using a specific antibody. For this aim, U2OS cells were electroporated with TBE-LUC_NEO-EGFP RNA and plated. Cellular localization of viral non-structural proteins as well as the expression of EGFP cassette from the replicon was studied over time. From the Figure 12, the expression of both non-structural proteins and EGFP are increased with time. Together, these results indicate that TBE-LUC-NEO_EGFP replicated in U2OS cell line.

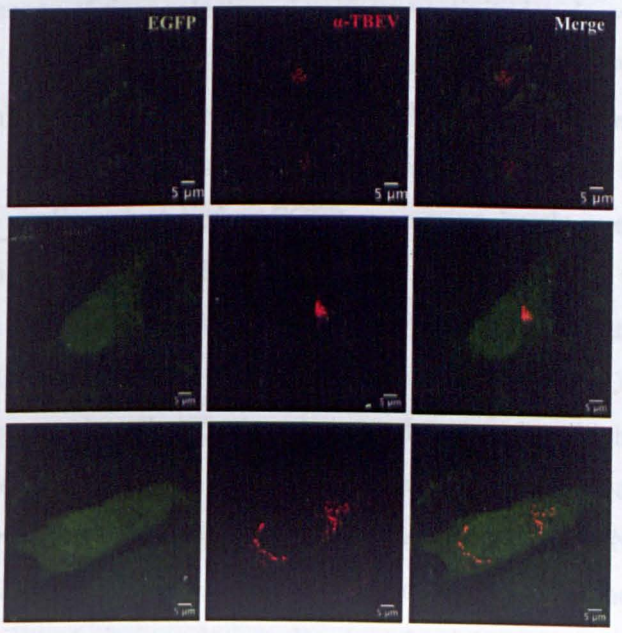


**Figure 12: TBE-LUC_NEO-EGFP replication over time**

Confocal images of U2OS cells electroporated with the TBE-LUC_NEO-EGFP replicon. After the indicated time points (hours post transfection) cells were fixed and incubated with an antiserum used against TBEV viral proteins (middle panel, red). EGFP expression is shown in the first panel (green)

### 3.1.2. Generation of a stable cell line supporting autonomous replication of TBE-LUC_NEO-EGFP

TBE-LUC-NEO_EGFP replication in U2OS cells

Having established that TBE-LUC-NEO_EGFP replicated transiently in U2OS cells, replicon RNA was introduced in U2OS cells. 24 hours post transfection cells were exposed to G418 antibiotic. After three days under drug selection a massive cell death was observed. Therefore I hypothesized that due to the low rate of viral replication neomycin expression levels were not high enough to keep the cells alive at the used drug concentration. For this reason, different G418 concentrations were used between 0,2-1 mg/ml but no changes in cell survival were obtained. In order to understand if viral replication was maintained for longer time points and in how many cells this was occurring I decided to monitor GFP expression and the luciferase activity over seven days in the absence of drug selection. Luciferase activity levels were indicating active replication of TBE-LUC_NEO-EGFP over time (Figure 13A). Flow cytometry analysis was showing a reduced number of cells containing the replicon over time (Figure 13B). Another observation from this experiment was that cells that were containing the replicon had higher EGFP expression levels over time. Due to this latter observation G418 was added at different time points post transfection without changes in the cellular survival rate. Altogether, this data indicates that even though TBE-LUC_NEO-EGFP replicon is replicating efficiently in U2OS cells, the number of cells that supported replication was decreased during time in the absence of G418. One possible idea is that these cells have a strong cellular response against viruses since it has been shown they are able to respond to known IFN response inducers (Miorin et al, 2012). Therefore, I tried to obtain a stable cell line by using BHK-21 cells which are permissive to virus replication since they do not produce IFN (Nagai et al, 1981).

A

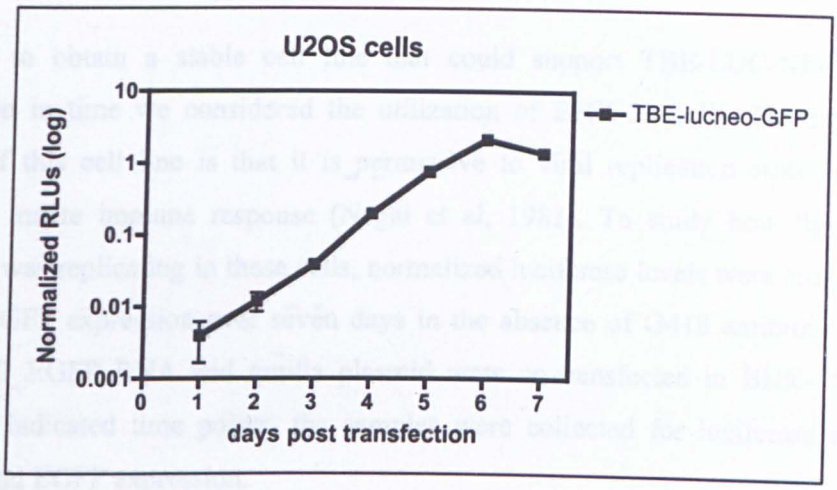


B

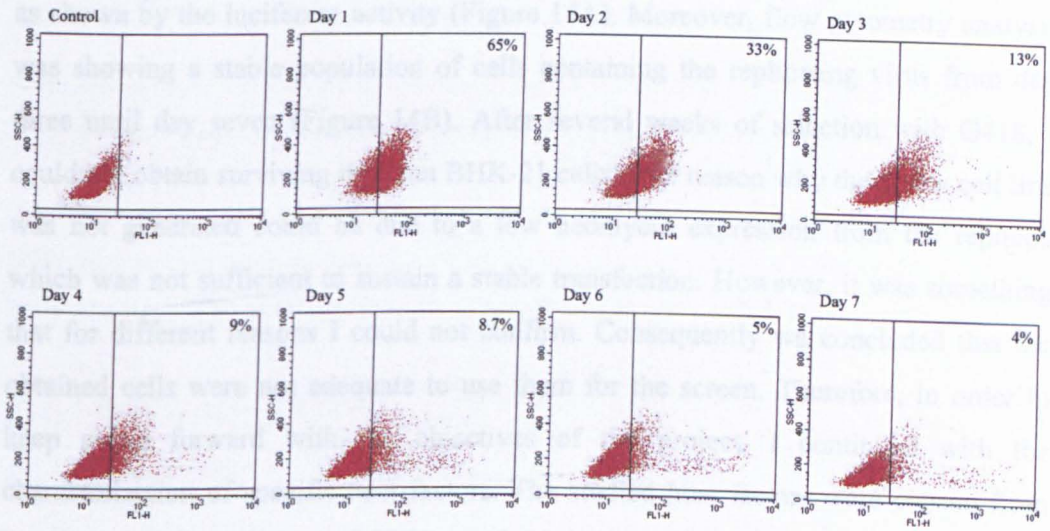


**Figure 13: TBEV-LUC_NEO-EGFP replication in U2OS cells**

Characterization of TBE-LUC_NEO-EGFP replication in U2OS cells without drug selection. A) Luciferase activity assay of U2OS cells transfected with the TBE-LUC_NEO-EGFP replicon over seven days. B) Cytofluorimetric analysis conducted in replicon U2OS cells. As shown in the graph, the percentage of eGFP positive cells is decreasing upon time. The first panel corresponds to mock transfected cells. Data were averaged from three independent experiments and are represented as mean ± standard deviation.

TBE-LUC-NEO_EGFP replication in BHK-21 cells

In order to obtain a stable cell line that could support TBE-LUC-NEO_EGFP replication in time we considered the utilization of BHK-21 cells. The important feature of this cell line is that it is permissive to viral replication since it has a defective innate immune response (Nagai et al, 1981). To study how the TBEV construct was replicating in these cells, normalized luciferase levels were analyzed as well as EGFP expression over seven days in the absence of G418 antibiotic. TBE-LUC-NEO_EGFP RNA and renilla plasmid were co-transfected in BHK-21 cells. After the indicated time points, the samples were collected for luciferase activity analysis and EGFP expression.

TBE-LUC-NEO_EGFP replication was well supported in BHK-21 cells during time as shown by the luciferase activity (Figure 14A). Moreover, flow cytometry analysis was showing a stable population of cells containing the replicating virus from day three until day seven (Figure 14B). After several weeks of selection with G418, I could not obtain surviving replicon BHK-21 cells. One reason why the stable cell line was not generated could be due to a low neomycin expression from the replicon which was not sufficient to sustain a stable transfection. However, it was something that for different reasons I could not confirm. Consequently we concluded that the obtained cells were not adequate to use them for the screen. Therefore, in order to keep going forward with the objectives of the project, I continued with the characterization of specific host factors. The studied host factors were chosen from literature for their role in viral RNA metabolism.

A

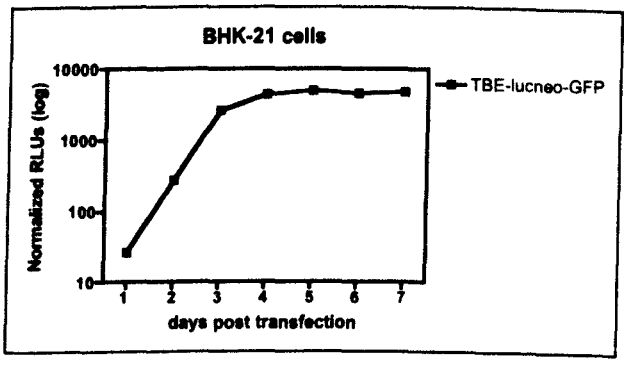

**B**

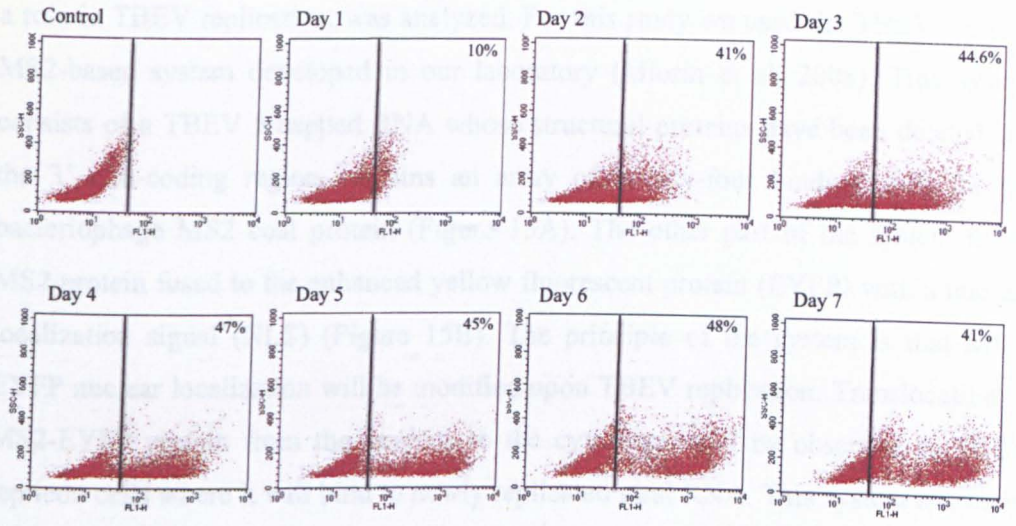


**Figure 14: TBEV-LUC_NEO-EGFP replication in BHK-21 cells**

Characterization of the TBE-LUC_NEO-EGFP replication in BHK-21 cells. A) Luciferase activity assay of cells transfected with TBE-LUC_NEO-EGFP replicon over seven days. Data were averaged from three independent experiments and are represented as mean ± standard deviation. B) Cytofluorimetric analysis conducted of GFP BHK-21 cells. As shown in the graph, the percentage of EGFP positive cells increases from day one to day two and then there is a stable population of cells expressing the reporter gene. The first panel corresponds to the mock transfected cells.

## 3.2. Characterization of Host RNA-binding proteins during TBEV replication

As mentioned before, the flavivirus genome is composed by a positive-polarity single strand-RNA, which needs to be translated by the cellular machinery. A polyprotein is produced that contains only ten proteins from which seven will be part of replication complexes. Viral replication occurs in virus-induced host cell membranes, which serve as a scaffold for replication complexes. Viral RNA, viral proteins and possibly cellular proteins compose these replication complexes. Different host factors have been found to regulate flaviviral replication but the functional relevance of these events is still unknown. In order to study the possible role of determined RNA-binding proteins in viral replication we performed immunofluorescence and over-

expression analysis. A battery of host proteins, which are possible candidates to have a role in TBEV replication, was analyzed. For this study we used the TBEV replicon MS2-based system developed in our laboratory (Miorin et al, 2008). This system consists of a TBEV 5'capped RNA whose structural proteins have been deleted and the 3' non-coding region contains an array of twenty-four binding sites for the bacteriophage MS2 coat protein (Figure 15A). The other part of the system is the MS2 protein fused to the enhanced yellow fluorescent protein (EYFP) with a nuclear localization signal (NLS) (Figure 15B). The principle of the system is that MS2-EYFP nuclear localization will be modified upon TBEV replication. Translocation of MS2-EYFP protein from the nucleus to the cytoplasm will be observed in TBEV replicon cells where it will bind to newly replicated viral RNA. This system allows us to detect TBEV replicating RNAs by fluorescence microscopy. As a control we used a TBEV replicon (pTNd/ΔME_GAA) that contains the GDD to GAA mutation in the catalytic domain of the NS5 protein, which does not allow viral replication.

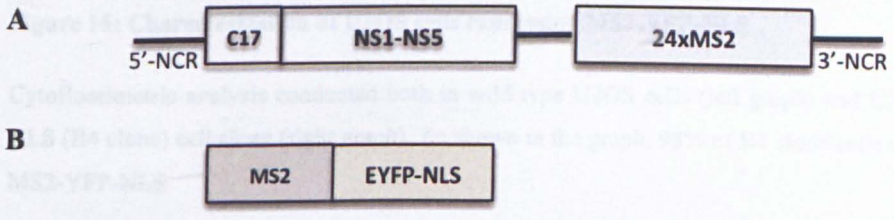


**Figure 15: TBEV replicon system used for the microscopy analysis**

The rectangles show the main parts of the constructs. A) The *in vitro* transcribed RNA is 5' capped, contains the first seventeen aminoacids of capsid protein (C) whereas the rest of the structural proteins have been deleted. In the variable region of 3'NCR an array of biding sites for the bacteriophage MS2 coat protein (24xMS2) is localized. B) The MS2-EYFP fusion protein

### 3.2.1. Development of human stable cell lines expressing MS2-EYFP-NLS

The variability in the efficiencies of transfection of the constructs was reducing the number of cells that could be studied. Therefore, in order to have an homogenous cell line expressing MS2-EYFP-NLS for the analysis of host factors, a stable U2OS cell line expressing the fusion protein was established. Upon transfection with MS2-EYFP-NLS plasmid, U2OS cells were grown in the presence of G418. Isolated clones

were expanded and characterized. U2OS clone B4-MS2-EYFP-NLS was used for the analysis of host factors since it was showing high percentage of EYFP positive cells both by flow cytometry (Figure 16) and by fluorescence analysis (data not shown).

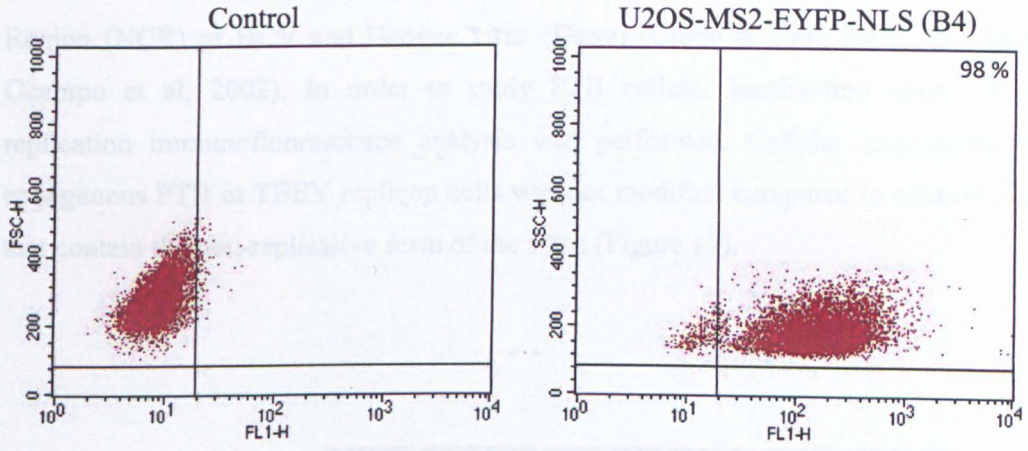


**Figure 16: Characterization of U2OS cells expressing MS2-YFP-NLS**

Cytofluorimetric analysis conducted both in wild type U2OS cells (left graph) and U2OS-MS2-YFP-NLS (B4 clone) cell clone (right graph). As shown in the graph, 98% of B4 clone cells were expressing MS2-YFP-NLS

### 3.2.2. Study of cellular localization of RNA binding proteins in TBEV replicon cells

For the study of the cellular localization of host factors in TBEV replicon cells, I used specific antibodies for some of them which are organized in section 3.2.2.1 and for other factors I used the corresponding plasmids that are located in section 3.2.2.2

3.2.2.1 Endogenous protein analysis

In order to understand the role of determined RNA binding proteins in TBEV replication, an immunofluorescence experiment was performed. U2OS cell line-expressing MS2-EYFP-NLS was electroporated with pTNd/ΔME_24xMS2 and control replicon pTNd/ΔME_GAA. The host proteins studied by this approach were PTB, TIA-1 and RIG-I.

The Polypirimidine Tract Binding (PTB) protein is an RNA binding protein, which shuttles between the nucleus and the cytoplasm. In the nucleus, it has a role in

alternative pre-mRNA splicing (Wagner & Garcia-Blanco, 2001). PTB was clearly important for hepatitis C virus (HCV) replication. In Huh7 cells (a human hepatocyte cell line) transfected with the HCV replicon, the endogenous PTB goes from the nucleus to the cytoplasm, where it co-localizes with the viral NS5B protein (Domitrovich et al, 2005). *In vitro* studies shows that PTB binds to 3'-Non-Coding Region (NCR) of HCV and Dengue virus (Denv) (Clerte & Hall, 2006; De Nova-Ocampo et al, 2002). In order to study PTB cellular localization upon TBEV replication immunofluorescence analysis was performed. Cellular localization of endogenous PTB in TBEV replicon cells was not modified compared to control cells that contain the non-replicative form of the virus (Figure 17).

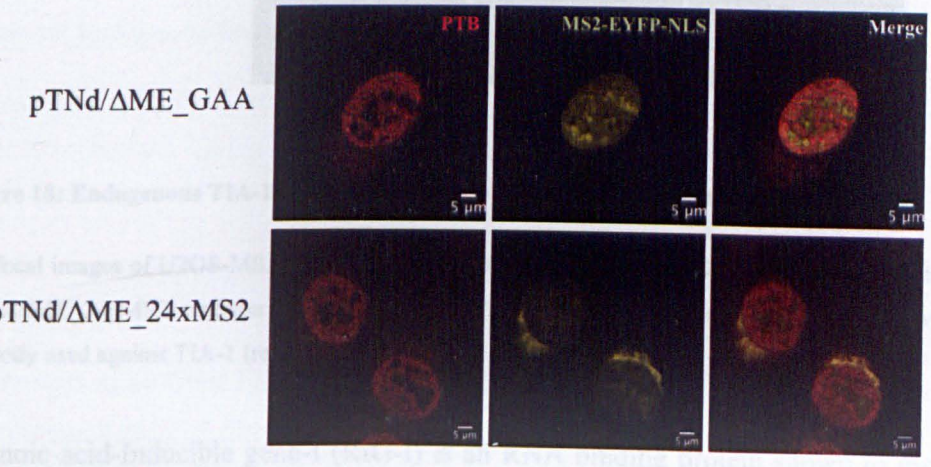


**Figure 17: Endogenous PTB cellular localization in TBEV replicon cells**

Confocal images of U2OS-MS2-YFP-NLS cells electroporated with pTNd/ΔME_GAA (first row) and pTNd/ΔME_24xMS2 replicon (second row). After 24h.p.t cells were fixed and incubated with an antiserum used against PTB (red).

T-Cell Intracellular Antigen-1 (TIA-1) is an RNA binding protein involved in RNA metabolism. In the nucleus, it is implicated in alternative pre-mRNA splicing and in the cytoplasm as a negative regulator of translation (Izquierdo et al, 2005; Kedersha et al, 1999; Piecyk et al, 2000). TIA-1 has been shown to bind 3'NCR of West Nile virus (WNV) and the protein co-localizes at sites of WNV replication

(Emara & Brinton, 2007; Li et al, 2002). In order to study TIA-1 cellular localization upon TBEV replication U2OS MS2-EYFP-NLS cells were electroporated. In cells transfected with pTNd/ΔME_24xMS2, TIA-1 was accumulating in the perinuclear region of the cytoplasm and colocalizing with MS2-EYFP tagged viral RNA (Figure 18). pTNd/ΔME_GAA control cells were showing normal TIA-1 cellular localization.

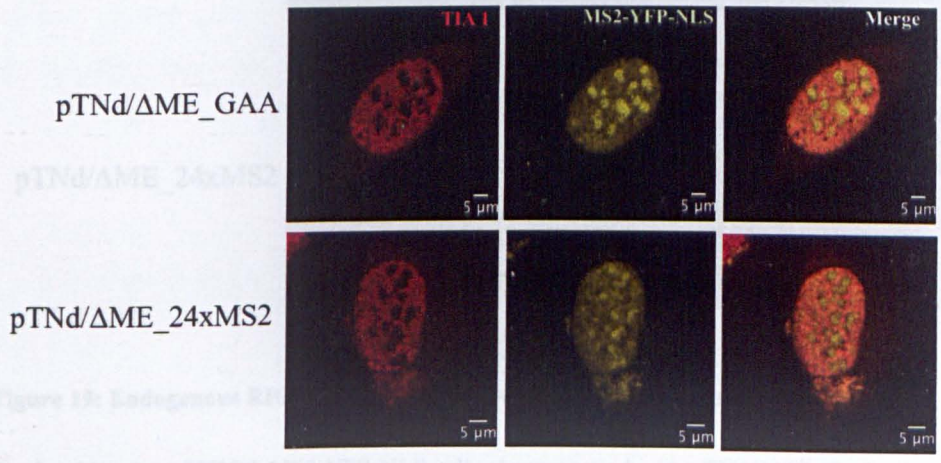


**Figure 18: Endogenous TIA-1 cellular localization in TBEV replicon cells**

Confocal images of U2OS-MS2-YFP-NLS cells electroporated with pTNd/ΔME_GAA (first row) and pTNd/ΔME_24xMS2 replicon (second row). After 24h.p.t cells were fixed and incubated with an antibody used against TIA-1 (red).

Retinoic acid-Inducible gene-I (RIG-I) is an RNA binding protein shown to mediate intracellular response to viral RNA. RIG-I consists of a C-terminal DExD/H box RNA helicase domain and two N-terminal caspase recruitment domains (CARD). Binding of dsRNA to the helicase domain of RIG-I is postulated to induce conformational changes that allow its interaction with downstream effector molecules via the CARD domain (Takahasi et al, 2008). These interactions initiate a signaling cascade that results in the expression of interferon (IFN)(Yoneyama et al, 2004). With the objective to test RIG-I cellular localization upon TBEV replication, I performed immunofluorescence analysis using a specific antibody that recognizes the C-terminal domain of RIG-I. In these experiments we could observe a speckle-like re-distribution of the protein in the cytoplasm of U2OS containing pTNd/ΔME_24xMS2 replicon (Figure 19) while control pTNd/ΔME_GAA cells, RIG-I was dispersed throughout

the cell. Moreover these sites of RIG-I accumulation were distinct from sites of viral replication.

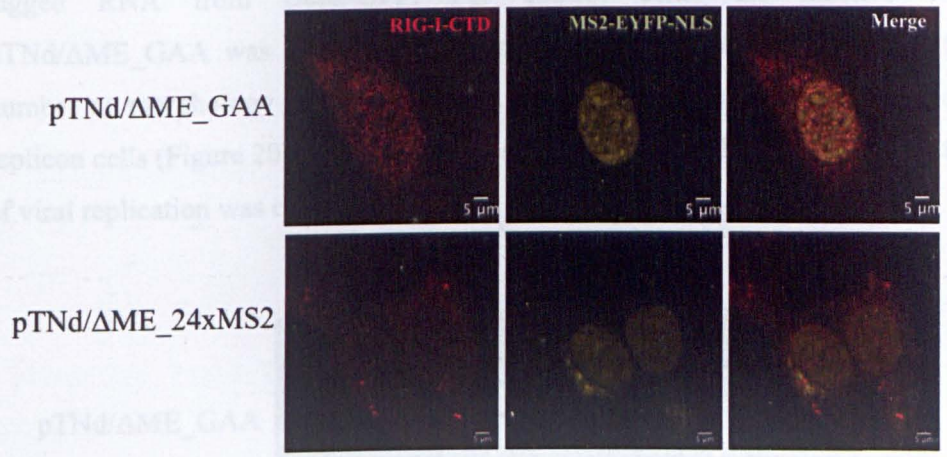


**Figure 19: Endogenous RIG-I cellular localization in TBEV replicon cells**

Confocal images of U2OS-MS2-YFP-NLS cells electroporated with pTNd/ΔME_GAA (first row) and pTNd/ΔME_24xMS2 replicon (second row). After 24h.p.t cells were fixed and incubated with an antibody used against RIG-I-CTD (red).

### 3.2.2.2 Host proteins over-expression analysis

Decapping enzyme 1 (Dcp1) is involved in mRNA decay, most specifically 5'-3' RNA degradation. After deadenylation, mRNA can be decapped by Dcp1/Dcp2 decapping enzyme leading to 5' to 3' degradation by the exonuclease Xrn-1. This process needs the formation of a translationally repressed mRNP complex (mRNA and proteins) that can aggregate into specific foci named Processing-bodies (P-bodies) (Anderson & Kedersha, 2006; Eulalio et al, 2007). The RNA contained in these complexes can either be degraded or stored for later return to translation. The fundamental role of P-bodies in the translation repression and degradation of host transcripts suggests that these complexes and the proteins within them affect the metabolism of viral mRNAs. Interestingly, in some cases key components of these complexes are involved in viral RNA processing such as Xrn-1 exonuclease, which has been shown to produce sub-genomic fragments (sfRNA) in flaviviruses, which are important for virus-induced cytopathic effects and pathogenicity (Pijlman et al, 2008).

To assess the possible role of Dcp1 during TBEV replication, U2OS cells were co-transfected with Dcp1-GFP, MS2-Cherry-NLS and pTNd/ΔME_24xMS2. The variant MS2 fused to Cherry-NLS was used in order to differentiate the localization of the tagged RNA from Dcp2-GFP. For control cells, the inactive replicon pTNd/ΔME_GAA was co-transfected. Confocal images show no change either in number or morphology in P-bodies from TBEV replicon cells compared to control replicon cells (Figure 20). Importantly, no co-localization of Dcp1-GFP foci with sites of viral replication was observed.

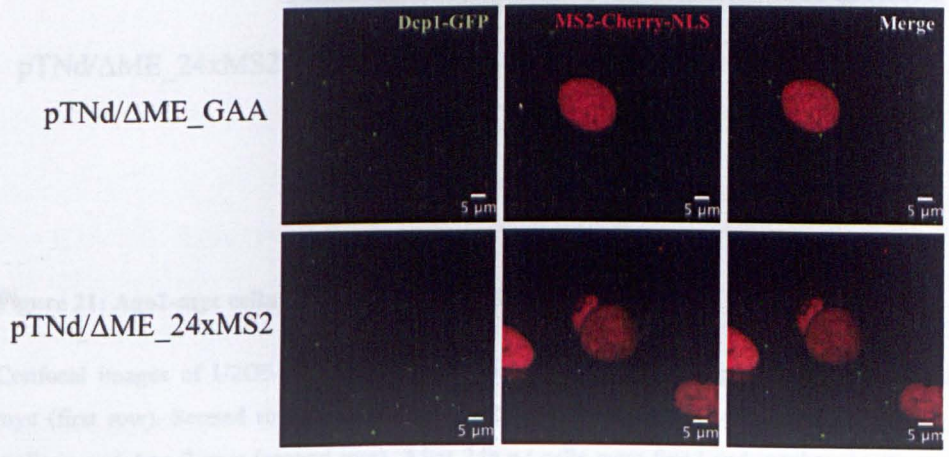


**Figure 20: Dcp1-GFP cellular localization in TBEV replicon cells**

Confocal images of U2OS cells electroporated with pTNd/ΔME_GAA, Dcp1-GFP and MS2-Cherry-NLS (first row). Second row, U2OS cells electroporated with pTNd/ΔME_24xMS2 replicon, Dcp1-GFP and MS2-Cherry-NLS (second row). After 24h.p.t cells were fixed and analyzed.

Argonaute 2 (Ago-2) is an important sensor and effector of the RNAi pathway. It is a fundamental component of the RNA-induced silencing complex (RISC). The complex is activated by a small RNA associated with an Argonaute protein, which regulates gene expression mediated by the sequence complementarity between the small RNA and the target mRNA. Ago-2 contains a PIWI domain that has endonuclease activity and a PAZ and Mid domains to interact with small RNA molecules and proteins involved in translation. Previous data have shown the important role of RNAi pathway in the innate immune response in mosquito cells against Denv-2 virus (Sanchez-Vargas et al, 2009). Therefore, with the purpose of

understanding the role of Ago-2 in TBEV replication, U2OS-MS2-YFP-NLS cells were co-transfected with Ago-2-Myc and pTNd/ΔME_24xMS2. No co-localization of Ago-2 foci with sites of RNA replication was observed in TBEV replicon cells (Figure 21). The number of Ago-2 foci was similar under both conditions.

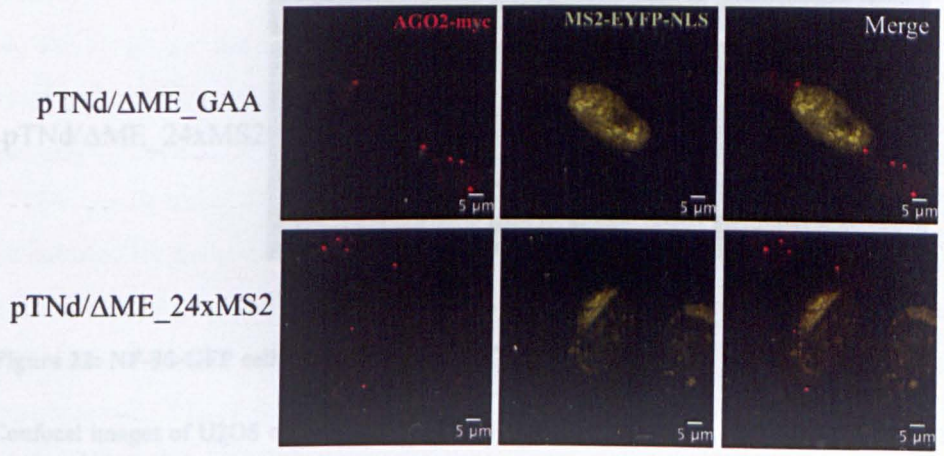


**Figure 21: Ago2-myc cellular localization in TBEV replicon cells**

Confocal images of U2OS-MS2-YFP-NLS cells electroporated with pTNd/ΔME_GAA and Ago-2-myc (first row). Second row, U2OS-MS2-YFP-NLS cells electroporated with pTNd/ΔME_24xMS2 replicon and Ago-2-myc (second row). After 24h.p.t cells were fixed and incubated with an antibody against myc (red).

Nuclear factor 90 (NF-90) is a double-stranded RNA (dsRNA) binding protein that interacts with other proteins, dsRNA, small non-coding RNAs and mRNA to regulate gene expression and mRNA stability. Previous evidence shows that the protein binds to the 5'NCR and 3'NCR of Hepatitis C viral RNA, which are very important for viral replication (Isken et al, 2007). More recent data has described the role of NF-90 as a positive regulator of Dengue virus (DENV) replication by binding to the 3'NCR of viral RNA (Gomila et al, 2011). In order to study the possible involvement of NF-90 during TBEV replication, U2OS cells were co-transfected with NF-90-GFP, MS2-Cherry-NLS and either pTNd/ΔME_24xMS2 or pTNd/ΔME_GAA. NF-90-GFP nuclear localization remained unchanged in TBEV replicon cells compared to control cells (Figure 22).

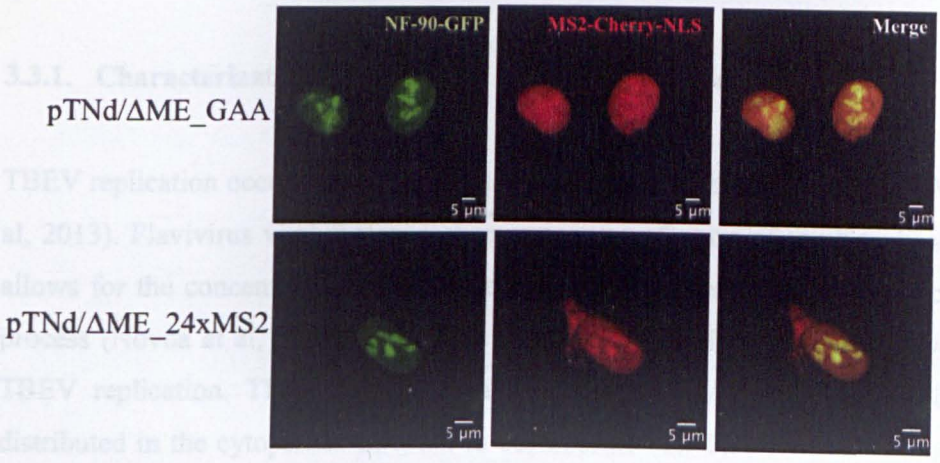


**Figure 22: NF-90-GFP cellular localization in TBEV replicon cells**

Confocal images of U2OS cells electroporated with pTNd/ΔME_GAA, NF-90-GFP and MS2-Cherry-NLS (first row). Second row, U2OS cells electroporated with pTNd/ΔME_24xMS2 replicon, NF-90-GFP (first column) and MS2-Cherry-NLS (second column). After 24h.p.t cells were fixed and analyzed.

In summary, the data shown here revealed that the cellular localization of the majority of the host factors analyzed were not modified in TBEV replicon cells compared to control replicon cells. There were two proteins whose cellular localization was modified during TBEV replication. TIA-1 was recruited to sites of viral replication while RIG-I protein was presenting a speckle-like distribution in TBEV replicon cells but not in control cells. Thus, I decided to further characterize the possible role of these proteins during TBEV replication and infection.

## 3.3. Characterization of TIA-1 upon TBEV replication

### 3.3.1. Characterization of TIA-1 in TBEV replicon cells

TBEV replication occurs in virus-induced host cytoplasmic ER membranes (Miorin et al, 2013). Flavivirus viral factories share a common feature of virus replication that allows for the concentration of viral factors thereby increasing the efficiency of the process (Novoa et al, 2005). Very little is known about the host factors involved in TBEV replication. TIA-1 cellular localization is mainly nuclear and is diffusely distributed in the cytoplasm. In order to corroborate that TIA-1 was accumulating at sites of viral replication, U2OS-MS2-YFP-NLS cells were electroporated with pTNd/ΔME_24xMS2 or pTNd/ΔME_GAA as control. In pTNd/ΔME_24xMS2 replicon cells TIA-1 was co-localizing with MS2-YFP tagged viral RNA. Moreover, co-localization with TBEV proteins was observed when specific antibody was used (Figure 23A). TIA-1 was also co-localizing with double-strand RNA (dsRNA) as observed by using an antibody that recognizes the intermediary of viral replication (Figure 23B).

**A**

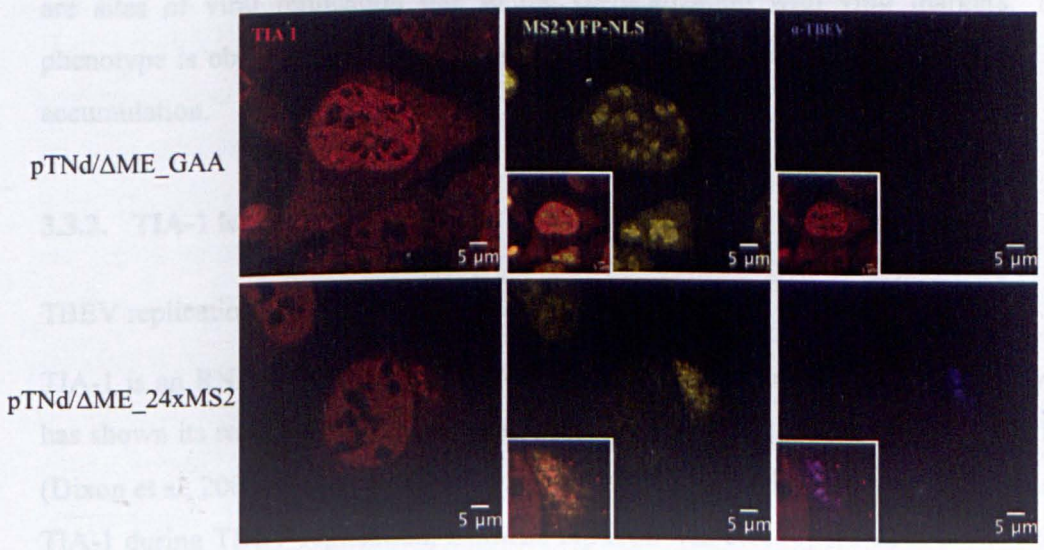

B

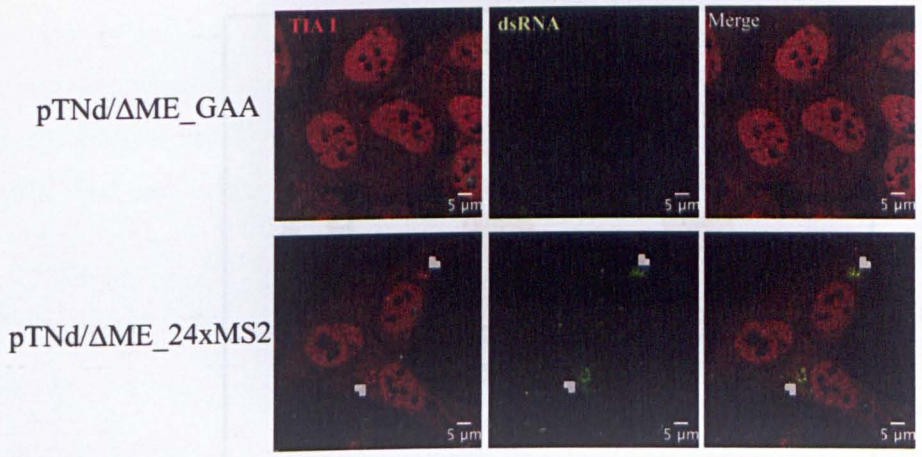


**Figure 23: Characterization of TBEV replication sites**

Confocal images of U2OS cells electroporated with pTNd/ΔME_GAA and pTNd/ΔME_24xMS2 A) U2OS-MS2-YFP-NLS cells electroporated with pTNd/ΔME_GAA (first row) and pTNd/ΔME_24xMS2 replicon (second row). After 24 h.p.t cells were fixed and incubated with antiserum against TBEV proteins (blue) and TIA-1 (red) antibodies. B) U2OS cells electroporated with pTNd/ΔME_GAA (first row) and pTNd/ΔME_24xMS2 replicon (second row). After 24 h.p.t cells were fixed and incubated with TIA-1 (red) and dsRNA (middle panel, green) antibodies.

Together these results confirm that the sites of TIA-1 accumulation in the cytoplasm are sites of viral replication due to the co-localization with viral markers. This phenotype is observed only in cells where there is active viral replication and RNA accumulation.

### 3.3.2. TIA-1 is a negative regulator of TBEV replication

TBEV replication in TIA-1 knockout cells

TIA-1 is an RNA binding protein involved in host RNA metabolism. Previous work has shown its role as a post-transcriptional regulator of host genes Cox-2 and TNF-α (Dixon et al, 2003; Piecyk et al, 2000). In order to evaluate the functional relevance of TIA-1 during TBEV replication, 24xMS2 replicon was electroporated in MEF TIA-1 knockout cells and MEF WT as control. Normalized luciferase levels in MEF TIA-1 knockout cells were increased over MEF WT cells indicating that TIA-1 was acting as a restriction factor for TBEV replication (Figure 24).

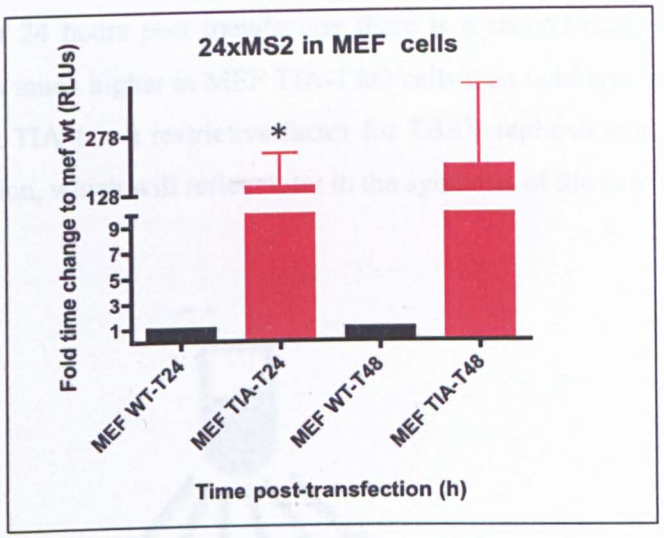


**Figure 24: TIA-1 is a negative factor for TBEV replication**

MEF WT and MEF TIA-1 knockout cells were electroporated with 24xMS2 TBEV replicon. Samples were collected after 24 and 48 hours post transfection. Luciferase fold time enrichment is shown for 24xMS2 in MEF WT (black bar) and MEF TIA-1 kO (red bar). Data were averaged from three independent experiments and are represented as mean ± standard deviation. Significant *p*-values were calculated with paired *t*-test ($p<0.01$=**; $p<0.05$=*).

Next, I took advantage of this replicon to further understand at which level of viral replication was TIA-1 acting. Hoenninger and collaborators showed that 24xMS2 replicon exhibited a biphasic pattern of luciferase activity over a time course of 48 h.p.t. The first peak, which appears within the first 4 h after transfection, shows that the initial input RNA was translated in the cell, yielding a functional luciferase enzyme. After a subsequent decrease in luciferase activity indicative of a decrease in translation, a second peak represented luciferase that was expressed from newly synthesized sense-strand RNA after replication of the input RNA (Hoenninger et al, 2008). In order to assess viral replication I co-transfected *in vitro* transcribed 24xMS2 replicon with renilla luciferase plasmid in MEF TIA-1 kO and MEF WT cells. After the indicated time points cells were harvested (Figure 25A). According to Hoenninger and collaborators for firefly luciferase activity normalization I used for the first time points (0-8 h.p.t.) renilla luciferase *in vitro* transcribed RNA. For the subsequent time

points I transfected DNA (Hoenninger et al, 2008). As shown in figure 25B, during the first peak the TBEV luciferase levels are increased in MEF TIA-1 kO with respect to MEF WT. After 24 hours post transfection there is a second peak of luciferase expression which is much higher in MEF TIA-1 kO cells than wild type MEFs. These results suggest that TIA-1 is a restrictive factor for TBEV replication at the level of initial viral translation, which will reflect later in the synthesis of the new viral RNA.

**A**

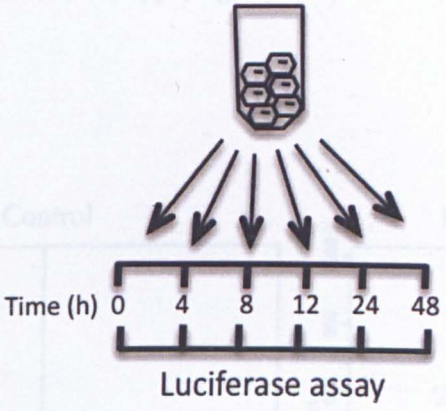


**B**

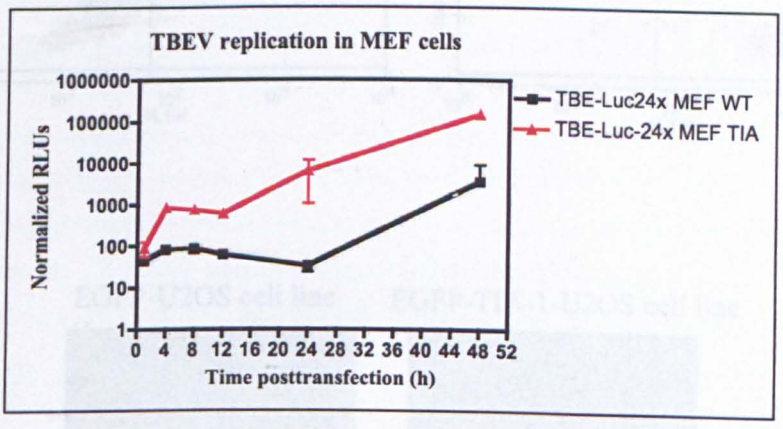


Figure 25: TIA-1 is involved in the initial round of TBEV translation

Time course of 24xMS2 replication in MEF WT and MEF TIA-1 kO cells. A) Schematic diagram of the experiment. MEF WT and TIA-1 kO cells were electroporated and samples were harvested at the indicated time point after transfection. B) Normalized luciferase levels of 24xMS2 in MEF WT (black curve) and MEF TIA-1 cells (red curve) at different time points. Data were averaged from three independent experiments and are represented as mean ± standard deviation.

TIA-1 over-expression in U2OS cells

With the purpose of understanding the specificity of the negative role of TIA-1 in TBEV replication, TIA-1 over-expression analysis was performed. In order to obtain reproducible results, a stable U2OS cell line over-expressing TIA-1 was produced. Upon transfection with EGFP-TIA-1 plasmid, U2OS cells were grown in the presence of G418. Isolated clones were expanded and characterized by FACS analysis (Figure 26A), fluorescent microscopy (Figure 26B) and Western blot studies (Figures 26 C and D).

**A**

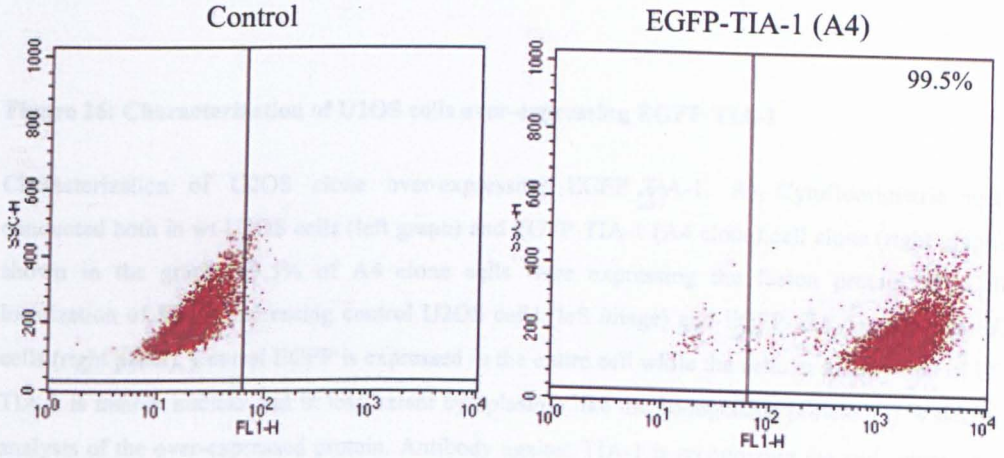


**B**

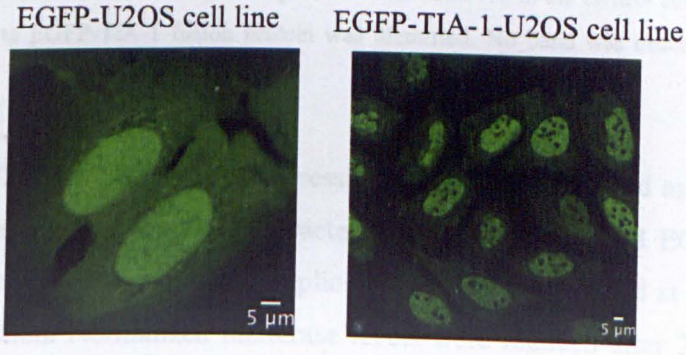

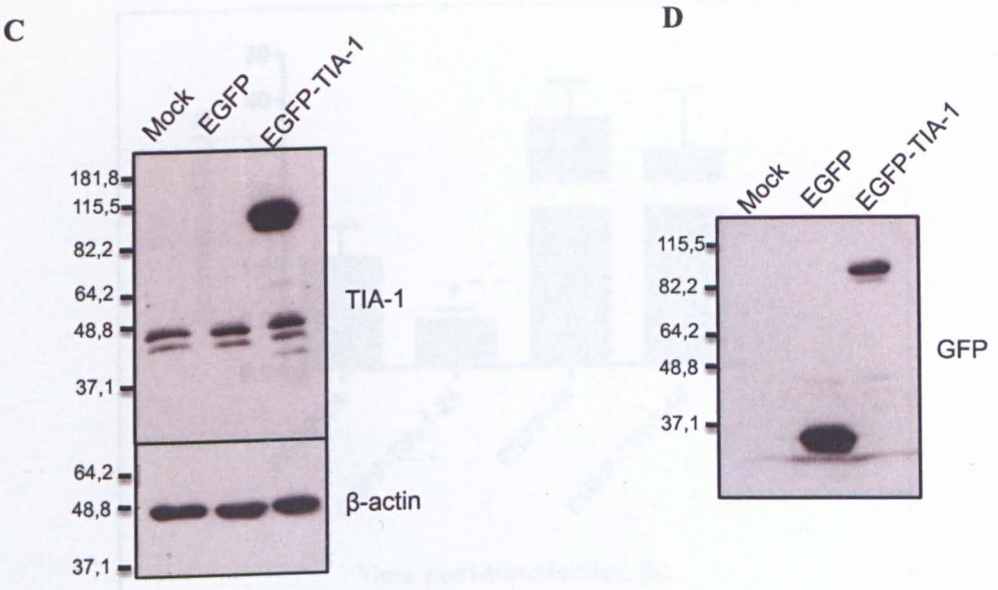


**Figure 26: Characterization of U2OS cells over-expressing EGFP-TIA-1**

Characterization of U2OS clone over-expressing EGFP_TIA-1. A) Cytofluorimetric analysis conducted both in wt U2OS cells (left graph) and EGFP-TIA-1 (A4 clone) cell clone (right graph). As shown in the graph, 99,5% of A4 clone cells were expressing the fusion protein. B) Cellular localization of EGFP expressing control U2OS cells (left image) and EGFP-TIA-1 expressing U2OS cells (right panel). Control EGFP is expressed in the entire cell while the cellular localization of EGFP-TIA-1 is mainly nuclear and in less extent cytoplasmic like the endogenous protein. C) Western Blot analysis of the over-expressed protein. Antibody against TIA-1 is recognizing the endogenous protein in every sample. Moreover there was a higher band only in EGFP-TIA-1 lane which corresponds to the fusion protein. β-actin was used as a loading control. D) Antibody that recognizes GFP was used in the same membrane (C). A band corresponding to GFP was observed in the control cells and a higher band corresponding to EGFP-TIA-1 fusion protein was identified. No band was observed in U2OS mock cells.

Moreover, U2OS cell line stably expressing EGFP was generated as over-expression control. Once the cell line was characterized, EGFP-TIA-1 and EGFP U2OS cells were transfected with the 24xMS2 replicon. Cells were harvested at 24 and 48 hours after transfection. Normalized luciferase levels were reduced after 24 hpt in EGFP-TIA-1 cells with respect to control EGFP U2OS cells (Figure 27). This data supports the knockout results performed in MEF cells confirming the negative role of TIA-1 in TBEV replication.

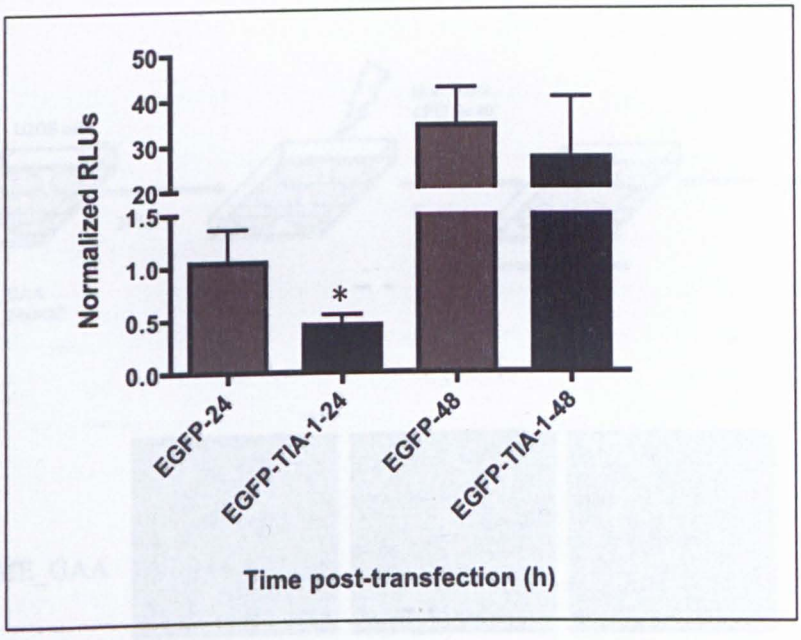


**Figure 27: TIA-1 is a negative factor during TBEV replication**

TBE-24xMS2 replication in EGFP-TIA-1 over-expressed U2OS cells. U2OS A4 clone was electroporated with 24xMS2 replicon. Samples were collected after 24 and 48 hpt. Normalized luciferase levels in control EGFP cells (grey bars) and EGFP-TIA-1 cells (black bars) are shown in the graph. Data were averaged from three independent experiments and are represented as mean ± standard deviation. Significant *p*-values were calculated with unpaired *t*-test ($p<0.01$=**; $p<0.05$=*).

## TBEV replication affects TIA-1 stress granule formation

TIA-1 is involved in the cellular stress-induced response (Kedersha et al, 2000). When cells are exposed to stresses such us UV radiation, oxidative stress, heat shock or viruses, TIA-1 aggregates to form stress granules (SG). SG assembly is a consequence of abortive translational initiation in which TIA-1 binds to the RNA and forms a deficient pre-initiation complex. Until now I have demonstrated that TIA-1 accumulates at sites of viral replication, however no TIA-1 stress granules were observed in these cells. For this reason, I sought to understand whether viral replication was inhibiting TIA-1 SG formation. For this aim, U2OS cells were transfected either with pTNd/ΔME_24xMS2 or pTNd/ΔME_GAA and 24 h.p.t. cells were exposed to stress (heat shock) before fixation (Figure 28A). Next, in order to evaluate the cellular response to stress in replicon cells the number of TIA-1 SG per cell were counted and compared to control pTNd/ΔME_GAA cells (Figure 28B).

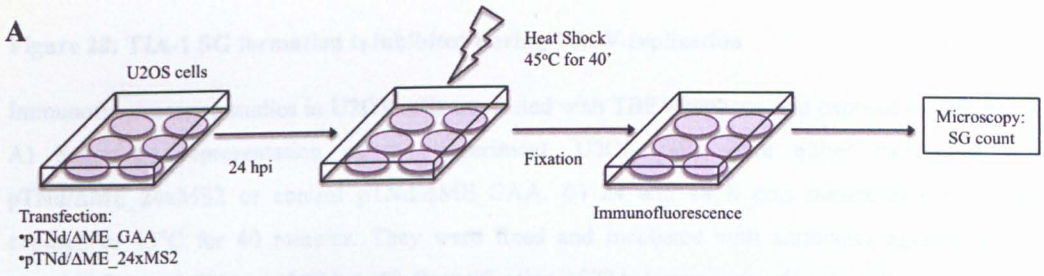
A
U2OS cells
24 hpi
Heat Shock
45°C for 40'
Fixation
Microscopy:
SG count
Transfection:
•pTNd/ΔME_GAA
•pTNd/ΔME_24xMS2
Immunofluorescence

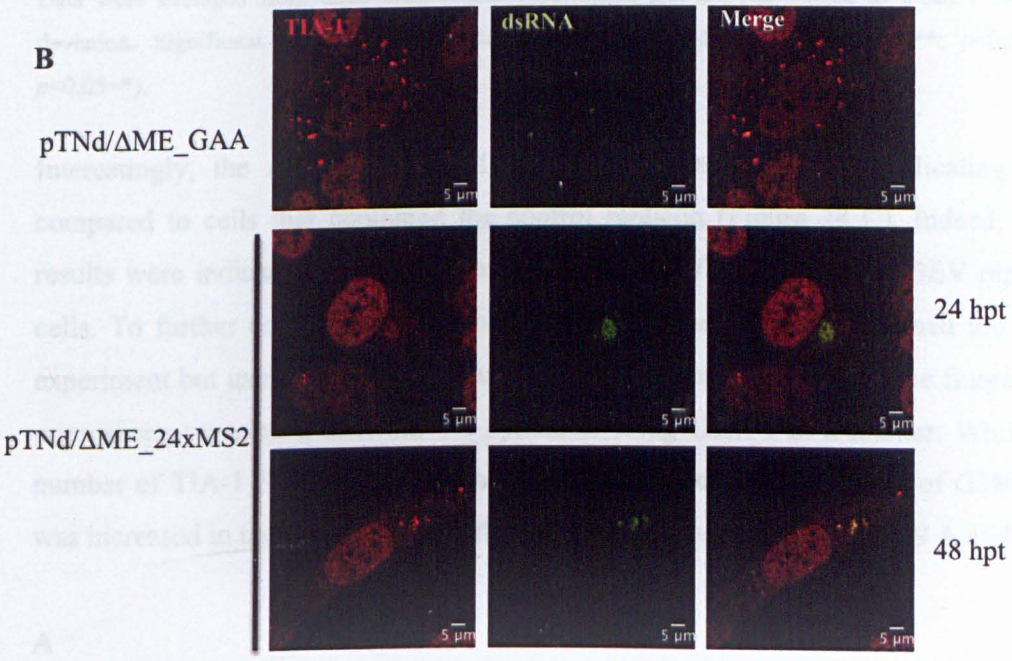
B
TIA-1
dsRNA
Merge
pTNd/ΔME_GAA
pTNd/ΔME_24xMS2
24 hpt
48 hpt
5 µm

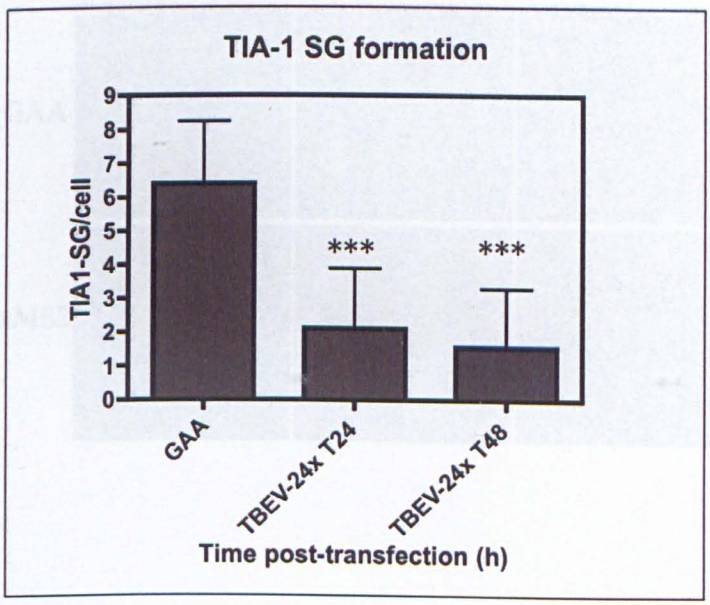
C
TIA-1 SG formation
TIA1-SG/cell
0
1
2
3
4
5
6
7
8
9
***
***
GAA
TBEV-24x T24
TBEV-24x T48
Time post-transfection (h)

**Figure 28: TIA-1 SG formation is inhibited during TBEV replication**

Immunofluorescence studies in U2OS cells tranfected with TBEV replicon and exposed to heat shock. A) Schematic representation of the experiment. U2OS cells were either transfected with pTNd/ΔME_24xMS2 or control pTNd/ΔME_GAA. B) 24 and 48 h post transfection cells were exposed to 45°C for 40 minutes. They were fixed and incubated with antibodies against double-stranded RNA (dsRNA) and TIA-1. C) Quantification of TIA-1 stress granules per cell in control (M) cells and TBEV replicon cells after 24 and 48 hpt. A number of 100 cells per condition were counted. Data were averaged from three independent experiments and are represented as mean ± standard deviation. Significant *p*-values were calculated with unpaired *t*-test ($p<0.001$=***; $p<0.01$=**; $p<0.05$=*).

Interestingly, the number of TIA-1 SG was reduced in TBEV replicating cells compared to cells that contained the control replicon (Figure 28 C). Indeed, these results were indicating that there was an inhibition of TIA-1 SG in TBEV replicon cells. To further corroborate the specificity of the phenotype I performed the same experiment but using another SG marker G3BP1. Observations under the fluorescent microscope revealed a different SG dynamics using G3BP1 as a marker. While the number of TIA-1 SG was reduced in TBEV replicon cells, the number of G3BP SG was increased in these cells compared to control replicon cells (Figures 29 A and B).

**A**

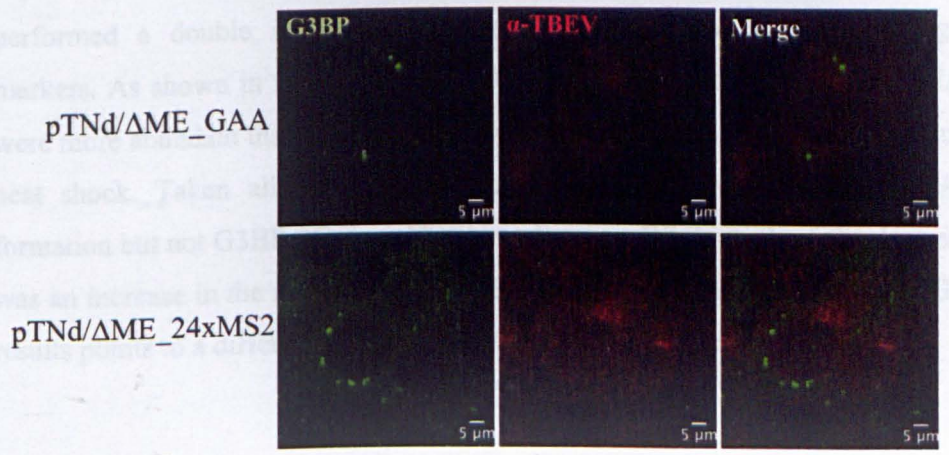

**B**

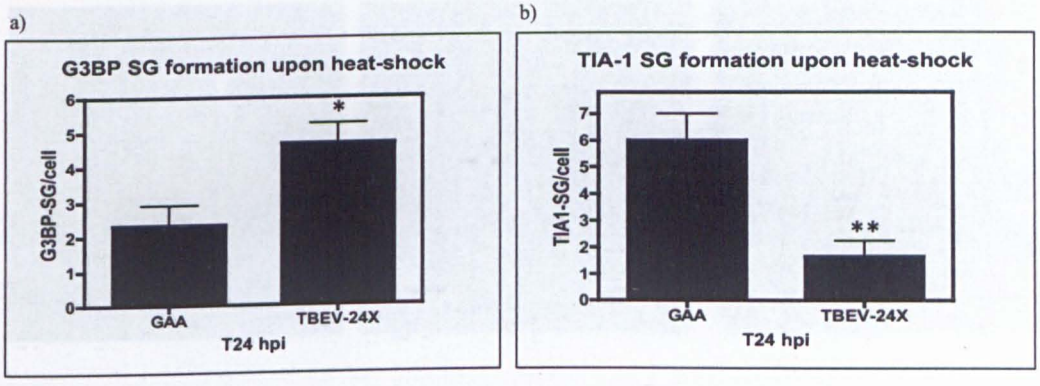


**Figure 29: TBEV replication does not inhibit G3BP stress granules formation**

Immunofluorescence studies in U2OS cells exposed to heat shock and tranfected with TBEV replicon. A) U2OS cells were either transfected with pTNd/ΔME_24xMS2 or control pTNd/ΔME_GAA. 24 post transfection cells were exposed to 45°C for 40 minutes. They were fixed and incubated with antibodies against α-TBEV and G3BP. B) a) Quantified G3BP stress granules per cell in replicon TBE-24X cells and control TBE-GAA cells (left panel). b) In the right panel, quantification of TIA-1 SG is shown as comparison. A number of 100 cells were counted per condition. Data were averaged from three independent experiments and are represented as mean ± standard deviation. Significant *p*-values were calculated with unpaired *t*-test ($p<0.001$=***; $p<0.01$=**; $p<0.05$=*).

Therefore I hypothesized from these results that there was a differential SG dynamics depending on the stress. To confirm this idea I exposed to heat shock U2OS cells and performed a double immunofluorescence for TIA-1 and G3BP stress granules markers. As shown in figure 30 A and B, upon heat shock the number of TIA-1 SG were more abundant than G3BP SG indicating a differential protein composition upon heat shock. Taken all together these experiments showed a reduced TIA-1 SG formation but not G3BP SG upon TBEV replication. While for heat shock stress there was an increase in the number of TIA-1 SG formation compared to G3BP SG. These results points to a differential cellular stress response dependent on the stress.

A

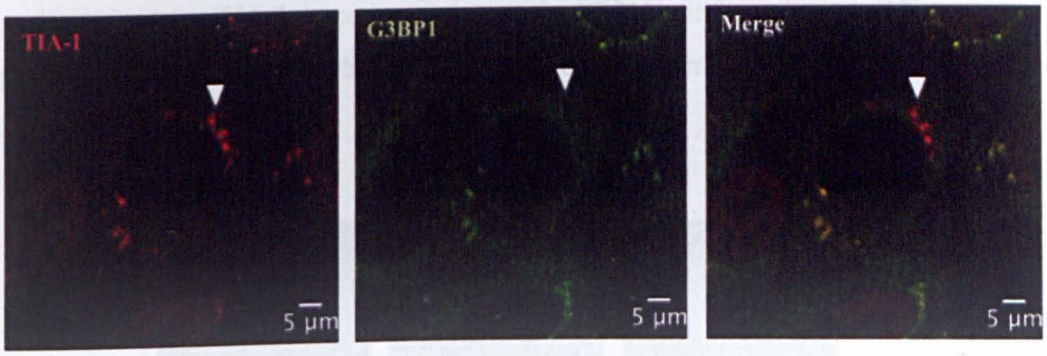


B

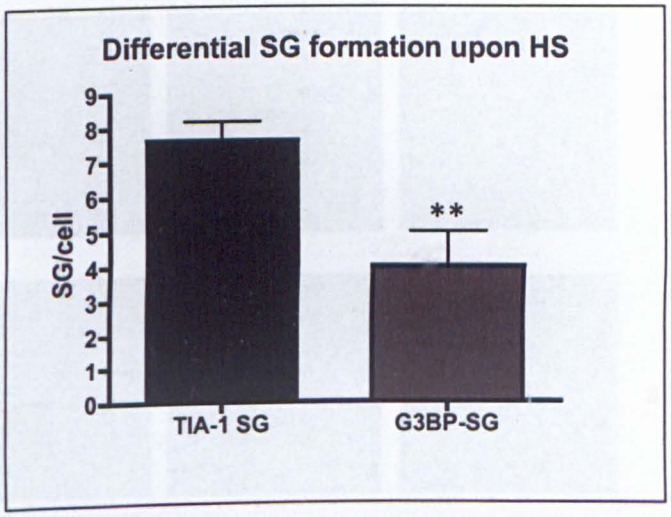


**Figure 30: Comparison of TIA-1 stress granules formation during heat shock**

G3BP and TIA-1 stress granules formation upon heat shock in U2OS cells. A) U2OS cells were exposed to heat shock at 45°C for 40 minutes, fixed and incubated with G3BP and TIA-1 antibodies. B) Quantification of TIA-1 (dark grey bar) and G3BP (light grey bar) stress granules in cells exposed to heat shock. A number of 100 cells were counted per condition. Data were averaged from three independent experiments and are represented as mean ± standard deviation. Significant *p*-values were calculated with unpaired *t*-test ($p<0.001$=***; $p<0.01$=**; $p<0.05$=*).

### 3.3.3. Characterization of TIA-1 in TBEV infected cells

In order to further explore the involvement of TIA-1 in TBEV replication, TBEV full-length virus was used. U2OS cells were infected with the Western TBEV Hypr strain

at a multiplicity of infection (MOI) of 2. After different time points cells were fixed and immunofluorescence analysis was performed. As previously observed with the replicon system, TIA-1 is co-localizing with dsRNA viral marker at different time points after infection. This phenotype was not observed in mock infected cells (Figure 31).

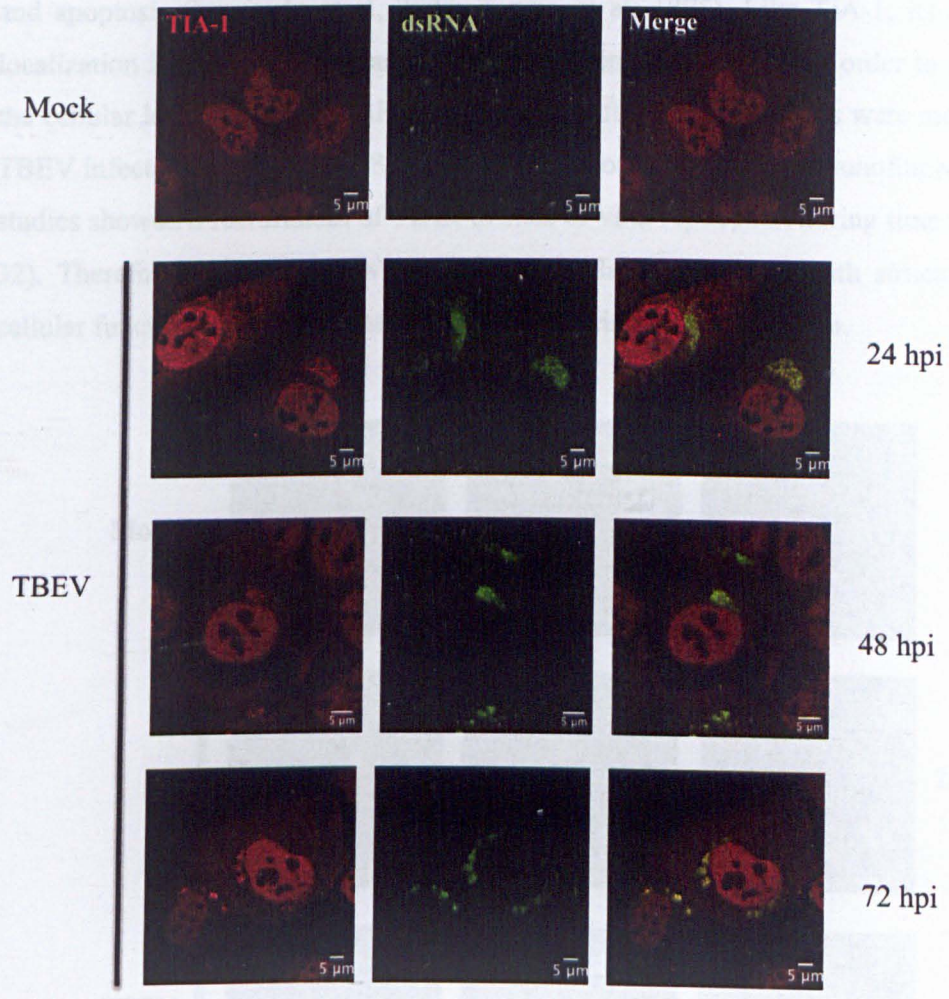


**Figure 31: Cellular localization of TIA-1 in TBEV infected cells**

Time course of TIA-1 cellular localization in TBEV infected cells. U2OS cells were either mock and TBEV infected at a MOI of 2. Cells were fixed after 24, 48 and 72 hours post infection. After fixation immunofluorescence analysis was performed using anti-TIA-1 (red) and anti-dsRNA (green) antibodies.

As previously observed in TBEV replicon cells, TIA-1 was re-localized to replication sites without formation of TIA-1 stress granules. With the objective to further understand if this phenotype was specific for TIA-1, I explored the cellular localization of other stress response markers in TBEV infected cells. TIAR is a TIA1-related protein, which binds to adenine-uridine rich domains in mRNA and pre-mRNA of a wide range of genes. It has been involved in translational control, splicing and apoptosis (Izquierdo et al, 2005; Taupin et al, 1995). Like TIA-1, its cellular localization is mainly nuclear and to a lesser extent cytoplasmic. In order to explore the cellular localization of TIAR during TBEV infection, U2OS cells were mock and TBEV infected. After 24 and 48 hours post infection were fixed. Immunofluorescence studies showed a recruitment of TIAR to sites of viral replication during time (Figure 32). Therefore, this protein, which is very similar to TIA-1 in both structure and cellular functions, also was behaving similarly during TBEV infection.

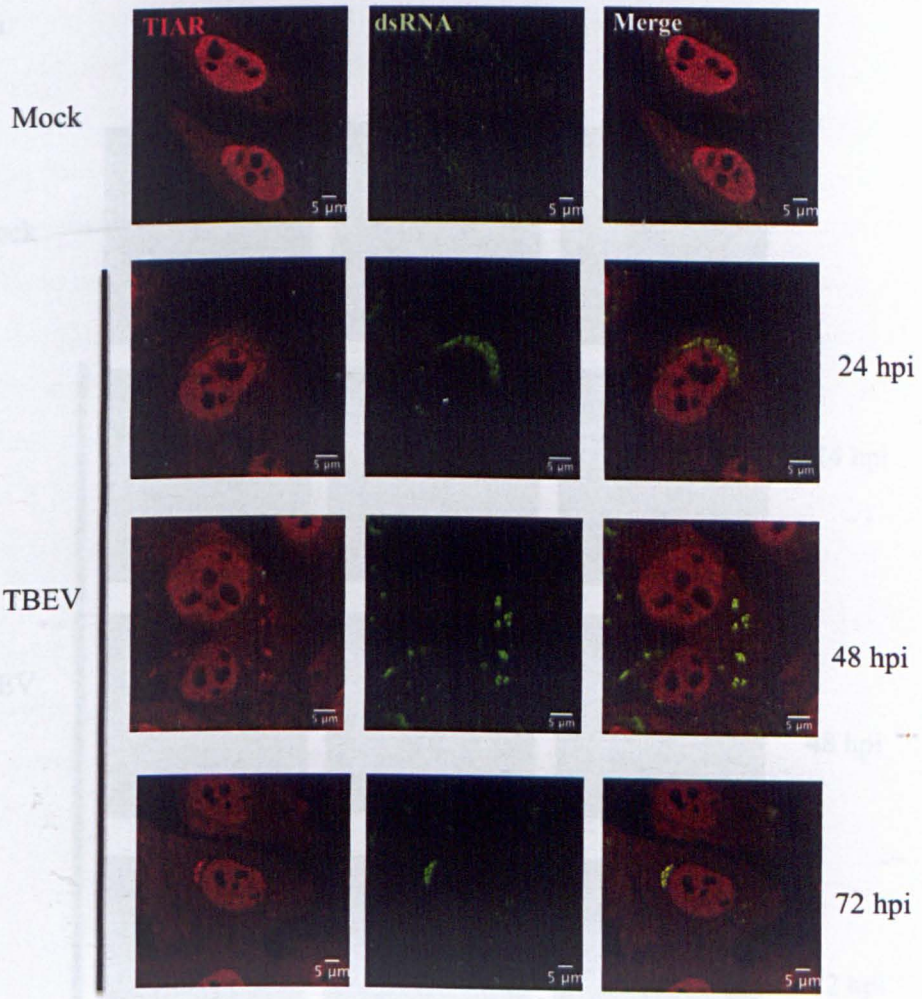

**Figure 32: Cellular localization of TIAR in TBEV infected cells**

Time course of TIAR cellular localization in TBEV infected cells. U2OS cells were either mock and TBEV infected at a MOI of 2. Cells were fixed after 24, 48 and 72 hours post infection. After fixation immunofluorescence analysis was performed using anti-TIAR (red) and anti-dsRNA (green) antibodies.

Another stress protein marker already used in this work is G3BP, which is an RNA binding protein that has been shown to have endoribonuclease activity and therefore is involved is mRNA decay (Tourriere et al, 2001). To address the cellular localization of the protein during TBEV infection, U2OS cells were infected and after the indicated time points immunofluorescence analysis was performed. Interestingly, formation of G3BP SGs was observed without co-localization of the granules in replication complexes as observed for TIA-1 and TIAR proteins (Figure 33). These results point to a differential response of stress marker proteins during TBEV infection.

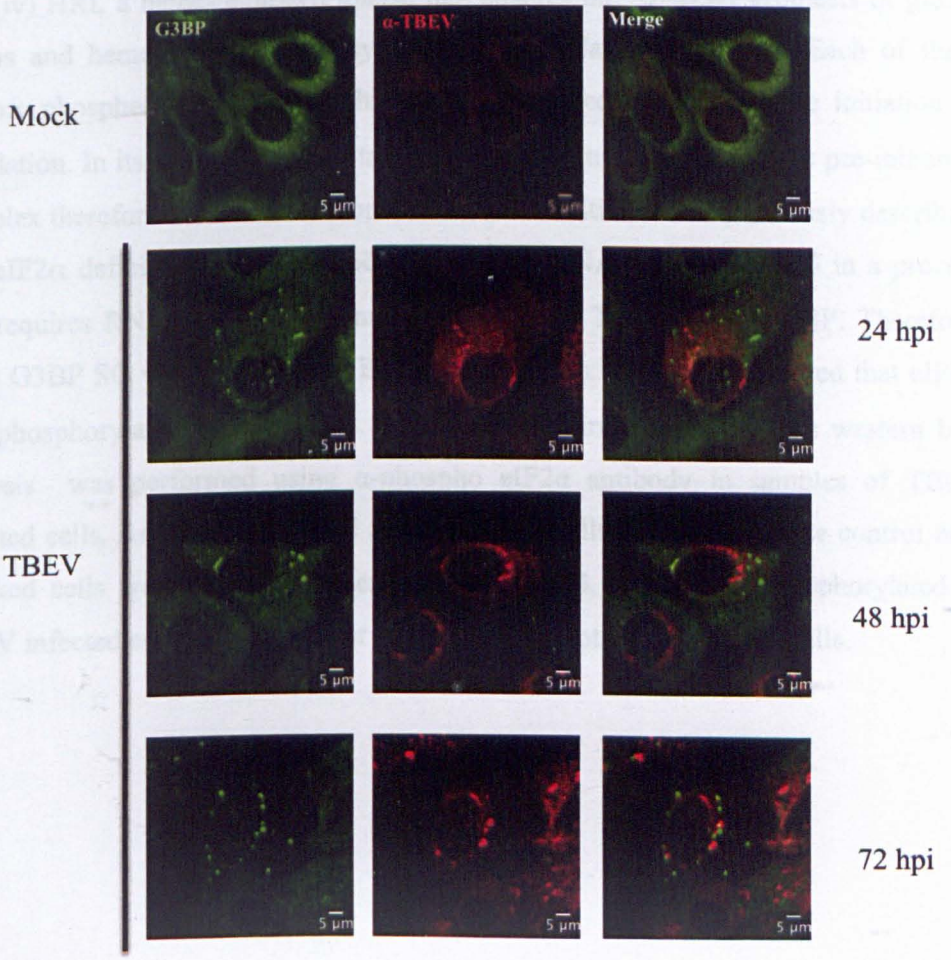

**Figure 33: Cellular localization of G3BP in TBEV infected cells**

Time course of G3BP cellular localization in TBEV infected cells. U2OS cells were either mock and TBEV infected at a MOI of 2. Cells were fixed after 24, 48 and 72 hours post infection. After fixation immunofluorescence analysis was performed using anti-G3BP (green) and anti-TBEV (red) antibodies.

## eIF2α is phosphorylated in TBEV infected cells

In response to environmental stress, eukaryotic cells shut down the translation of the "housekeeping" transcripts whereas the translation of heat shock proteins and some transcription factors is maintained or enhanced. In the apex of the stress response signalling cascade, there is the family of serine/threonine kinases which are the sensors of environmental stress. Members of this family are: (i) PKR, a double-stranded RNA-dependent kinase that is activated by viral infection, heat shock and UV irradiation (Williams, 2001);(Harding et al, 2000) (ii) PERK/PEK, a resident ER protein that is activated when unfolded proteins accumulate in the ER (Harding et al, 2000); (iii) GCN2, a protein that responds to amino acid deprivation (Kimball, 2001); and (iv) HRI, a heme-regulated kinase that ensures the balanced synthesis of globin chains and heme during erythrocyte maturation (Han et al, 2001). Each of these sensors phosphorylates eIF2α, which is a critical component for the initiation of translation. In its phosphorylated state this protein is not loaded into the pre-initiation complex therefore there is inhibition of translation initiation. As previously described, this eIF2α deficient complex associated to the mRNA is routed to SG in a process that requires RNA binding proteins such us TIA-1, TIAR and/or G3BP. Therefore, since G3BP SG were present in TBEV infected cells then I hypothesized that eIF2α was phosphorylated in these cells. In order to confirm this hypothesis western blot analysis was performed using α-phospho eIF2α antibody in samples of TBEV infected cells. As negative control mock infected cells and as a positive control heat shocked cells were used. As observed in figure 34, eIF2α was phosphorylated in TBEV infected cells as well as heat shock cells but not mock infected cells.

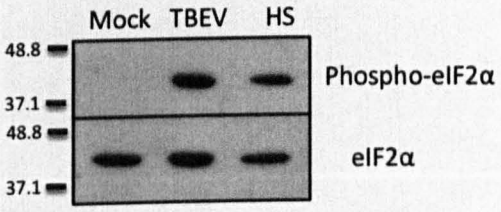


**Figure 34: eIF2α is phosphorylated in TBEV infected cells**

The phosphorylation of eIF2α was assessed by Western blot analysis. The first lane corresponds to mock infected cells, second lane to TBEV infected cells after 24 hpi and the third lane to heat shock cells used as positive control. Antibody that recognizes the phosphorylated form of eIF2α was used in the upper panel and another antibody that recognizes the total eIF2α protein was used in the lower panel.

Until now all these results show a recruitment of TIA-1 and TIAR to sites of viral replication during TBEV infection. On the other hand, the other stress marker G3BP protein is forming stress granules accompanied by a stalling of translation revealed by the phosphorylated state of eIF2α.

As mentioned above, stress granules are characterized by the presence of mRNA, translation initiation factors as well as specific RNA binding proteins (Anderson & Kedersha, 2009). White and colleagues have demonstrated the presence of pseudo-stress granules in Poliovirus infected cells. These granules are self aggregated TIA-1 protein which does not contain the other components of stress granules (White & Lloyd, 2011). In order to confirm that G3BP SG induced in TBEV infected cells were not pseudo-granules, immunofluorescence studies using translation initiation factor 3 (eIF3) antibody was performed. U2OS cells were mock and TBEV infected at MOI of 2. After 24 hpi were fixed and immunostaining with G3BP and eIF3 was carried out. From the figure 35, it is possible to observe that eIF3 protein is co-localizing with G3BP SG in TBEV infected cells. Therefore this data corroborates the presence of *bona fide* SGs during TBEV infection.

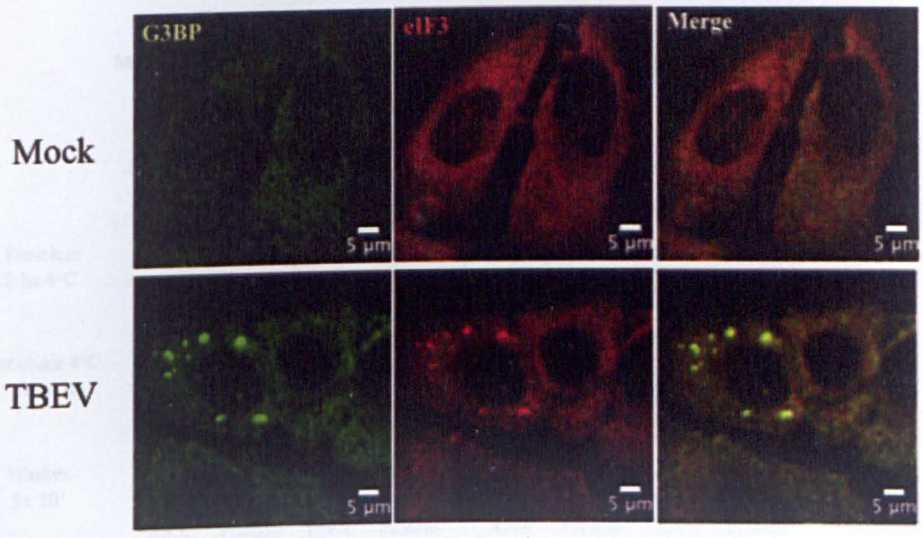


**Figure 35: Formation of bona fide SGs in TBEV infected cells**

G3BP and eIF3 cellular localization in TBEV infected cells. U2OS cells were either mock and TBEV infected at a MOI of 2. Cells were fixed after 24hours post infection. After fixation immunofluorescence analysis was performed using anti-G3BP (green) and anti-eIF3 (red) antibodies.

### 3.3.4. TIA-1 binds to viral RNA and TIAR during TBEV infection

To further explore the role of TIA-1 during TBEV infection a TIA-1 pull down from TBEV infected and mock infected U2OS cells was performed (Figure 36A). Western blot analysis confirmed successful TIA-1 pull-down (Figure 36 Ba). Moreover, by using specific antibodies the presence of TIAR but not G3BP was observed in TIA-1 pull down during infection (Figures 36 Bb and Bc, respectively). Furthermore, viral proteins NS1 and prM were not present in TIA-1 beads from infected cells (Figures 36 Be and Bf, respectively). From the immunofluorescence data I hypothesized that TIA-1 was binding viral RNA in the replication complexes.

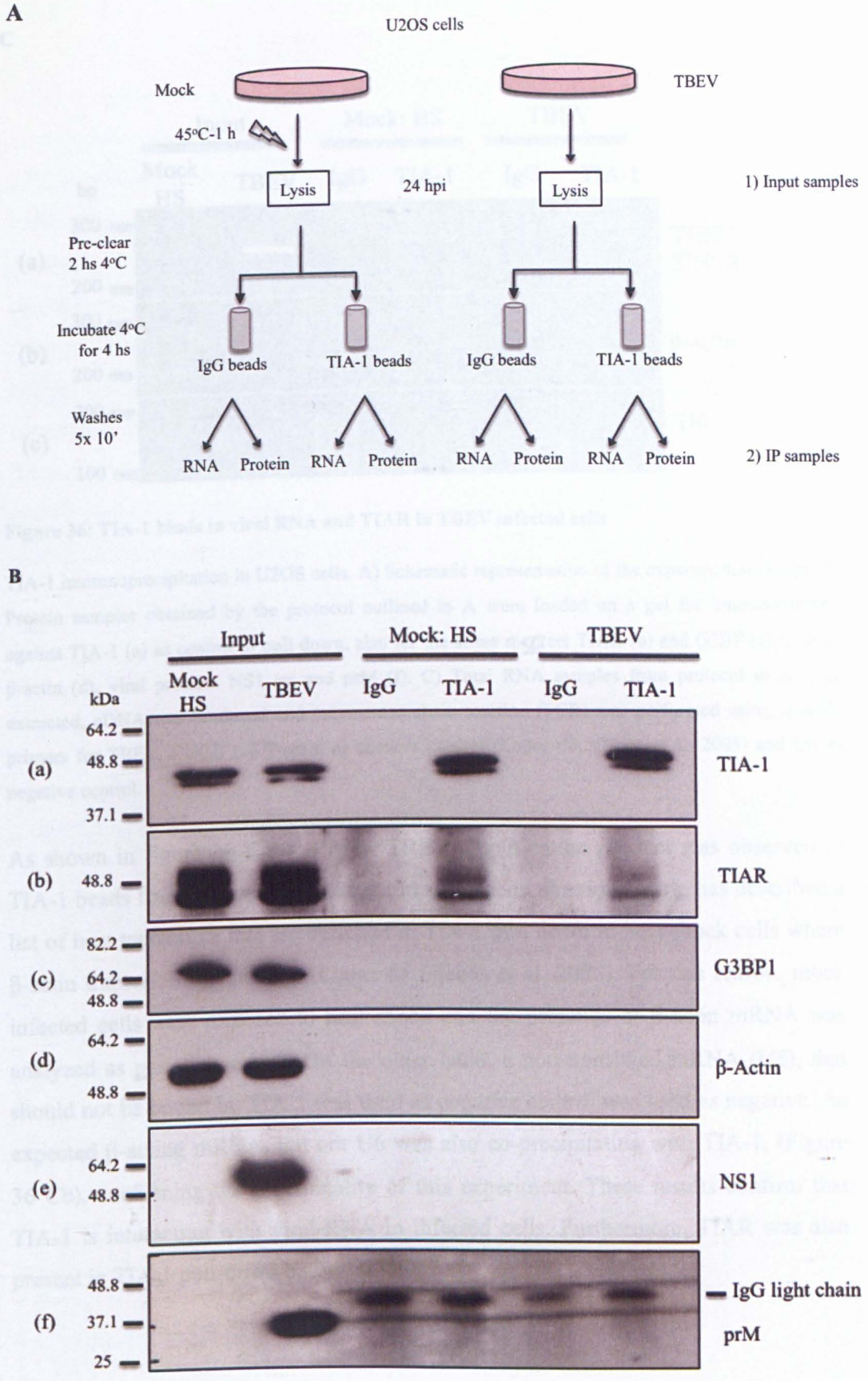
A
U2OS cells
Mock
TBEV
45°C-1 h
Lysis
24 hpi
Lysis
1) Input samples
Pre-clear
2 hs 4°C
Incubate 4°C
for 4 hs
IgG beads
TIA-1 beads
IgG beads
TIA-1 beads
Washes
5x 10'
RNA
Protein
RNA
Protein
RNA
Protein
RNA
Protein
2) IP samples
B
Input
Mock: HS
TBEV
Mock HS
TBEV
IgG
TIA-1
IgG
TIA-1
kDa
64.2
48.8
37.1
(a)
TIA-1
48.8
(b)
TIAR
82.2
64.2
48.8
(c)
G3BP1
64.2
48.8
(d)
β-Actin
64.2
48.8
(e)
NS1
48.8
37.1
25
(f)
IgG light chain
prM

C

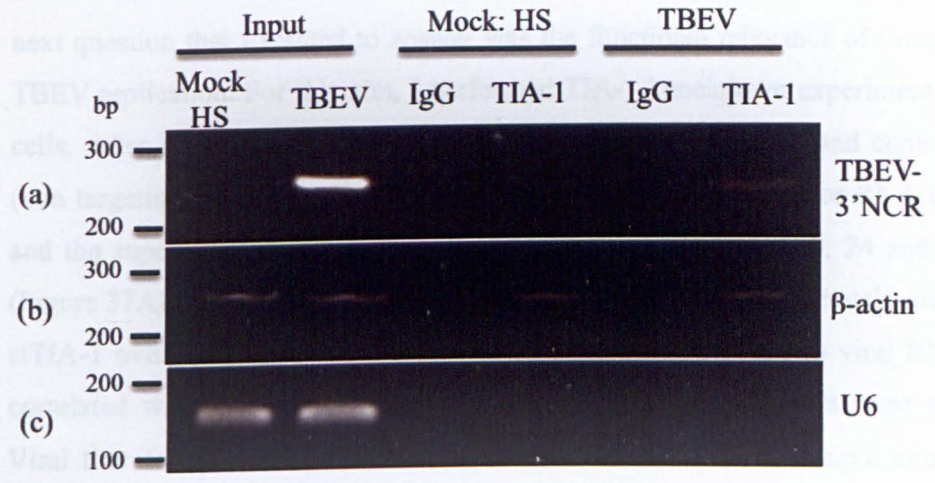


**Figure 36: TIA-1 binds to viral RNA and TIAR in TBEV infected cells**

TIA-1 immunoprecipitation in U2OS cells. A) Schematic representation of the experimental design. B) Protein samples obtained by the protocol outlined in A were loaded on a gel for immunoblotting against TIA-1 (a) as control of pull down, also for the stress markers TIAR (b) and G3BP (c), control β-actin (d), viral proteins NS1 (e) and prM (f). C) Total RNA samples from protocol in A were extracted, cDNA was produced and polymerase chain reaction (PCR) was performed using specific primers for TBEV 3'NCR (a), β-actin as positive control (Lopez de Silanes et al, 2005) and U6 as negative control.

As shown in figure 36 Ca, a 3'NCR TBEV amplification product was observed in TIA-1 beads from infected cells but not in mock cells. Previous work, has described a list of host transcripts that are enriched in TIA-1 pull down in heat shock cells where β-actin transcript was present (Lopez de Silanes et al, 2005). For this reason, mock infected cells were exposed to heat shock and the presence of β-actin mRNA was analyzed as positive control. On the other hand, a non-translated mRNA (U6), that should not be bound by TIA-1 was used as negative control was used as negative. As expected β-acting mRNA, but not U6 was also co-precipitating with TIA-1, (Figure 36 Cb), confirming the functionality of this experiment. These results confirm that TIA-1 is interacting with viral RNA in infected cells. Furthermore, TIAR was also present in TIA-1 pull-down but not G3BP.

### 3.3.5. TIA-1 is a negative regulator of TBEV replication during infection

After the observation that TIA-1 binds TBEV RNA at sites of viral replication the next question that I wanted to answer was the functional relevance of this protein in TBEV replication. For this aim, I performed TIA-1 knockdown experiment in U2OS cells. After 48 hours post transfection of the cells with siTIA-1 and control siNTG (non targeting), cells were infected at a MOI of 2. The samples for RNA extraction and the supernatants for plaque assay were collected after time 0, 24 and 48 hours (Figure 37A). As shown in figure 37 Ba, viral RNA levels are moderately increased in siTIA-1 over the siNTG. To test whether the observed increase in viral RNA levels correlated with increase of infectious particle release, virus titers were measured. Viral titer from TIA-1 knockdown cells was increased after 24 h.p.i. compared to siNTG treated cells (Figure 37 Bb). Efficient TIA-1 protein knockdown was observed during the time points of infection (Figure 37C)

**A**

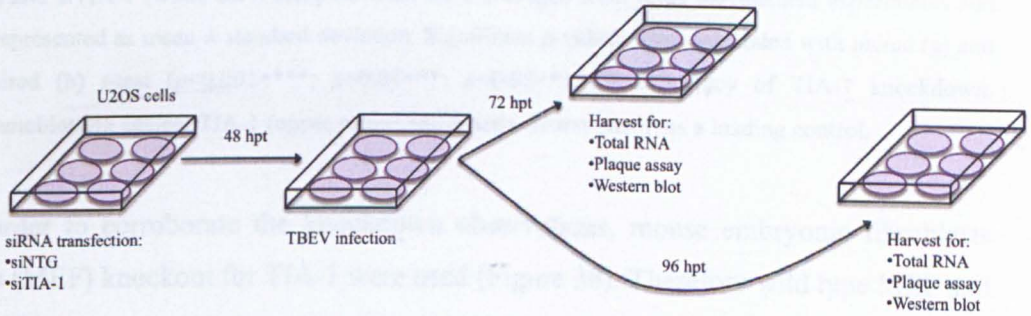


**B**

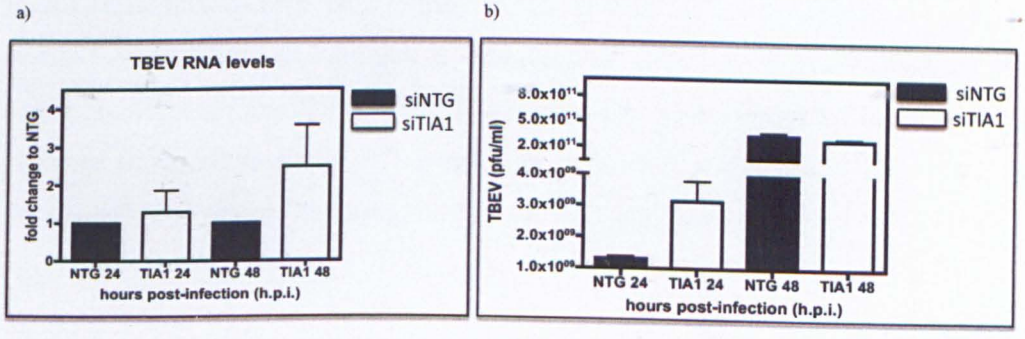

C


**Figure 37: TIA-1 is a negative regulator of TBEV replication in infected cells**

TIA-1 knockdown experiment in U2OS cells. A) Schematic design of the experiment. U2OS cells were transfected with siNTG (small interfering non targeting RNA) and siTIA-1. After 48 h post transfection, cells were infected at a MOI of 2. Samples for RNA extraction, immunoblotting and supernatants were collected after 24 and 48 h post infection. B) a) Viral RNA quantification by qRT-PCR from siNTG (black bars) and siTIA-1 (white bars) samples. Total RNA was extracted and reverse transcribed. TBEV amplification products were normalized to β-actin. b) Plaque assay from siNTG and siTIA-1 supernatants. Viral particle production per mililiter (pfu/ml) was measured from siNTG (black bars) and siTIA-1 (white bars) samples. Data were averaged from three independent experiments and are represented as mean ± standard deviation. Significant *p*-values were calculated with paired (a) and unpaired (b) *t*-test ($p<0.001$=***; $p<0.01$=**; $p<0.05$=*). C) Efficiency of TIA-1 knockdown. Immunoblotting against TIA-1 (upper panel) and β-actin (lower panel) as a loading control.

In order to corroborate the knockdown observations, mouse embryonic fibroblasts cells (MEF) knockout for TIA-1 were used (Figure 38). Therefore wild type MEF and TIA-1 kO cells were infected at MOI of 2. Cells and supernatants were collected after 0, 24 and 48 hours post infection. Viral RNA levels were increased at 24 and 48 h.p.i. in MEF TIA-1 kO cells with respect to MEF WT (Figure 38 A). Moreover, viral titer was increased in these cells compared to control MEF cells (Figure 38 B).

A B

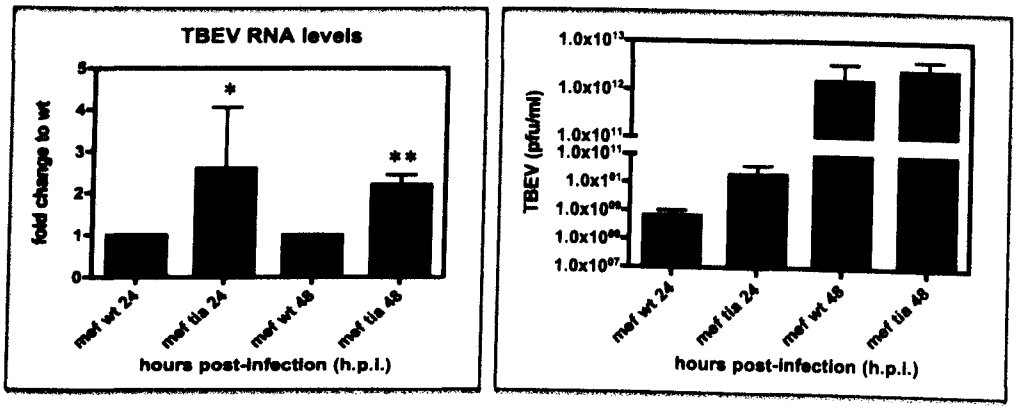


**Figure 38: TBEV replication in MEF wt and TIA-1 knockout cells**

TBEV replication in MEF TIA-1 knockout cells. MEF wt and TIA-1 kO were infected with TBEV at a MOI of 2. After 24 and 48 hours, samples for RNA extraction and supernatants were harvested. A) Viral RNA quantification by qRT-PCR from MEF wt (black bars) and MEF TIA-1 kO (grey bars) samples. Total RNA was extracted and reverse transcribed. TBEV amplification products were normalized to β-actin. B) Plaque assay from MEF wt and MEF TIA-1 kO supernatants. Viral particle production per mililiter (pfu/ml) was measured from MEF wt (black bars) and MEF TIA-1 kO (grey bars) samples. Data were averaged from three independent experiments and are represented as mean ± standard deviation. Significant *p*-values were calculated with paired (a) and unpaired (b) *t*-test ($p<0.001$=***; $p<0.01$=**; $p<0.05$=*).

In order to compare the functional relevance of TIA-1 with other stress-response proteins during TBEV infection, knockdown analysis for TIAR was performed (Figure 39). After 48 hours siTIAR and siNTG transfection, U2OS cells were infected at a MOI of 2. Cells were harvested at 0-24-48 hours post infection (hpi) and total RNA extracts were analyzed for viral RNA expression by RT-qPCR. Supernatants were collected at 24 and 48 hpi to evaluate extracellular infectivity (Figure 39A). As shown in figures 39 Ba and Bb, viral RNA levels and viral particle production are increased in siTIAR cells with respect to siNTG over the time, respectively. After 48 hours post infection, no changes in extracellular infectivity was observed between both conditions (Figure 39 Bb), which can be due to saturation in the amount of viral particles produced therefore it was difficult to observe a difference. Efficient TIAR knockdown was observed during the time of infection (Figure 39 C). .

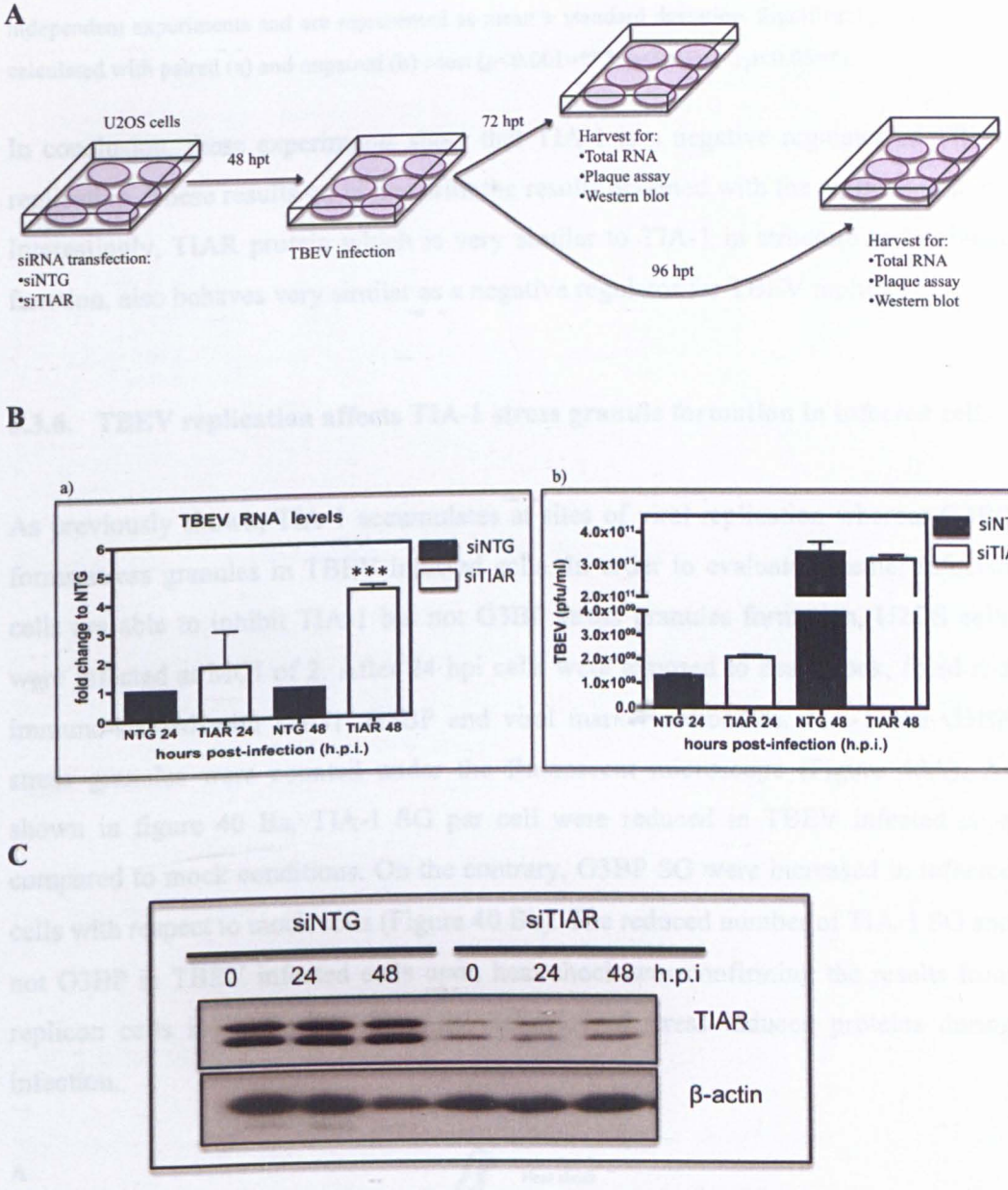


**Figure 39: TIAR is a negative regulator of TBEV replication in infected cells**

TIAR knockdown experiment in U2OS cells. A) Schematic design of the experiment. U2OS cells were transfected with siNTG (small interfering non targeting RNA) and siTIAR. After 48 h post transfection, cells were infected at a MOI of 2. Samples for RNA extraction, immunoblotting and supernatants were collected after 24 and 48 h post infection. B) a) Viral RNA quantification by qRT-PCR from siNTG (black bars) and siTIAR (grey bars) samples. Total RNA was extracted and reverse transcribed. TBEV amplification products were normalized to β-actin. b) Plaque assay from siNTG and siTIAR supernatants. Viral particle production per mililiter (pfu/ml) was measured from siNTG (black

bars) and siTIAR (white bars) samples. C) Efficiency of TIAR knockdown. Immunoblotting against TIAR (upper panel) and β-actin (lower panel) as a loading control. Data were averaged from three independent experiments and are represented as mean ± standard deviation. Significant *p*-values were calculated with paired (a) and unpaired (b) *t*-test ($p<0.001$=***; $p<0.01$=**; $p<0.05$=*).

In conclusion, these experiments show that TIA-1 is a negative regulator of TBEV replication. These results go in line with the results obtained with the replicon system. Interestingly, TIAR protein which is very similar to TIA-1 in structure and cellular function, also behaves very similar as a negative regulator for TBEV replication.

### 3.3.6. TBEV replication affects TIA-1 stress granule formation in infected cells

As previously shown, TIA-1 accumulates at sites of viral replication whereas G3BP forms stress granules in TBEV infected cells. In order to evaluate whether infected cells are able to inhibit TIA-1 but not G3BP stress granules formation, U2OS cells were infected at MOI of 2. After 24 hpi cells were exposed to heat shock, fixed and immuno-stained with TIA-1, G3BP and viral marker antibodies. TIA-1 and G3BP stress granules were counted under the fluorescent microscope (Figure 40A). As shown in figure 40 Ba, TIA-1 SG per cell were reduced in TBEV infected cells compared to mock conditions. On the contrary, G3BP SG were increased in infected cells with respect to mock cells (Figure 40 Bb). The reduced number of TIA-1 SG and not G3BP in TBEV infected cells upon heat shock was confirming the results from replicon cells indicating a differential behavior of stress induced proteins during infection.

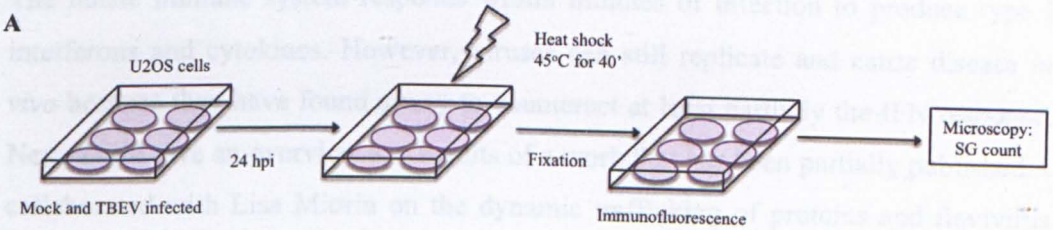

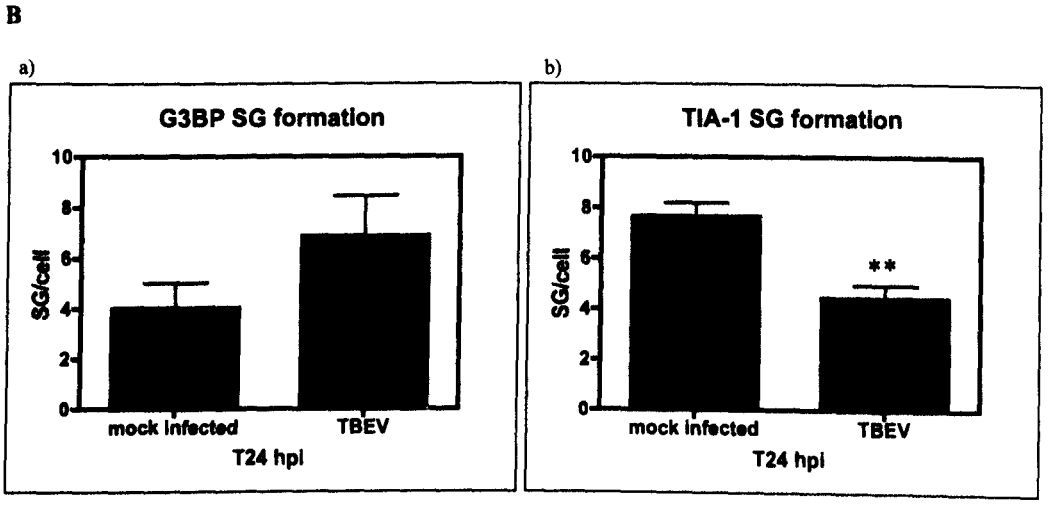


**Figure 40: TBEV replication does not inhibit G3BP stress granules formation**

Immunofluorescence studies in U2OS cells exposed to heat shock and infected with TBEV. A) Schematic representation of the experiment. U2OS cells were either mock and TBEV infected. 24 h post infection cells were exposed to 45°C for 40 minutes, fixed and incubated with specific antibodies. B) a) Quantified TIA-1 stress granules per cell in mock infected and TBEV infected cells. b) Quantified G3BP stress granules per cell in mock infected and TBEV infected cells. A number of 100 cells were counted per condition. Data were averaged from three independent experiments and are represented as mean ± standard deviation. Significant *p*-values were calculated with unpaired *t*-test ($p<0.001$=***; $p<0.01$=**; $p<0.05$=*).

## 3.4. Immune response to viral infection

The innate immune system responds within minutes of infection to produce type I interferons and cytokines. However, viruses can still replicate and cause disease *in vivo* because they have found a way to counteract at least partially the IFN response. Next, I will give an overview and results of a work that has been partially published. I collaborated with Lisa Miorin on the dynamic trafficking of proteins and flavivirus RNAs between replication compartments and the cytosol. RNA viruses like TBEV induce host cell membrane rearrangements to replicate efficiently and possibly to escape from innate immunity. In this work she exploited the tick-borne encephalitis flavivirus as a model to address the dynamics of virus-induced vesicle formation. She initially observed a consistent delay of interferon induction following virus

replication. Delay in interferon induction correlated with a defect in pattern recognition receptor's signalling. However, viral proteins could not directly inhibit the pathway suggesting an indirect mechanism. In order to dissect the role of replication compartments in this delay we explored protein and viral RNA trafficking in the living cell. We found that the replication compartment is able to exchange proteins with the cytosol. However, replicated viral RNA trafficking to the cytosol was significantly impaired. We conclude that TBEV replication compartments established early during infection allow exchange of proteins with the cytosol, but this is insufficient to allow IRF-3 signaling and interferon induction (Miorin et al, 2012).

### 3.4.1. RIG-I characterization during TBEV infection

A wide range of cells in the body is capable of displaying antiviral innate immunological responses upon viral infection. RLRs sense cytoplasmic viral RNA and activate the immunological response, including the production of type I interferon (IFN) and cytokines (Yoneyama et al, 2005; Yoneyama et al, 2004). Members of this family such us RIG-I and MDA-5 have been shown to sense specific types of viruses. Whereas MDA-5 recognizes picornaviruses (Kato et al, 2006), RIG-I senses viruses like Japanese encephalitis (JEV) and West Nile (WNV) (Fredericksen & Gale, 2006; Kato et al, 2006) among others. In order to identify the pattern recognition receptor/s that is involved in triggering interferon expression during TBEV infection, a knockdown experiment was performed in U2OS cells (Figure 41). Cells were transfected in parallel with control siRNA (NTG), siRNA against MDA-5 and siRNA for RIG-I. After 48 hours post transfection, U2OS cells were infected at a MOI of 2. Samples were collected after T0, 4, 8 and 24 hours post infection for total RNA extraction, cDNA production and quantification by qRT-PCR (Figure 41A). As shown in figure 41Ba, after 24 hpi IFN expression in siNTG cells was increased. Interestingly, in RIG-I knockdown cells, interferon expression was reduced but not siMDA-5 compared to siNTG. Efficient RIG-I and MDA-5 mRNA knockdown was observed (Figures 41Bb and Bc, respectively). This data suggested that RIG-I is the pattern recognition receptor that was triggering IFN expression during TBEV infection.

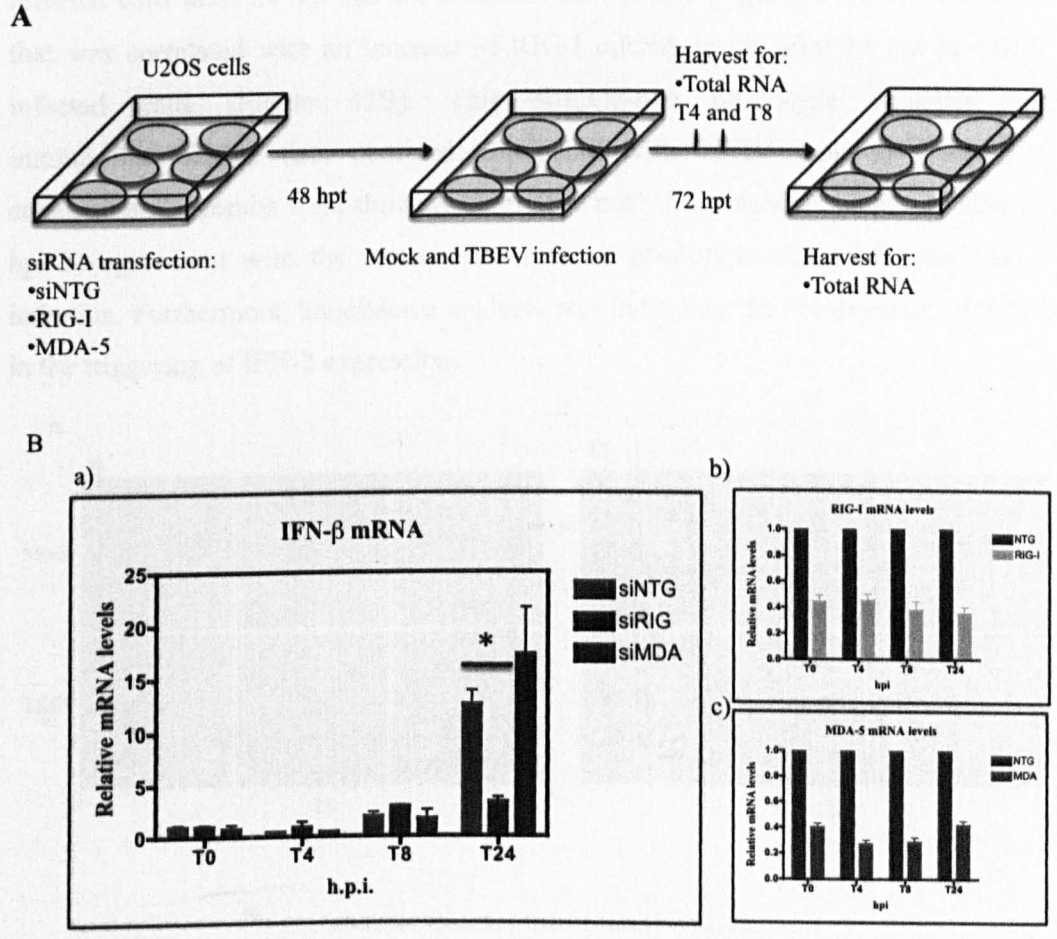


**Figure 41: RIG-I but not MDA-5 is involved in triggering IFN b expression in TBEV infected cells**

RIG-I and MDA-5 knockdown in U2OS cells. A) Flow chart of the experiment. U2OS cells were transfected with siNTG (non targeting), siRIG-I and siMDA-5. After 48 hpt, cells were mock and TBEV infected. Samples for RNA extraction were collected at T0, 4, 8 and 24 hours post infection. B) a) IFN-β mRNA quantification by qRT-PCR from siNTG (grey bars), siRIG-I (red bars) and siMDA-5 (blue bars) samples in TBEV infected cells. Total RNA was extracted and reverse transcribed. IFN-β amplification products were normalized to β-actin (Miorin, 2012). b) Efficiency of RIG-I knockdown. Quantification of RIG-I mRNA levels in control NTG cells (grey bars) and siRIG-I cells (yellow bars). c) Quantification of MDA-5 mRNA levels in control NTG cells (grey bars) and siMDA-5 cells (yellow bars). Data were averaged from three independent experiments and are represented as mean ± standard deviation. Significant *p*-values were calculated with unpaired *t*-test ($p<0.001$=***; $p<0.01$=**; $p<0.05$=*).

Immunofluorescence analysis showed a speckle-like distribution of RIG-I in TBEV infected cells after 24 hpi but not at earlier time points (Figure 42A), a observation that was correlated with an increase of RIG-I mRNA levels after 24 hpi in TBEV infected cells (Figure 42B). This speckle-like phenotype validated the immunofluorescence data obtained previously with TBEV replicon system. In conclusion, the results were showing that RIG-I mRNA levels were increased after 24 hpi in agreement with the immunofluorescence phenotype observed upon TBEV infection. Furthermore, knockdown analysis was indicating the involvement of RIG-I in the triggering of IFN-β expression.

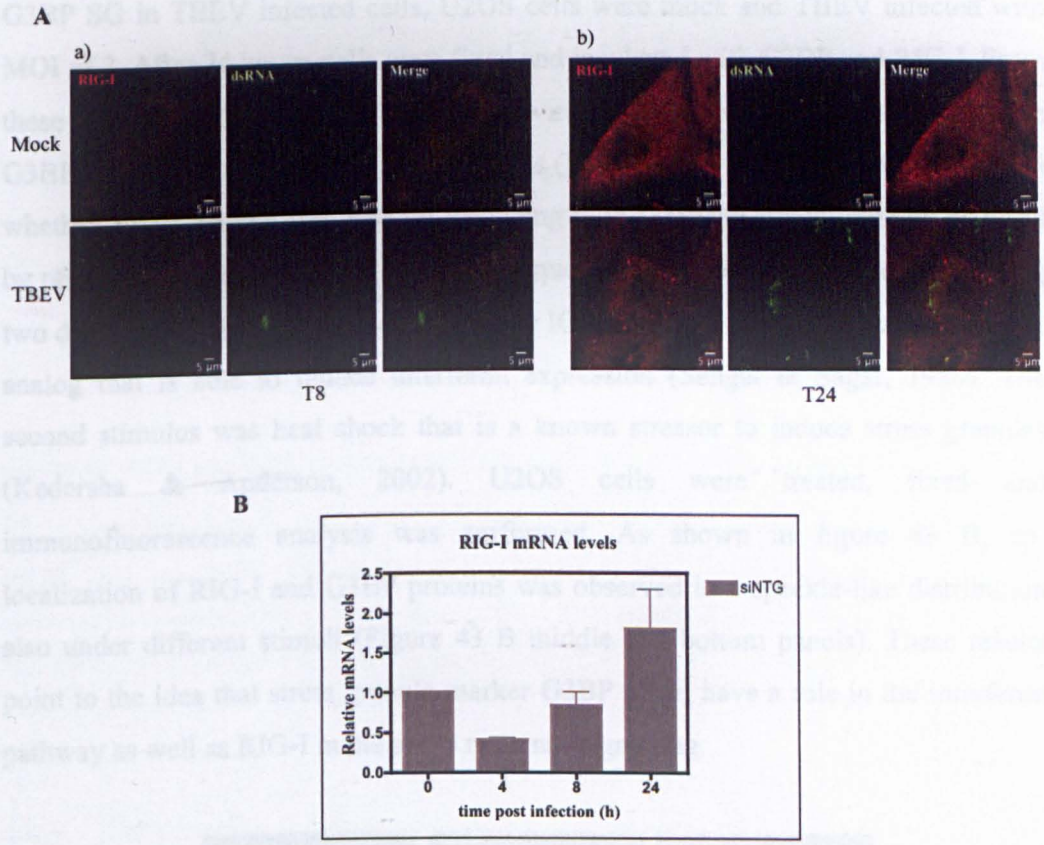


**Figure 42: Characterization of RIG-I in TBEV infected cells**

Cellular localization and expression levels of RIG-I in TBEV infected cells. A) U2OS cells were mock and TBEV infected. After 8 and 24 hours post infection were fixed and incubated with antibodies against RIG-I (red) and dsRNA(green). a) Mock (upper panels) and TBEV (lower panels) infected U2OS cells after 8 hours of infection. b) Mock (upper panels) and TBEV (lower panels) infected U2OS cells after 24 hours of infection. B) RIG-I mRNA quantification by qRT-PCR from siNTG (grey bars) samples in infected cells. Data were averaged from three independent experiments and are represented

as mean ± standard deviation. Significant *p*-values were calculated with unpaired *t*-test ($p<0.001$=***; $p<0.01$=**; $p<0.05$=*).

### 3.4.2. Stress granules from TBEV infected cells contain G3BP and RIG-I

RIG-I speckle-like distribution in TBEV replicon and infected cells was very similar to the G3BP SG phenotype observed in TBEV infected cells. Furthermore, there was shown in a recent publication, that RIG-I co-localized with G3BP in Influenza A infected cells (Onomoto et al, 2012). To test whether RIG-I was co-localizing with G3BP SG in TBEV infected cells, U2OS cells were mock and TBEV infected with MOI of 2. After 24 hours, cells were fixed and incubated with G3BP and RIG-I. From these experiments, I could confirm that antiviral RIG-I protein was co-localizing with G3BP stress granules in TBEV infected cells (Figure 43A). Next, I asked the question whether RIG-I protein was also co-localizing with G3BP in stress granules induced by other stimuli than virus. To address this question I performed an experiment using two different stimuli. The first one was Poly IC which is a long double-stranded RNA analog that is able to induce interferon expression (Sehgal & Sagar, 1980). The second stimulus was heat shock that is a known stressor to induce stress granules (Kedersha & Anderson, 2002). U2OS cells were treated, fixed and immunofluorescence analysis was performed. As shown in figure 43 B, co-localization of RIG-I and G3BP proteins was observed in a speckle-like distribution also under different stimuli (Figure 43 B middle and bottom panels). These results point to the idea that stress granule marker G3BP could have a role in the interferon pathway as well as RIG-I in the stress response signalling.

A

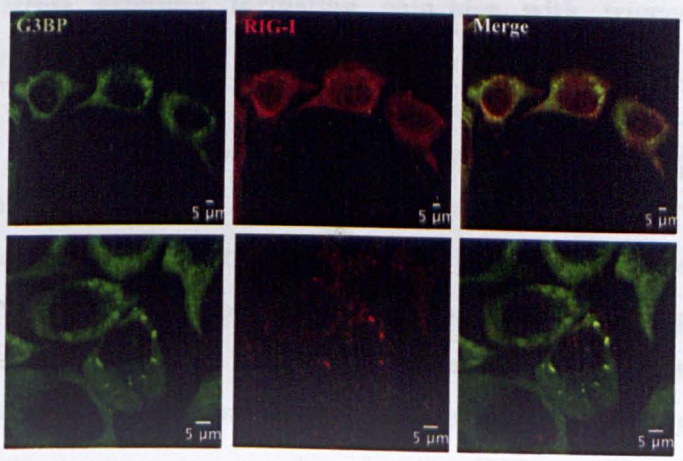

**B**

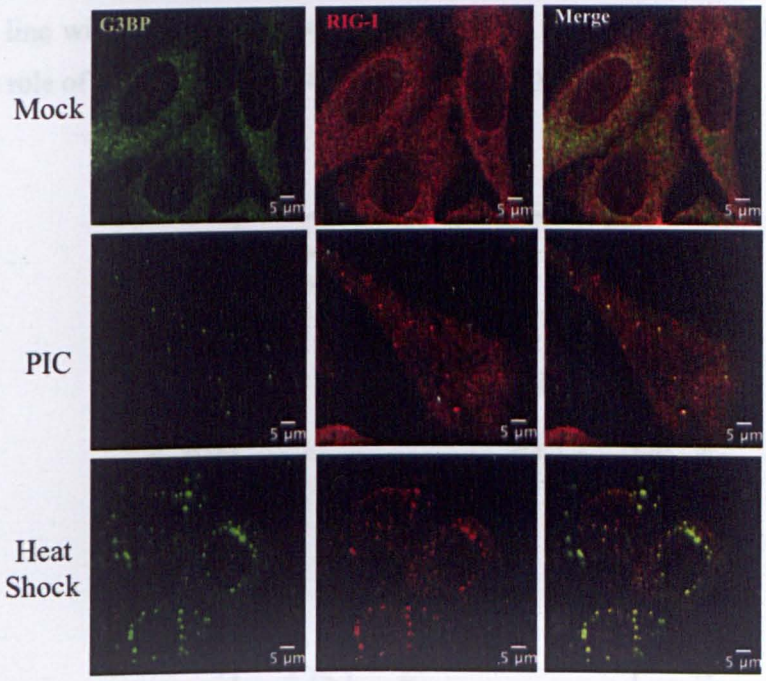


**Figure 43: RIG-I and G3BP co-localize in SG in TBEV infected cells and under different stresses**

RIG-I and G3BP cellular localization in U2OS cells exposed to different stressors. A) Cells were mock (upper row) and TBEV infected (lower row). After 24 hours post infection were fixed and immunostained with specific antibodies against RIG-I (red) and G3BP (green). B) U2OS were exposed to different stimuli: without stress (upper panel), Poly IC (PIC) (middle panel) and 45°C for 40' heat shock (lower panel).

### 3.4.3. G3BP stress granules formation coincides with triggering of IFN expression

From previous published data, we showed a delay in interferon expression upon TBEV infection. We could show an increase of viral RNA levels between 4 and 8 hours after infection, while induction of IFN-β levels started only after 12 hours in TBEV infected cells with a stronger increment between 16-20 h post infection (Miorin et al, 2012) (Figure 44 A). Therefore, in order to gain insight into the possible link between G3BP SG formation and interferon response, a time course during

TBEV infection was performed. U2OS cells were infected with TBEV at MOI of 2 and were fixed every 4 hours after infection until 24 hpi. Immunofluorescence analysis was performed using anti-TBEV and G3BP antibodies. As observed in figure 44 B, G3BP stress granules start to appear around 16 h post infection. These data were in line with the increment of IFN expression leading to the conclusion of the possible role of G3BP SG during innate immune response.

**A**

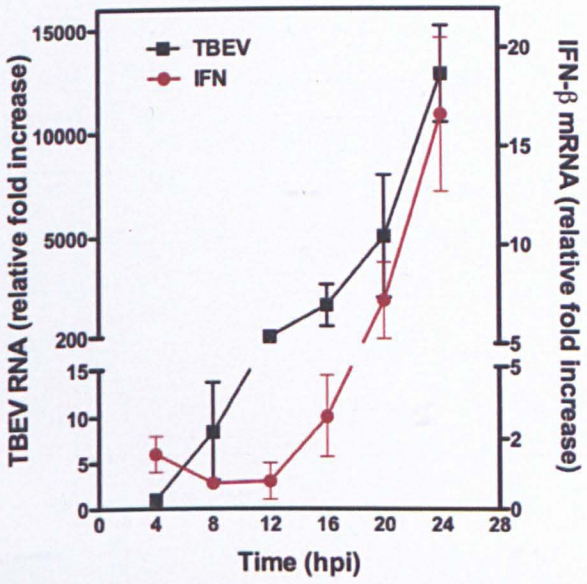


**B**

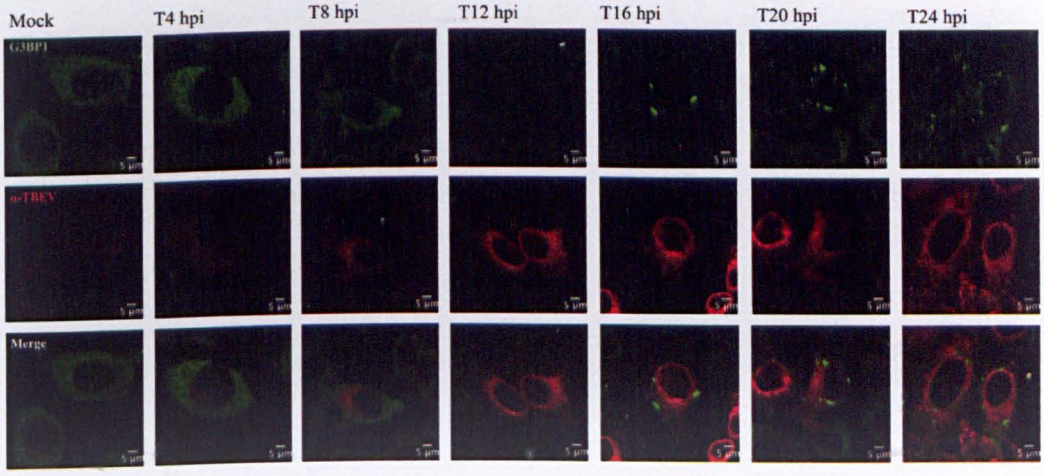


**Figure 44: G3BP stress granules formation coincides with triggering of IFN expresión**

Time course of TBEV replication in U2OS cells. A) Delayed induction of IFNβ by TBEV. U2OS cells were either mock infected or infected with TBEV. At different time points, cell extracts were collected.

Total RNA was isolated, retro-transcribed and quantified by qRT-PCR. TBEV RNA levels (black squares) and IFNβ mRNA (red circles) levels are expressed as fold increase relative to time 4 hpi TBEV RNA and to mock infected U2OS cells for IFNβ mRNA (graph taken from Miorin, 2012). B) Time course of G3BP stress granules formation during TBEV infection. U2OS cells were mock or TBEV infected at a MOI of 2. Cells were fixed every 4 hours after infection until 24 hours. U2OS cells were immunostained with antibodies against G3BP (green) and anti-TBEV (red).

# 4. DISCUSSION

Viruses are intracellular parasites that require the cellular machinery to initiate and maintain a productive infection. In particular, positive-strand RNA viruses have the need to rapidly translate genomic RNA. The viral non structural proteins produced serve as a scaffold to induce host membrane rearrangement that are required for replication. These replication sites are associated with perinuclear membranes and are composed of viral RNA as well as viral and possibly host proteins. During the viral life cycle, genomic RNA is exposed to different cellular responses such us the RNA decay machinery, the stress response pathway and the immune response. In the present thesis I have studied the cellular localization of host cellular factors involved in the host response with respect to flavivirus infection. I could characterize the role of the stress response protein TIA-1 during TBEV replication. Taking advantage of both infectious virus and a sub-genomic replicon system I could specifically study viral replication. I could demonstrate that TIA-1 and its related protein TIAR localize at the viral replication sites while G3BP, another stress response protein, was not. These results were indicative of the specific response of TIA-1 and not a general feature of stress response proteins. Moreover, TIA-1 bound to viral RNA indicating its participation in viral RNA metabolism. Interestingly, this phenotype was observed in cells where active viral RNA synthesis occurred indicating a specific response during TBEV replication. TBEV infected cells were showing a reduced number of TIA-1 cytoplasmic granules compared to the other stress granule marker G3BP when cells were exposed to stress. Also, I could show that TIA-1 depletion, greatly enhanced the early step of subgenomic replicon luciferase activity, consistent with an inhibitory role in early viral RNA translation. Furthermore I described the involvement of the innate immune response protein RIG-I as the pattern recognition receptor that triggers IFNβ expression during TBEV infection. In addition to these results, RIG-I co-localized with stress response protein G3BP during TBEV infection. This co-localization was also observed when cells were exposed to other non-viral stresses, suggesting an interplay between stress pathway and innate immune response proteins. Whether stress granule formation is inducing IFNβ expression is a question under study.

## 4.1. Identification and functional characterization of putative host factors involved in Tick-borne Encephalitis virus infection.

### 4.1.1. Development of a cell line that recapitulates TBEV replication for RNAi screening

RNA interference (RNAi) screens have become important tools to identify host factors involved in the viral life cycle. Several RNAi screens have been performed for HCV but much less for flaviviruses. Even though they belong to the same family there are differences in the host factors required for replication. An example is PI4KIIIα which was found to be essential for HCV replication (Berger et al, 2009). On the contrary, the absence of this factor did not cause any effect in the replication of Dengue and West Nile viruses (Martin-Acebes et al, 2011; Reiss et al, 2011). A common characteristic of these screens was the use of fully infectious viruses in a susceptible cell line. The information obtained concerns all steps of the virus life cycle including entry, replication, assembly and egress, that must be then validated by conventional techniques. Therefore, in order to narrow the study to host factors that were involved only during viral replication I tried to generate a TBEV replicon cell line. For this purpose, I produced a TBEV replicon that encoded for the non-structural proteins (from NS1 to NS5) as well as the firefly luciferase-neomycin phosphotransferase fusion protein. Moreover, it contained an ECMV IRES-EGFP cassette at the 3'NCR (Figure 10C). Such a construct allows for: i) selection of the clones carrying the replicon with the neomycin gene upon exposure of cells to G418, ii) a reporter for viral replication like the luciferase gene, iii) a reporter for replication like GFP that permits cell imaging as a readout for high-throughput analysis. The replication ability of the engineered sub-genomic replicon was assessed in U2OS cells by different approaches, as described in section 1.2.1 from results.

Firefly luciferase activity is a linear function of replicon RNA copy number and therefore permits sensitive and rapid quantitation of TBEV replication. Consistently, through luciferase activity assay I could demonstrate that TBE-LUC-NEO_EGFP construct was efficiently replicating after three days of transfection in U2OS cells (Figure 11 B) and EGFP was also expressed during this period of time (Figure 12). On the other hand, by the characterization of TBEV replication for a longer period of time I was able to show through EGFP expression analysis that the number of cells

containing the replicon was decreasing over time (Figure 13 B). The increased levels of luciferase activity as well as intensity of EGFP expression over time were indicative of active replication (Figures 13 A and B, respectively). However, only a low number of cells in the culture supported TBEV replication. This idea prompted me to add the antibiotic for selection at different concentrations and time points after transfection in order to find a suitable condition for selection. The absence of surviving clones upon drug selection suggested that the cell line used might be non permissive or support only low levels of viral RNA replication.

Baby hamster kidney (BHK-21) cells have been shown to be a more permissive cell line for flaviviruses (Lo et al, 2003). Therefore, in order to obtain a stably TBEV replicating cell line I characterized TBE-LUC-NEO_EGFP replication in these cells. The increase in luciferase activity over seven days was suggesting active viral replication (Figure 14 A). Moreover, through flow cytometry analysis I could demonstrate the presence of a stable EGFP positive population over seven days (Figure 14 B). Disappointingly, after weeks of selection with G418 I was not able to detect any surviving clone. One reason why the stable cell line was not generated could be due to low neomycin expression from the replicon which was not sufficient to sustain a stable transfection. However, there is no sensitive assay to address this question. Finally, I concluded that the replicon was not efficiently replicating in order to obtain the stable cell line. Tai and co-workers validated the reporter luciferase-neomycin fusion approach by using a HCV replicon cell line to perform a whole-genome RNAi screen. By using this system, they were able to identify host factors affecting viral replication. Among those factors, PI4KA was found to strongly inhibit HCV replication. These results were confirmed with the fully infectious JFH1 HCV strain (Tai et al, 2009). For the future, I would propose to clone the neomycin reporter gene separate from luciferase gene under the control of another translation promoter such as EMCV IRES or HCV IRES (Supekova et al, 2008). Another possibility would be to replace the luciferase gene with the neomycin gene since this replicon already contains the EGFP reporter gene for the readout. The idea to place the neomycin gene under a control of an independent translation promoter was to ensure proper translation. Alternatively, to change neomycin for another selectable gene such as blasticidin S deaminase or hygromycin phosphotransferase which have been shown to be successful in the selection of positives clones (Appel et al, 2005; Evans et al, 2004).

### 4.1.2. Study of cellular localization of RNA binding proteins in TBEV replicon cells

Another possibility to study host factors involved in viral replication is based on careful identification of protein candidates and their validation. Since I was interested in the study of host factors involved in viral RNA replication, I analyzed cellular RNA binding proteins taking advantage of the TBEV MS2 replicon system developed in our laboratory (Miorin et al, 2008). The method, was based on the binding of the MS2 phage core protein to its related RNA binding sites has been proposed for the detection of viral RNA genomes (Basyuk et al, 2003; Beckham et al, 2007; Boireau et al, 2007). The possibility of detecting viral RNA in living cells allows the analysis of the dynamic recruitment of host and viral factors to the viral genome to be measured in real time in order to build a kinetic model of the process (Dundr & Misteli, 2003; Molle et al, 2007). In this study I investigated the cellular localization of determined host factors upon TBEV RNA biosynthesis. Among the cellular proteins that were studied only TIA-1 and RIG-I proteins showed a different cellular localization in TBEV replicon cells compared to the non-replicative construct (Figures 18 and 19, respectively). The fact that I could not observe any difference in the cellular localization of PTB, DCP1, AGO2 and NF-90 proteins during TBEV replication does not mean they have no role in other steps of the viral life cycle. Perhaps the use of full-length virus could give us a deeper understanding of the role of these host proteins in the entire process. Moreover, RNAi studies can contribute to determining the functional relevance of the proteins in TBEV viral replication. By knocking down the expression of the protein it is possible to study the possible involvement of the RNA-binding proteins in viral RNA metabolism.

### 4.1.3. Characterization of TIA-1 upon TBEV replication

TIA-1 cellular localization in TBEV cells

As previously mentioned, I used the MS2-tagging system to monitor viral RNA replication in human cells. I could demonstrate by using a specific antibody that TIA-1 was accumulating at sites of viral replication due to the co-localization with MS2-tagged viral RNA. Consistent with these results I could confirm that the sites of TIA-1 accumulation were viral replication factories by the co-localization with TBEV viral proteins and double-stranded RNA (Figures 23 A and B, respectively). The fact that TIA-1 exhibited a normal cellular localization in GAA-mutant replicon cells suggested that the re-localization was in response to either active replication and/or RNA accumulation (Figure 23). Furthermore, TIA-1 recruitment to sites of viral replication was demonstrated by using fully infectious TBEV (Figure 31). Cellular localization of stress granules markers TIAR and G3BP was also analyzed in TBEV infected cells. A TIAR immunofluorescence assay showed recruitment of the protein to sites of viral replication as observed for TIA-1 consistent with their functional redundancy (Figure 32) (Kawakami et al, 1992). Moreover I could not observe neither the presence of TIA-1 nor TIAR SGs in infected cells. On the contrary, by immunofluorescence studies I could observe that G3BP stress protein formed SG in TBEV infected cells without co-localization to sites of viral replication (Figure 33). Additionally, I confirmed that these G3BP SG were also positive for the eIF3 initiation of translation factor (Figure 34). These results reinforce the notion that there is SG formation following TBEV infection but they lack TIA-1 and TIAR. Accordingly, with SG formation, the phosphorylation of eIF2α was observed. Consistent with our data the recruitment of TIA-1 and TIAR proteins to replication complexes without SG formation has been also observed for West Nile virus (WNV) and Dengue virus (Denv2) in BHK-21 cells (Emara, 2007). In this work they showed through immunofluorescence studies that TIA-1 and TIAR were present in the replication complexes of WNV and Denv2 infected cells without formation of TIA-1/TIAR cytoplasmic granules concluding that flaviviruses did not induce SG. On the other hand, a recent work has shown that G3BP protein is also recruited to sites of viral replication during Denv2 infection (Ward et al, 2011). Although Emara's work did not study G3BP cellular localization, the data from both publications indicate that

during Denv2 infection the recruitment of stress response proteins could be due to a general response pathway than to specific proteins itself . In conclusion, our results reveal that the stress response pathway is induced upon TBEV infection indicated by the presence of G3BP SG formation. However, recruitment of TIA-1 and TIAR to sites of viral replication seems to be a specific function of these proteins and independent of SG formation. Evidence that supports this idea comes from immunofluorescence studies performed in MEF TIA-1 knockout TBEV infected cells where G3BP SG formation is observed (data not shown).

The observation of TIA-1 recruitment to sites of viral replication prompted me to study whether the host protein was binding to viral RNA. To address this question I performed TIA-1 pull-down analysis in TBEV infected cells and mock infected cells (Figure 36A). PCR on RNA extracted pull-downs revealed the presence of viral RNA in TIA-1 samples (Figure 36 C). Additionally, in this study TIAR protein was found in TIA-1 pull-down samples but not G3BP stress protein (Figure 36 B). The accuracy of the experiment was confirmed by using β-Actin as positive control since it has been shown that actin transcripts interact with TIA-1 in heat shock cells (Lopez de Silanes et al, 2005). Moreover from biochemical studies, the binding of TIA-1 as well as TIAR to the negative strand of WNV 3'-NCR was described (Li et al, 2002). In this work, *in vitro* transcribed WNV 3(-) SL RNA was attached to an agarose adipic acid matrix and subsequently cell extracts from BHK-21 were passed through the column. Each elution from the column was tested for viral RNA binding activity using gel mobility shift and UV-induced cross-linking assays. The interaction between WNV 3(-) SL and TIA-1/TIAR was confirmed using recombinant proteins. However these biochemical analyses were described using a partial portion of genomic viral RNA and even more they did not prove it in infected cells. During the different steps of the life cycle, viral RNA is exposed to diverse cellular pathways. In the TIA-1 pull down assay of TBEV infected cells I was able to demonstrate that after 24 hpi TIA-1 bound to viral RNA. In agreement with these results, the binding of stress response proteins such as Caprin-1, G3BP1 and G3BP2, and USP10 to the variable region of the 3'NCR of Denv2 has been shown (Ward et al, 2011). They proposed that the various mRNP complexes that bind to the viral 3'NCR and the viral RNA might act as a platform for recruitment of protein complexes that function in different steps of viral life cycle.

In conclusion, I could show that TIA-1 and TIAR proteins are recruited to sites of viral replication in human cells in response to TBEV infection. Moreover the binding of TIA-1 to viral RNA leads to speculation about a possible role of these proteins during TBEV replication.

TIA-1 restricts viral replication

In order to understand the functional relevance of this phenotype I transfected the TBEV replicon into mouse embryonic fibroblast (MEF) knockout cells for TIA-1. In these cells I could show a significant increase in the luciferase activity from the replicon compared to WT MEF (Figure 24). Since luciferase activity is directly proportional to viral replication I concluded that TIA-1 has a negative role during TBEV replication. Moreover, I confirmed these results by infecting TIA-1 siRNA U2OS cells as well as MEF TIA-1 knockout cells with fully infectious TBEV (Figures 37 and 38, respectively). Increased TBEV RNA levels and extracellular infectivity was also observed in TIAR knockdown cells validating the functional similarity of these two proteins. The modest effect caused in viral RNA synthesis in the absence of TIA-1 raises the possibility that other proteins such as TIAR might complement its function. Next, the question that rose from these results was at what level of viral replication TIA-1 was affecting either viral translation and/or RNA synthesis. For this aim, I used the TBEV replicon system that describes two peaks of luciferase activity: i) the first peak of luciferase activity within the first 4 hpt is due to the translation of the input RNA; ii) the second peak of luciferase activity comes from the translation of the newly synthesized RNA (Hoenninger et al, 2008). Briefly, any alteration in the first peak of luciferase activity is due to problems in translation, whereas alterations in the second peak indicate problems in RNA synthesis. MEF TIA-1 replicon cells showed significantly higher luciferase activity at the first peak than MEF wt replicon cells after 4 hpt. This difference was even greater at the second peak after 24 hours post transfection in MEF TIA-1 KO cells (Figure 25). These data suggested that TIA-1 was affecting viral replication at the level of the first round of translation and consequently, RNA synthesis. Piecyk and collaborators have shown the role of TIA-1 as a translational silencer for TNF-α transcripts (Piecyk et al, 2000). In this work, they have demonstrated that the absence of TIA-1 in LPS-stimulated cells significantly increases the proportion of TNF-α transcripts that associate with

polysomes suggesting its role as a translational repressor. Expression of TNF-α mRNA was similar between wt and TIA-1$^{-/-}$ macrophages indicating that the increased secretion of this factor is not due to higher levels of RNA. The stability of these transcripts was not significantly different in these cells. Similar work with another cellular factor COX-2 demonstrated the negative role of TIA-1 during translation (Dixon et al, 2003). This evidence suggested a role for TIA-1 as a translational silencer that regulates the cellular and micro-organismal response to stress: i) at the cellular level, by contributing to general translational arrest that accompanies environmental stress; ii) at the micro-organismal level, by regulating the expression of cytokines in response to microbial infections. Even though it has been described the role of TIA-1 as a translational repressor for a set of cellular genes, this is the first time that it has been shown to regulate a viral system.

To confirm the negative role of TIA-1 during TBEV replication I transfected the TBEV replicon containing the luciferase gene in U2OS cells stably expressing EGFP-TIA-1 and control EGFP. Normalized luciferase levels from the TBEV replicon were reduced in these cells compared to control EGFP expressing cells at 24 hpt and the difference was less significant after 48 hpt (Figure 27). These data corroborate the specificity of the negative effect of TIA-1 during TBEV replication. The observation of a reduced TBEV replication in TIA-1 over-expressing cells can be explained by the fact that the initial translation is impaired leading to a reduced production of viral proteins that consequently reduce viral RNA synthesis.

#### 4.1.3.3 TIA-1 SG formation upon TBEV replication

In response to environmental stress TIA-1 accumulates in the cytoplasm to form stress granules (SG) (Kedersha et al, 1999). In TBEV replicon cells I did not observe TIA-1 SG formation, therefore prompted by this observation I examined whether TBEV replication was the cause of this phenotype. In order to address this question I transfected cells with the TBEV replicon and with replication-deficient TBEV construct as control. After 24 hours post transfection I exposed cells to heat shock under known stress inducing conditions (Kedersha & Anderson, 2002). TIA-1 immunofluorescence experiments indicated that the number of TIA-1 SG produced per cell in TBEV replicon cells was reduced compared to cells containing the non-replicative form of the virus. Additionally, TIA-1 was localizing at sites of viral

replication in TBEV replicon cells but not control cells (Figure 28). Furthermore, I used the G3BP SG marker in order to assess if the phenotype observed was specific for the TIA-1 protein or was a general feature of the stress response to TBEV replication. Interestingly, the number of G3BP SG per cell was increased in TBEV replicon cells compared to control replicon cells (Figure 29 B) indicating a specific behaviour of TIA-1 upon TBEV replication. This data was confirmed using TBEV infectious virus. The different protein composition in SG generally depends on the type of virus. Different viruses can block SGs such as poliovirus, HIV-1, and WNV among others (Abrahamyan et al, 2010; Emara & Brinton, 2007; White et al, 2007) but the mechanism for blocking SG has been described for only a few of them. A common pattern emerging is the destruction or sequestration of key host factors required for SG formation: i) White and colleagues showed that poliovirus 3C protease cleaves the SG-nucleating factor G3BP but there is still the presence of TIA-1 SG in infected cells. They observed G3BP SG early during infection but they would disappear at later time points post infection. Moreover, G3BP cleavage resulted in higher yields of virus but they did not show the significance of the observation. Later, they showed that TIA-1 granules were not canonical SGs but they were self-aggregated protein (White et al, 2007; White & Lloyd, 2011) ii) consistent with our data, Emara and colleagues described the observation of a reduced number of TIA-1/TIAR SG upon viral replication but they did not test other SG markers. In this work, they were suggesting a possible inhibition of TIA-1 stress granules formation driven by WNV through the sequestration of the protein to sites of replication but the potential mechanism was not addressed (Emara & Brinton, 2007). One possible mechanism of hijacking host factors such as TIA-1 recruitment to replication complexes is the production of viral sub-genomic fragments (sfRNA) by flaviviruses (Pijlman et al, 2008). Viral sub-genomic fragments (sfRNA) are products of incomplete degradation of viral genomic RNA by cellular ribonucleases, more specifically a part of 3'UTR that is resistant to cleavage. These sfRNA may contribute to the pathogenesis of the virus by antagonizing or inactivating host proteins involved in the cellular response pathway.

On the other hand, TIA-1 SG inhibition upon heat shock of infected cells can be explained by the inability of TIA-1 to exit once inside the replication complex. TBEV replication complexes are surrounded by rearranged membranes that allow the exchange of host proteins with the cytoplasm but the viral RNA is confined into

reduced areas where it is not free to move (Miorin et al, 2013). In response to TBEV infection TIA-1 relocates to sites of replication to bind viral RNA (Figure 31). Therefore, when the cell is exposed to stress such as heat shock, TIA-1 is not able to exit to the cytoplasm to form SG (Figure 28). This idea is supported by the fact that in TBEV infected cells, G3BP is not located at the sites of viral replication hence is free to form SG upon heat shock in infected cells.

### 4.1.4. Is RIG-I the bridge between innate immune response and stress response upon TBEV infection?

In eukaryotic cells, there are different cellular responses that can be triggered by viral infection. In the previous sections I discussed about the stress response and described the role of different stress response proteins during TBEV replication. Another cellular response against viruses is the innate immune response. Host pathogen recognition receptors (PRR) such as RIG-I-like receptors recognize specific pathogen-molecular patterns, which activate the transcription of several genes including interferons (IFN) and antiviral proteins. In order to identify the PRR involved in the activation of IFNβ expression during TBEV infection I performed knockdown of RIG-I and MDA-5 in U2OS cells. After 24 hours upon TBEV infection the IFNβ expression levels were reduced in RIG-I but not MDA-5 knockdown cells (Figure 41). The competence of these cells for IFNβ induction was already properly assessed (Miorin, 2012). The differential role of RIG-I and MDA-5 in the recognition of RNA viruses has been shown by Kato and colleagues. They have demonstrated that MDA-5 but not RIG-I is essential in the triggering of IFNβ production during Encephalo-myocarditis virus (EMCV) infection. On the other hand, RIG-I but not MDA-5 is involved in IFNβ induction upon Japanese encephalitis virus (JEV) infection which belongs to the flavivirus genus like TBEV (Kato et al, 2006).

Furthermore, I demonstrated that RIG-I mRNA levels were increased in TBEV infected cells and that the distribution was speckle-like in the cytoplasm (Figures 42 A and B, respectively). This specific distribution of RIG-I in the cytoplasm was observed also with the TBEV replicon. Moreover, the punctuate distribution of the antiviral protein was very similar to G3BP stress protein localization in TBEV infected cells. This observation prompted me to address whether RIG-I and G3BP

proteins were co-localizing upon TBEV infection. Immunofluorescence studies performed in TBEV infected cells confirmed the hypothesis (Figure 43). Interestingly, the co-localization of both proteins was observed also following a non-viral stimulus such us Poly I:C and heat shock (Figure 43 B). Polyinosinic-polycytidylic acid (Poly I:C) is an artificial double-stranded (ds) RNA which induces IFN expression through RIG-I or MDA-5 depending on its length (Kato et al, 2008). The co-localization observed between G3BP stress response protein with RIG-I immune response protein under different stimuli suggests interplay between both pathways. Onomoto and collaborators have shown the co-localization of RIG-I with G3BP and TIAR stress proteins in cells infected with a mutant Influenza A virus (IAV) that lacks NS1 viral protein, a potent inhibitor of IFN production. They also observed this phenotype under oxidative stress conditions but they showed that only infected cells display an increase in IFNβ expression (Onomoto et al, 2012). In this work it is suggested that the granules that contain RIG-I are antiviral and therefore their composition is different from the conventional granules. Moreover, it is proposed that the antiviral granules are involved in the immune response however the over-expression of IPS-1 which triggers IFNβ expression was not inducing SGs.

In the work of Miorin and collaborators we have demonstrated a delay in INFβ expression upon TBEV infection (Figure 44 A) (Miorin et al, 2012). Moreover, we could show that this delay was not imputable to the lack of TBEV agonists but to the protected environment where they are contained. It has been shown that positive strand RNA viruses manipulate host cell membranes in order to build the replication complexes which protect viral RNA from RNase treatment (Miorin et al, 2012; Welsch et al, 2009). Therefore, the replication complexes not only represent the site of viral replication but also a barrier for PRR detection. The observation of a delayed IFNβ expression prompted me to assess if there was a relation between this event and G3BP stress granule formation. To address this question I performed a TBEV infection time course and analyzed G3BP SG formation through immunofluorescence studies (Figure 44B). Clearly, I could demonstrate that the formation of G3BP SG at different time points post infection was correlated with an increase in IFNβ expression. Whether these two events are directly related is something that must be investigated. A recent report showed that non-structural protein 1 (NS1) from Influenza A virus, which is a known inhibitor of the IFN pathway, also inhibited stress granules (Khaperskyy et al, 2012). On the other hand, Langereis and colleagues

have evidence that stress granule formation is not required for triggering of IFN expression during EMCV infection (Langereis et al, 2013). Moreover, activation of the RIG-I like receptor (RLR) pathway did not trigger and was not a prerequisite for SG formation. The lack of connection between both pathways observed by Langereis can be specific for the viral system used, type of cell line or treatment conditions applied. Our preliminary results indicate that treatment of uninfected MEF cells with IFN is inducing G3BP stress granules formation and this effect is increased when cells are infected with TBEV. Further analysis should be performed in order to address a direct relation between these two events such us knocking-down RIG-I protein levels and assessing G3BP SG formation upon TBEV infection.

## 4.2. Conclusions

In summary, I have described the cellular stress response upon TBEV replication, more specifically the role of the TIA-1 protein. The recruitment of TIA-1 to replication complexes seems to be specific for the protein and not to stress response proteins in general such as G3BP (Figure 31 and Figure 33, respectively). Consistent with its role as a translational repressor TIA-1 seems to regulate viral translation by binding to viral RNA. This idea does not support the work of Li and collaborators where they postulate the role of TIA-1 as a transcription factor during WNV RNA synthesis. From the binding of TIA-1 to WNV 3 (-) SL they were suggesting its involvement during RNA synthesis. Furthermore, I could show a decrease in TIA-1 stress granule formation but not G3BP SG in the context of stress induction by heat shock (Figure 40). Miorin and collaborators have shown that replication complexes are accessible for proteins from the cytosol but rather impermeable to replicated viral RNA egress (Miorin et al, 2013). This evidence suggests the possibility that once TIA-1 protein binds to viral RNA it is more difficult to exit the replication complexes to form stress granules unlike G3BP protein which does not enter. G3BP SG formation is also a way for the cell to respond to a stress, in this case TBEV infection (Figure 33). In this context I could demonstrate that RIG-I antiviral protein is present in the granules (Fig. 43 A). Moreover, I showed that RIG-I protein is the pattern recognition receptor involved in the activation of IFNβ expression upon TBEV infection (Figure 41 Ba). The relationship between G3BP SG formation and the

increase in IFNβ expression during TBEV infection suggests that these two events maybe connected (Figure 44). Whether G3BP-RIG-I SG formation is required for activating IFNβ expression in TBEV infected cells is something that needs to be further addressed. Another question that rises from this work is whether TIA-1 recruitment to replication complexes is an event connected to IFNβ expression. Preliminary results, suggests that in TBEV infected TIA-1 knockout MEF cells, IFNβ levels are reduced compared to WT MEF cells. Nevertheless, this work opens new questions that certainly require to be addressed in order to have a more detailed picture of the cellular response during TBEV infection.

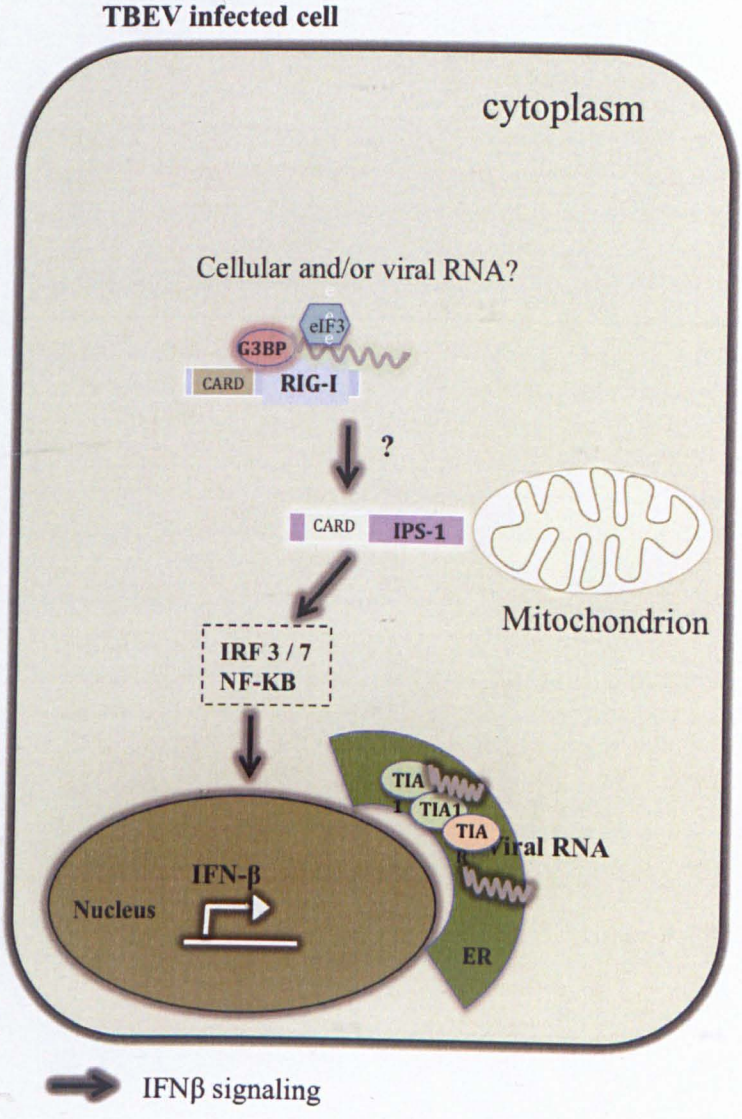

**Figure 45: Schematic model of stress and innate immune response in TBEV infected cells**

Upon TBEV infection, cytoplasmic G3BP SG (pink circle) are formed and TIA-1 and TIAR (yellow circles) proteins are localized at sites of viral replication without SG formation. Moreover, the presence of eIF3 protein in SG, indicates the possibility that also RNA is present in the granules. Perhaps, the presence and the nature of the RNA would give further information about the events during cellular response. The existence of RIG-I protein (light blue) in SG suggests a possible participation of SG formation during innate immune response. Whether G3BP-RIG-I SG formation is connected to increased IFNβ levels (black arrows) during TBEV infection, is an issue that has to be addressed. On the other hand, TIA-1 is present in sites of viral replication binding viral RNA. Further analysis to understand if this event is involved in triggering IFNβ response or is specific for stress pathway, has to be performed.

# 5. REFERENCES

## 5. References

Abrahamyan LG, Chatel-Chaix L, Ajamian L, Milev MP, Monette A, Clement JF, Song R, Lehmann M, DesGroseillers L, Laughrea M, Boccaccio G, Mouland AJ (2010) Novel Staufen1 ribonucleoproteins prevent formation of stress granules but favour encapsidation of HIV-1 genomic RNA. *J Cell Sci* **123:** 369-383

Akira S, Takeda K (2004) Toll-like receptor signalling. *Nat Rev Immunol* **4:** 499-511

Akira S, Uematsu S, Takeuchi O (2006) Pathogen recognition and innate immunity. *Cell* **124:** 783-801

Alvarez DE, Lodeiro MF, Luduena SJ, Pietrasanta LI, Gamarnik AV (2005) Long-range RNA-RNA interactions circularize the dengue virus genome. *J Virol* **79:** 6631-6643

Anderson P, Kedersha N (2002) Stressful initiations. *J Cell Sci* **115:** 3227-3234

Anderson P, Kedersha N (2006) RNA granules. *J Cell Biol* **172:** 803-808

Anderson P, Kedersha N (2009) RNA granules: post-transcriptional and epigenetic modulators of gene expression. *Nat Rev Mol Cell Biol* **10:** 430-436

Appel N, Herian U, Bartenschlager R (2005) Efficient rescue of hepatitis C virus RNA replication by trans-complementation with nonstructural protein 5A. *J Virol* **79:** 896-909

Arrigo AP, Suhan JP, Welch WJ (1988) Dynamic changes in the structure and intracellular locale of the mammalian low-molecular-weight heat shock protein. *Mol Cell Biol* **8:** 5059-5071

Ashour J, Laurent-Rolle M, Shi PY, Garcia-Sastre A (2009) NS5 of dengue virus mediates STAT2 binding and degradation. *J Virol* **83:** 5408-5418

Avirutnan P, Punyadee N, Noisakran S, Komoltri C, Thiemmeca S, Auethavornanan K, Jairungsri A, Kanlaya R, Tangthawornchaikul N, Puttikhunt C, Pattanakitsakul SN, Yenchitsomanus PT, Mongkolsapaya J, Kasinrerk W, Sittisombut N, Husmann M, Blettner M, Vasanawathana S, Bhakdi S, Malasit P (2006) Vascular leakage in severe dengue virus infections: a potential role for the nonstructural viral protein NS1 and complement. *J Infect Dis* **193:** 1078-1088

Basyuk E, Galli T, Mougel M, Blanchard JM, Sitbon M, Bertrand E (2003) Retroviral genomic RNAs are transported to the plasma membrane by endosomal vesicles. *Dev Cell* **5:** 161-174

Beck AR, Medley QG, O'Brien S, Anderson P, Streuli M (1996) Structure, tissue distribution and genomic organization of the murine RRM-type RNA binding proteins TIA-1 and TIAR. *Nucleic Acids Res* **24:** 3829-3835

Beckham CJ, Light HR, Nissan TA, Ahlquist P, Parker R, Noueiry A (2007) Interactions between brome mosaic virus RNAs and cytoplasmic processing bodies. *J Virol* **81:** 9759-9768

Berger KL, Cooper JD, Heaton NS, Yoon R, Oakland TE, Jordan TX, Mateu G, Grakoui A, Randall G (2009) Roles for endocytic trafficking and phosphatidylinositol 4-kinase III alpha in hepatitis C virus replication. *Proc Natl Acad Sci U S A* **106:** 7577-7582

Bertrand E, Chartrand P, Schaefer M, Shenoy SM, Singer RH, Long RM (1998) Localization of ASH1 mRNA particles in living yeast. *Mol Cell* **2:** 437-445

Best SM, Morris KL, Shannon JG, Robertson SJ, Mitzel DN, Park GS, Boer E, Wolfinbarger JB, Bloom ME (2005) Inhibition of interferon-stimulated JAK-STAT signaling by a tick-borne flavivirus and identification of NS5 as an interferon antagonist. *J Virol* **79:** 12828-12839

Bohnsack MT, Czaplinski K, Gorlich D (2004) Exportin 5 is a RanGTP-dependent dsRNA-binding protein that mediates nuclear export of pre-miRNAs. *RNA* **10:** 185-191

Boireau S, Maiuri P, Basyuk E, de la Mata M, Knezevich A, Pradet-Balade B, Backer V, Kornblihtt A, Marcello A, Bertrand E (2007) The transcriptional cycle of HIV-1 in real-time and live cells. *J Cell Biol* **179:** 291-304

Brandenburg B, Lee LY, Lakadamyali M, Rust MJ, Zhuang X, Hogle JM (2007) Imaging poliovirus entry in live cells. *PLoS Biol* **5:** e183

Bray M, Zhao BT, Markoff L, Eckels KH, Chanock RM, Lai CJ (1989) Mice immunized with recombinant vaccinia virus expressing dengue 4 virus structural proteins with or without nonstructural protein NS1 are protected against fatal dengue virus encephalitis. *J Virol* **63:** 2853-2856

Bressanelli S, Stiasny K, Allison SL, Stura EA, Duquerroy S, Lescar J, Heinz FX, Rey FA (2004) Structure of a flavivirus envelope glycoprotein in its low-pH-induced membrane fusion conformation. *EMBO J* **23:** 728-738

Brinkworth RI, Fairlie DP, Leung D, Young PR (1999) Homology model of the dengue 2 virus NS3 protease: putative interactions with both substrate and NS2B cofactor. *J Gen Virol* **80 ( Pt 5):** 1167-1177

Brinton MA, Dispoto JH (1988) Sequence and secondary structure analysis of the 5'-terminal region of flavivirus genome RNA. *Virology* **162:** 290-299

Brummelkamp TR, Bernards R, Agami R (2002) A system for stable expression of short interfering RNAs in mammalian cells. *Science* **296:** 550-553

Buckley A, Gaidamovich S, Turchinskaya A, Gould EA (1992) Monoclonal antibodies identify the NS5 yellow fever virus non-structural protein in the nuclei of infected cells. *J Gen Virol* **73 ( Pt 5):** 1125-1130

Chambers TJ, Hahn CS, Galler R, Rice CM (1990) Flavivirus genome organization, expression, and replication. *Annu Rev Microbiol* **44:** 649-688

Chen CJ, Kuo MD, Chien LJ, Hsu SL, Wang YM, Lin JH (1997) RNA-protein interactions: involvement of NS3, NS5, and 3' noncoding regions of Japanese encephalitis virus genomic RNA. *J Virol* **71:** 3466-3473

Chu JJ, Ng ML (2004) Infectious entry of West Nile virus occurs through a clathrin-mediated endocytic pathway. *J Virol* **78:** 10543-10555

Chu JJ, Yang PL (2007) c-Src protein kinase inhibitors block assembly and maturation of dengue virus. *Proc Natl Acad Sci U S A* **104:** 3520-3525

Cleaves GR, Dubin DT (1979) Methylation status of intracellular dengue type 2 40 S RNA. *Virology* **96:** 159-165

Cleaves GR, Ryan TE, Schlesinger RW (1981) Identification and characterization of type 2 dengue virus replicative intermediate and replicative form RNAs. *Virology* **111:** 73-83

Clerte C, Hall KB (2006) Characterization of multimeric complexes formed by the human PTB1 protein on RNA. *RNA* **12:** 457-475

Clum S, Ebner KE, Padmanabhan R (1997) Cotranslational membrane insertion of the serine proteinase precursor NS2B-NS3(Pro) of dengue virus type 2 is required for efficient in vitro processing and is mediated through the hydrophobic regions of NS2B. *J Biol Chem* **272:** 30715-30723

Cui T, Sugrue RJ, Xu Q, Lee AK, Chan YC, Fu J (1998) Recombinant dengue virus type 1 NS3 protein exhibits specific viral RNA binding and NTPase activity regulated by the NS5 protein. *Virology* **246:** 409-417

Cui ZQ, Zhang ZP, Zhang XE, Wen JK, Zhou YF, Xie WH (2005) Visualizing the dynamic behavior of poliovirus plus-strand RNA in living host cells. *Nucleic Acids Res* **33:** 3245-3252

De Nova-Ocampo M, Villegas-Sepulveda N, del Angel RM (2002) Translation elongation factor-1alpha, La, and PTB interact with the 3' untranslated region of dengue 4 virus RNA. *Virology* **295:** 337-347

Dember LM, Kim ND, Liu KQ, Anderson P (1996) Individual RNA recognition motifs of TIA-1 and TIAR have different RNA binding specificities. *J Biol Chem* **271:** 2783-2788

den Boon JA, Diaz A, Ahlquist P (2010) Cytoplasmic viral replication complexes. *Cell Host Microbe* **8:** 77-85

Diebold SS, Kaisho T, Hemmi H, Akira S, Reis e Sousa C (2004) Innate antiviral responses by means of TLR7-mediated recognition of single-stranded RNA. *Science* **303:** 1529-1531

Dixon DA, Balch GC, Kedersha N, Anderson P, Zimmerman GA, Beauchamp RD, Prescott SM (2003) Regulation of cyclooxygenase-2 expression by the translational silencer TIA-1. *J Exp Med* **198:** 475-481

Domitrovich AM, Diebel KW, Ali N, Sarker S, Siddiqui A (2005) Role of La autoantigen and polypyrimidine tract-binding protein in HCV replication. *Virology* **335:** 72-86

Droll DA, Krishna Murthy HM, Chambers TJ (2000) Yellow fever virus NS2B-NS3 protease: charged-to-alanine mutagenesis and deletion analysis define regions important for protease complex formation and function. *Virology* **275:** 335-347

Dundr M, Misteli T (2003) Measuring dynamics of nuclear proteins by photobleaching. *Curr Protoc Cell Biol* **Chapter 13:** Unit 13 15

Ecker M, Allison SL, Meixner T, Heinz FX (1999) Sequence analysis and genetic classification of tick-borne encephalitis viruses from Europe and Asia. *J Gen Virol* **80 ( Pt 1):** 179-185

Edelmann KH, Richardson-Burns S, Alexopoulou L, Tyler KL, Flavell RA, Oldstone MB (2004) Does Toll-like receptor 3 play a biological role in virus infections? *Virology* **322:** 231-238

Elbashir SM, Harborth J, Lendeckel W, Yalcin A, Weber K, Tuschl T (2001) Duplexes of 21-nucleotide RNAs mediate RNA interference in cultured mammalian cells. *Nature* **411:** 494-498

Emara MM, Brinton MA (2007) Interaction of TIA-1/TIAR with West Nile and dengue virus products in infected cells interferes with stress granule formation and processing body assembly. *Proc Natl Acad Sci U S A* **104:** 9041-9046

Eulalio A, Behm-Ansmant I, Izaurralde E (2007) P bodies: at the crossroads of post-transcriptional pathways. *Nat Rev Mol Cell Biol* **8:** 9-22

Evans MJ, Rice CM, Goff SP (2004) Genetic interactions between hepatitis C virus replicons. *J Virol* **78:** 12085-12089

Falgout B, Markoff L (1995) Evidence that flavivirus NS1-NS2A cleavage is mediated by a membrane-bound host protease in the endoplasmic reticulum. *J Virol* **69:** 7232-7243

Falgout B, Pethel M, Zhang YM, Lai CJ (1991) Both nonstructural proteins NS2B and NS3 are required for the proteolytic processing of dengue virus nonstructural proteins. *J Virol* **65:** 2467-2475

Fraefel C, Bittermann AG, Bueler H, Heid I, Bachi T, Ackermann M (2004) Spatial and temporal organization of adeno-associated virus DNA replication in live cells. *J Virol* **78:** 389-398

Fredericksen BL, Gale M, Jr. (2006) West Nile virus evades activation of interferon regulatory factor 3 through RIG-I-dependent and -independent pathways without antagonizing host defense signaling. *J Virol* **80:** 2913-2923

Fredericksen BL, Keller BC, Fornek J, Katze MG, Gale M, Jr. (2008) Establishment and maintenance of the innate antiviral response to West Nile Virus involves both RIG-I and MDA5 signaling through IPS-1. *J Virol* **82:** 609-616

Gallouzi IE, Brennan CM, Stenberg MG, Swanson MS, Eversole A, Maizels N, Steitz JA (2000) HuR binding to cytoplasmic mRNA is perturbed by heat shock. *Proc Natl Acad Sci U S A* **97:** 3073-3078

Gallouzi IE, Parker F, Chebli K, Maurier F, Labourier E, Barlat I, Capony JP, Tocque B, Tazi J (1998) A novel phosphorylation-dependent RNase activity of GAP-SH3 binding protein: a potential link between signal transduction and RNA stability. *Mol Cell Biol* **18:** 3956-3965

Gehrke R, Heinz FX, Davis NL, Mandl CW (2005) Heterologous gene expression by infectious and replicon vectors derived from tick-borne encephalitis virus and direct comparison of this flavivirus system with an alphavirus replicon. *J Gen Virol* **86:** 1045-1053

Gilks N, Kedersha N, Ayodele M, Shen L, Stoecklin G, Dember LM, Anderson P (2004) Stress granule assembly is mediated by prion-like aggregation of TIA-1. *Mol Biol Cell* **15:** 5383-5398

Gillespie LK, Hoenen A, Morgan G, Mackenzie JM (2010) The endoplasmic reticulum provides the membrane platform for biogenesis of the flavivirus replication complex. *J Virol* **84:** 10438-10447

Gitlin L, Benoit L, Song C, Cella M, Gilfillan S, Holtzman MJ, Colonna M (2010) Melanoma differentiation-associated gene 5 (MDA5) is involved in the innate immune response to Paramyxoviridae infection in vivo. *PLoS Pathog* **6:** e1000734

Gomila RC, Martin GW, Gehrke L (2011) NF90 binds the dengue virus RNA 3' terminus and is a positive regulator of dengue virus replication. *PLoS One* **6:** e16687

Grief C, Galler R, Cortes LM, Barth OM (1997) Intracellular localisation of dengue-2 RNA in mosquito cell culture using electron microscopic in situ hybridisation. *Arch Virol* **142:** 2347-2357

Gritsun TS, Gould EA (2007) Origin and evolution of flavivirus 5'UTRs and panhandles: trans-terminal duplications? *Virology* **366:** 8-15

Gueydan C, Droogmans L, Chalon P, Huez G, Caput D, Kruys V (1999) Identification of TIAR as a protein binding to the translational regulatory AU-rich element of tumor necrosis factor alpha mRNA. *J Biol Chem* **274:** 2322-2326

Habjan M, Andersson I, Klingstrom J, Schumann M, Martin A, Zimmermann P, Wagner V, Pichlmair A, Schneider U, Muhlberger E, Mirazimi A, Weber F (2008) Processing of genome 5' termini as a strategy of negative-strand RNA viruses to avoid RIG-I-dependent interferon induction. *PLoS One* **3:** e2032

Haglund M, Gunther G (2003) Tick-borne encephalitis--pathogenesis, clinical course and long-term follow-up. *Vaccine* **21 Suppl 1:** S11-18

Han AP, Yu C, Lu L, Fujiwara Y, Browne C, Chin G, Fleming M, Leboulch P, Orkin SH, Chen JJ (2001) Heme-regulated eIF2alpha kinase (HRI) is required for translational regulation and survival of erythroid precursors in iron deficiency. *EMBO J* **20:** 6909-6918

Harding HP, Novoa I, Zhang Y, Zeng H, Wek R, Schapira M, Ron D (2000) Regulated translation initiation controls stress-induced gene expression in mammalian cells. *Mol Cell* **6:** 1099-1108

Hoenninger VM, Rouha H, Orlinger KK, Miorin L, Marcello A, Kofler RM, Mandl CW (2008) Analysis of the effects of alterations in the tick-borne encephalitis virus 3'-noncoding region on translation and RNA replication using reporter replicons. *Virology* **377:** 419-430

Honda K, Ohba Y, Yanai H, Negishi H, Mizutani T, Takaoka A, Taya C, Taniguchi T (2005) Spatiotemporal regulation of MyD88-IRF-7 signalling for robust type-I interferon induction. *Nature* **434:** 1035-1040

Hua Y, Zhou J (2004) Rpp20 interacts with SMN and is re-distributed into SMN granules in response to stress. *Biochem Biophys Res Commun* **314:** 268-276

Iacono-Connors LC, Smith JF, Ksiazek TG, Kelley CL, Schmaljohn CS (1996) Characterization of Langat virus antigenic determinants defined by monoclonal antibodies to E, NS1 and preM and identification of a protective, non-neutralizing preM-specific monoclonal antibody. *Virus Res* **43:** 125-136

Isken O, Baroth M, Grassmann CW, Weinlich S, Ostareck DH, Ostareck-Lederer A, Behrens SE (2007) Nuclear factors are involved in hepatitis C virus RNA replication. *RNA* **13:** 1675-1692

Izquierdo JM, Majos N, Bonnal S, Martinez C, Castelo R, Guigo R, Bilbao D, Valcarcel J (2005) Regulation of Fas alternative splicing by antagonistic effects of TIA-1 and PTB on exon definition. *Mol Cell* **19:** 475-484

Izquierdo JM, Valcarcel J (2007) Two isoforms of the T-cell intracellular antigen 1 (TIA-1) splicing factor display distinct splicing regulation activities. Control of TIA-1 isoform ratio by TIA-1-related protein. *J Biol Chem* **282:** 19410-19417

Jaaskelainen AE, Tikkakoski T, Uzcategui NY, Alekseev AN, Vaheri A, Vapalahti O (2006) Siberian subtype tickborne encephalitis virus, Finland. *Emerg Infect Dis* **12:** 1568-1571

Kang DC, Gopalkrishnan RV, Wu Q, Jankowsky E, Pyle AM, Fisher PB (2002) mda-5: An interferon-inducible putative RNA helicase with double-stranded RNA-dependent ATPase activity and melanoma growth-suppressive properties. *Proc Natl Acad Sci U S A* **99:** 637-642

Kato H, Sato S, Yoneyama M, Yamamoto M, Uematsu S, Matsui K, Tsujimura T, Takeda K, Fujita T, Takeuchi O, Akira S (2005) Cell type-specific involvement of RIG-I in antiviral response. *Immunity* **23:** 19-28

Kato H, Takeuchi O, Mikamo-Satoh E, Hirai R, Kawai T, Matsushita K, Hiiragi A, Dermody TS, Fujita T, Akira S (2008) Length-dependent recognition of double-stranded ribonucleic acids by retinoic acid-inducible gene-I and melanoma differentiation-associated gene 5. *J Exp Med* **205:** 1601-1610

Kato H, Takeuchi O, Sato S, Yoneyama M, Yamamoto M, Matsui K, Uematsu S, Jung A, Kawai T, Ishii KJ, Yamaguchi O, Otsu K, Tsujimura T, Koh CS, Reis e Sousa C, Matsuura Y, Fujita T, Akira S (2006) Differential roles of MDA5 and RIG-I helicases in the recognition of RNA viruses. *Nature* **441:** 101-105

Kawakami A, Tian Q, Duan X, Streuli M, Schlossman SF, Anderson P (1992) Identification and functional characterization of a TIA-1-related nucleolysin. *Proc Natl Acad Sci U S A* **89:** 8681-8685

Kawakami A, Tian Q, Streuli M, Poe M, Edelhoff S, Disteche CM, Anderson P (1994) Intron-exon organization and chromosomal localization of the human TIA-1 gene. *J Immunol* **152:** 4937-4945

Kedersha N, Anderson P (2002) Stress granules: sites of mRNA triage that regulate mRNA stability and translatability. *Biochem Soc Trans* **30:** 963-969

Kedersha N, Chen S, Gilks N, Li W, Miller IJ, Stahl J, Anderson P (2002) Evidence that ternary complex (eIF2-GTP-tRNA(i)(Met))-deficient preinitiation complexes are core constituents of mammalian stress granules. *Mol Biol Cell* **13:** 195-210

Kedersha N, Cho MR, Li W, Yacono PW, Chen S, Gilks N, Golan DE, Anderson P (2000) Dynamic shuttling of TIA-1 accompanies the recruitment of mRNA to mammalian stress granules. *J Cell Biol* **151:** 1257-1268

Kedersha NL, Gupta M, Li W, Miller I, Anderson P (1999) RNA-binding proteins TIA-1 and TIAR link the phosphorylation of eIF-2 alpha to the assembly of mammalian stress granules. *J Cell Biol* **147:** 1431-1442

Kennedy D, French J, Guitard E, Ru K, Tocque B, Mattick J (2001) Characterization of G3BPs: tissue specific expression, chromosomal localisation and rasGAP(120) binding studies. *J Cell Biochem* **84:** 173-187

Khaperskyy DA, Hatchette TF, McCormick C (2012) Influenza A virus inhibits cytoplasmic stress granule formation. *FASEB J* **26:** 1629-1639

Khromykh AA, Sedlak PL, Westaway EG (2000) cis- and trans-acting elements in flavivirus RNA replication. *J Virol* **74:** 3253-3263

Khromykh AA, Westaway EG (1996) RNA binding properties of core protein of the flavivirus Kunjin. *Arch Virol* **141:** 685-699

Kiermayr S, Kofler RM, Mandl CW, Messner P, Heinz FX (2004) Isolation of capsid protein dimers from the tick-borne encephalitis flavivirus and in vitro assembly of capsid-like particles. *J Virol* **78:** 8078-8084

Kimball SR (2001) Regulation of translation initiation by amino acids in eukaryotic cells. *Prog Mol Subcell Biol* **26:** 155-184

Kofler RM, Hoenninger VM, Thurner C, Mandl CW (2006) Functional analysis of the tick-borne encephalitis virus cyclization elements indicates major differences between mosquito-borne and tick-borne flaviviruses. *J Virol* **80:** 4099-4113

Konishi E, Mason PW (1993) Proper maturation of the Japanese encephalitis virus envelope glycoprotein requires cosynthesis with the premembrane protein. *J Virol* **67:** 1672-1675

Krishnan MN, Ng A, Sukumaran B, Gilfoy FD, Uchil PD, Sultana H, Brass AL, Adametz R, Tsui M, Qian F, Montgomery RR, Lev S, Mason PW, Koski RA, Elledge SJ, Xavier RJ, Agaisse H, Fikrig E (2008) RNA interference screen for human genes associated with West Nile virus infection. *Nature* **455:** 242-245

Krishnan MN, Sukumaran B, Pal U, Agaisse H, Murray JL, Hodge TW, Fikrig E (2007) Rab 5 is required for the cellular entry of dengue and West Nile viruses. *J Virol* **81:** 4881-4885

Kula A, Guerra J, Knezevich A, Kleva D, Myers MP, Marcello A (2011) Characterization of the HIV-1 RNA associated proteome identifies Matrin 3 as a nuclear cofactor of Rev function. *Retrovirology* **8:** 60

Langereis MA, Feng Q, van Kuppeveld FJ (2013) MDA5 localizes to stress granules, but this localization is not required for the induction of type I interferon. *J Virol* **87:** 6314-6325

Lee HK, Lund JM, Ramanathan B, Mizushima N, Iwasaki A (2007) Autophagy-dependent viral recognition by plasmacytoid dendritic cells. *Science* **315:** 1398-1401

Lee JM, Crooks AJ, Stephenson JR (1989) The synthesis and maturation of a non-structural extracellular antigen from tick-borne encephalitis virus and its relationship to the intracellular NS1 protein. *J Gen Virol* **70 ( Pt 2):** 335-343

Lee Y, Jeon K, Lee JT, Kim S, Kim VN (2002) MicroRNA maturation: stepwise processing and subcellular localization. *EMBO J* **21:** 4663-4670

Leyssen P, De Clercq E, Neyts J (2000) Perspectives for the treatment of infections with Flaviviridae. *Clin Microbiol Rev* **13:** 67-82, table of contents

Li L, Lok SM, Yu IM, Zhang Y, Kuhn RJ, Chen J, Rossmann MG (2008) The flavivirus precursor membrane-envelope protein complex: structure and maturation. *Science* **319:** 1830-1834

Li W, Li Y, Kedersha N, Anderson P, Emara M, Swiderek KM, Moreno GT, Brinton MA (2002) Cell proteins TIA-1 and TIAR interact with the 3' stem-loop of the West Nile virus complementary minus-strand RNA and facilitate virus replication. *J Virol* **76:** 11989-12000

Lim LP, Lau NC, Garrett-Engele P, Grimson A, Schelter JM, Castle J, Bartel DP, Linsley PS, Johnson JM (2005) Microarray analysis shows that some microRNAs downregulate large numbers of target mRNAs. *Nature* **433:** 769-773

Lindenbach BD, Pragai BM, Montserret R, Beran RK, Pyle AM, Penin F, Rice CM (2007a) The C terminus of hepatitis C virus NS4A encodes an electrostatic switch that regulates NS5A hyperphosphorylation and viral replication. *J Virol* **81:** 8905-8918

Lindenbach BD, Rice CM (1997) trans-Complementation of yellow fever virus NS1 reveals a role in early RNA replication. *J Virol* **71:** 9608-9617

Lindenbach BD, Rice CM (1999) Genetic interaction of flavivirus nonstructural proteins NS1 and NS4A as a determinant of replicase function. *J Virol* **73:** 4611-4621

Lindenbach BD, Thiel HJ, Rice CM (2007b) Flaviviridae: the viruses and their replication. In *Fields Virology*, Knipe DM, Howley PM, Griffin DE, Lamb RA, Martin MA (eds), Fifth Edition edn, pp 1101-1152. Philadelphia: Lippincott, Williams & Wilkins

Lindquist ME, Lifland AW, Utley TJ, Santangelo PJ, Crowe JE, Jr. (2010) Respiratory syncytial virus induces host RNA stress granules to facilitate viral replication. *J Virol* **84:** 12274-12284

Liu WJ, Chen HB, Wang XJ, Huang H, Khromykh AA (2004) Analysis of adaptive mutations in Kunjin virus replicon RNA reveals a novel role for the flavivirus nonstructural protein NS2A in inhibition of beta interferon promoter-driven transcription. *J Virol* **78:** 12225-12235

Lo MK, Tilgner M, Shi PY (2003) Potential high-throughput assay for screening inhibitors of West Nile virus replication. *J Virol* **77:** 12901-12906

Lohmann V, Hoffmann S, Herian U, Penin F, Bartenschlager R (2003) Viral and cellular determinants of hepatitis C virus RNA replication in cell culture. *J Virol* **77:** 3007-3019

Lohmann V, Korner F, Dobierzewska A, Bartenschlager R (2001) Mutations in hepatitis C virus RNAs conferring cell culture adaptation. *J Virol* **75:** 1437-1449

Lohmann V, Korner F, Koch J, Herian U, Theilmann L, Bartenschlager R (1999) Replication of subgenomic hepatitis C virus RNAs in a hepatoma cell line. *Science* **285:** 110-113

Loo YM, Fornek J, Crochet N, Bajwa G, Perwitasari O, Martinez-Sobrido L, Akira S, Gill MA, Garcia-Sastre A, Katze MG, Gale M, Jr. (2008) Distinct RIG-I and MDA5 signaling by RNA viruses in innate immunity. *J Virol* **82:** 335-345

Lopez de Silanes I, Galban S, Martindale JL, Yang X, Mazan-Mamczarz K, Indig FE, Falco G, Zhan M, Gorospe M (2005) Identification and functional outcome of mRNAs associated with RNA-binding protein TIA-1. *Mol Cell Biol* **25:** 9520-9531

Ma L, Jones CT, Groesch TD, Kuhn RJ, Post CB (2004) Solution structure of dengue virus capsid protein reveals another fold. *Proc Natl Acad Sci U S A* **101:** 3414-3419

Mackenzie J (2005) Wrapping things up about virus RNA replication. *Traffic* **6:** 967-977

Mackenzie JM, Khromykh AA, Jones MK, Westaway EG (1998) Subcellular localization and some biochemical properties of the flavivirus Kunjin nonstructural proteins NS2A and NS4A. *Virology* **245:** 203-215

Mackenzie JM, Westaway EG (2001) Assembly and maturation of the flavivirus Kunjin virus appear to occur in the rough endoplasmic reticulum and along the secretory pathway, respectively. *J Virol* **75:** 10787-10799

Maiuri P, Knezevich A, Bertrand E, Marcello A (2011) Real-time imaging of the HIV-1 transcription cycle in single living cells. *Methods* **53:** 62-67

Mandl CW, Heinz FX, Stockl E, Kunz C (1989) Genome sequence of tick-borne encephalitis virus (Western subtype) and comparative analysis of nonstructural proteins with other flaviviruses. *Virology* **173:** 291-301

Martin-Acebes MA, Blazquez AB, Jimenez de Oya N, Escribano-Romero E, Saiz JC (2011) West Nile virus replication requires fatty acid synthesis but is independent on phosphatidylinositol-4-phosphate lipids. *PLoS One* **6:** e24970

Mason PW (1989) Maturation of Japanese encephalitis virus glycoproteins produced by infected mammalian and mosquito cells. *Virology* **169:** 354-364

Mazzon M, Jones M, Davidson A, Chain B, Jacobs M (2009) Dengue virus NS5 inhibits interferon-alpha signaling by blocking signal transducer and activator of transcription 2 phosphorylation. *J Infect Dis* **200:** 1261-1270

Meister G, Tuschl T (2004) Mechanisms of gene silencing by double-stranded RNA. *Nature* **431:** 343-349

Miorin L, Albornoz A, Baba MM, D'Agaro P, Marcello A (2012) Formation of membrane-defined compartments by tick-borne encephalitis virus contributes to the early delay in interferon signaling. *Virus Res* **163:** 660-666

Miorin L, Maiuri P, Hoenninger VM, Mandl CW, Marcello A (2008) Spatial and temporal organization of tick-borne encephalitis flavivirus replicated RNA in living cells. *Virology* **379:** 64-77

Miorin L, Romero-Brey I, Maiuri P, Hoppe S, Krijnse-Locker J, Bartenschlager R, Marcello A (2013) Three-dimensional architecture of tick-borne encephalitis virus replication sites and trafficking of the replicated RNA. *J Virol* **87:** 6469-6481

Molle D, Maiuri P, Boireau S, Bertrand E, Knezevich A, Marcello A, Basyuk E (2007) A real-time view of the TAR:Tat:P-TEFb complex at HIV-1 transcription sites. *Retrovirology* **4:** 36

Montero H, Arias CF, Lopez S (2006) Rotavirus Nonstructural Protein NSP3 is not required for viral protein synthesis. *J Virol* **80:** 9031-9038

Mukhopadhyay S, Kuhn RJ, Rossmann MG (2005) A structural perspective of the flavivirus life cycle. *Nat Rev Microbiol* **3:** 13-22

Munoz-Jordan JL, Laurent-Rolle M, Ashour J, Martinez-Sobrido L, Ashok M, Lipkin WI, Garcia-Sastre A (2005) Inhibition of alpha/beta interferon signaling by the NS4B protein of flaviviruses. *J Virol* **79:** 8004-8013

Muylaert IR, Galler R, Rice CM (1997) Genetic analysis of the yellow fever virus NS1 protein: identification of a temperature-sensitive mutation which blocks RNA accumulation. *J Virol* **71:** 291-298

Nagai Y, Ito Y, Hamaguchi M, Yoshida T, Matsumoto T (1981) Relation of interferon production to the limited replication of Newcastle disease virus in L cells. *J Gen Virol* **55:** 109-116

Nestorowicz A, Chambers TJ, Rice CM (1994) Mutagenesis of the yellow fever virus NS2A/2B cleavage site: effects on proteolytic processing, viral replication, and evidence for alternative processing of the NS2A protein. *Virology* **199:** 114-123

Nover L, Scharf KD, Neumann D (1983) Formation of cytoplasmic heat shock granules in tomato cell cultures and leaves. *Mol Cell Biol* **3:** 1648-1655

Nover L, Scharf KD, Neumann D (1989) Cytoplasmic heat shock granules are formed from precursor particles and are associated with a specific set of mRNAs. *Mol Cell Biol* **9:** 1298-1308

Novoa RR, Calderita G, Arranz R, Fontana J, Granzow H, Risco C (2005) Virus factories: associations of cell organelles for viral replication and morphogenesis. *Biol Cell* **97:** 147-172

Nykanen A, Haley B, Zamore PD (2001) ATP requirements and small interfering RNA structure in the RNA interference pathway. *Cell* **107:** 309-321

Onomoto K, Jogi M, Yoo JS, Narita R, Morimoto S, Takemura A, Sambhara S, Kawaguchi A, Osari S, Nagata K, Matsumiya T, Namiki H, Yoneyama M, Fujita T (2012) Critical role of an antiviral stress granule containing RIG-I and PKR in viral detection and innate immunity. *PLoS One* **7:** e43031

Orlinger KK, Hoenninger VM, Kofler RM, Mandl CW (2006) Construction and mutagenesis of an artificial bicistronic tick-borne encephalitis virus genome reveals an essential function of the second transmembrane region of protein e in flavivirus assembly. *J Virol* **80:** 12197-12208

Overby AK, Popov VL, Niedrig M, Weber F (2010) Tick-borne encephalitis virus delays interferon induction and hides its double-stranded RNA in intracellular membrane vesicles. *J Virol* **84:** 8470-8483

Paddison PJ, Caudy AA, Bernstein E, Hannon GJ, Conklin DS (2002) Short hairpin RNAs (shRNAs) induce sequence-specific silencing in mammalian cells. *Genes Dev* **16:** 948-958

Parker F, Maurier F, Delumeau I, Duchesne M, Faucher D, Debussche L, Dugue A, Schweighoffer F, Tocque B (1996) A Ras-GTPase-activating protein SH3-domain-binding protein. *Mol Cell Biol* **16:** 2561-2569

Pfeffer M, Dobler G (2010) Emergence of zoonotic arboviruses by animal trade and migration. *Parasit Vectors* **3:** 35

Pham JW, Pellino JL, Lee YS, Carthew RW, Sontheimer EJ (2004) A Dicer-2-dependent 80s complex cleaves targeted mRNAs during RNAi in Drosophila. *Cell* **117:** 83-94

Piecyk M, Wax S, Beck AR, Kedersha N, Gupta M, Maritim B, Chen S, Gueydan C, Kruys V, Streuli M, Anderson P (2000) TIA-1 is a translational silencer that selectively regulates the expression of TNF-alpha. *EMBO J* **19:** 4154-4163

Pijlman GP, Funk A, Kondratieva N, Leung J, Torres S, van der Aa L, Liu WJ, Palmenberg AC, Shi PY, Hall RA, Khromykh AA (2008) A highly structured, nuclease-resistant, noncoding RNA produced by flaviviruses is required for pathogenicity. *Cell Host Microbe* **4:** 579-591

Preugschat F, Yao CW, Strauss JH (1990) In vitro processing of dengue virus type 2 nonstructural proteins NS2A, NS2B, and NS3. *J Virol* **64:** 4364-4374

Randall G, Panis M, Cooper JD, Tellinghuisen TL, Sukhodolets KE, Pfeffer S, Landthaler M, Landgraf P, Kan S, Lindenbach BD, Chien M, Weir DB, Russo JJ, Ju J, Brownstein MJ, Sheridan R, Sander C, Zavolan M, Tuschl T, Rice CM (2007) Cellular cofactors affecting hepatitis C virus infection and replication. *Proc Natl Acad Sci U S A* **104:** 12884-12889

Randall RE, Goodbourn S (2008) Interferons and viruses: an interplay between induction, signalling, antiviral responses and virus countermeasures. *J Gen Virol* **89:** 1-47

Reiss S, Rebhan I, Backes P, Romero-Brey I, Erfle H, Matula P, Kaderali L, Poenisch M, Blankenburg H, Hiet MS, Longerich T, Diehl S, Ramirez F, Balla T, Rohr K, Kaul A, Buhler S, Pepperkok R, Lengauer T, Albrecht M, Eils R, Schirmacher P, Lohmann V, Bartenschlager R (2011) Recruitment and activation of a lipid kinase by hepatitis C virus NS5A is essential for integrity of the membranous replication compartment. *Cell Host Microbe* **9:** 32-45

Rey FA, Heinz FX, Mandl C, Kunz C, Harrison SC (1995) The envelope glycoprotein from tick-borne encephalitis virus at 2 A resolution. *Nature* **375:** 291-298

Reyes-Del Valle J, Chavez-Salinas S, Medina F, Del Angel RM (2005) Heat shock protein 90 and heat shock protein 70 are components of dengue virus receptor complex in human cells. *J Virol* **79:** 4557-4567

Roosendaal J, Westaway EG, Khromykh A, Mackenzie JM (2006) Regulated cleavages at the West Nile virus NS4A-2K-NS4B junctions play a major role in rearranging cytoplasmic membranes and Golgi trafficking of the NS4A protein. *J Virol* **80:** 4623-4632

Rothenfusser S, Goutagny N, DiPerna G, Gong M, Monks BG, Schoenemeyer A, Yamamoto M, Akira S, Fitzgerald KA (2005) The RNA helicase Lgp2 inhibits TLR-

independent sensing of viral replication by retinoic acid-inducible gene-I. *J Immunol* **175:** 5260-5268

Saito T, Hirai R, Loo YM, Owen D, Johnson CL, Sinha SC, Akira S, Fujita T, Gale M, Jr. (2007) Regulation of innate antiviral defenses through a shared repressor domain in RIG-I and LGP2. *Proc Natl Acad Sci U S A* **104:** 582-587

Sampath A, Padmanabhan R (2009) Molecular targets for flavivirus drug discovery. *Antiviral Res* **81:** 6-15

Sanchez-Vargas I, Scott JC, Poole-Smith BK, Franz AW, Barbosa-Solomieu V, Wilusz J, Olson KE, Blair CD (2009) Dengue virus type 2 infections of Aedes aegypti are modulated by the mosquito's RNA interference pathway. *PLoS Pathog* **5:** e1000299

Schlesinger JJ, Brandriss MW, Walsh EE (1985) Protection against 17D yellow fever encephalitis in mice by passive transfer of monoclonal antibodies to the nonstructural glycoprotein gp48 and by active immunization with gp48. *J Immunol* **135:** 2805-2809

Sehgal PB, Sagar AD (1980) Heterogeneity of poly(I) x poly(C)-induced human fibroblast interferon mRNA species. *Nature* **288:** 95-97

Shan G (2010) RNA interference as a gene knockdown technique. *Int J Biochem Cell Biol* **42:** 1243-1251

Sourvinos G, Everett RD (2002) Visualization of parental HSV-1 genomes and replication compartments in association with ND10 in live infected cells. *EMBO J* **21:** 4989-4997

Stadler K, Allison SL, Schalich J, Heinz FX (1997) Proteolytic activation of tick-borne encephalitis virus by furin. *J Virol* **71:** 8475-8481

Stiasny K, Fritz R, Pangerl K, Heinz FX (2009) Molecular mechanisms of flavivirus membrane fusion. *Amino Acids*

Stiasny K, Heinz FX (2006) Flavivirus membrane fusion. *J Gen Virol* **87:** 2755-2766

Stoecklin G, Stubbs T, Kedersha N, Wax S, Rigby WF, Blackwell TK, Anderson P (2004) MK2-induced tristetraprolin:14-3-3 complexes prevent stress granule association and ARE-mRNA decay. *EMBO J* **23:** 1313-1324

Supekova L, Supek F, Lee J, Chen S, Gray N, Pezacki JP, Schlapbach A, Schultz PG (2008) Identification of human kinases involved in hepatitis C virus replication by small interference RNA library screening. *J Biol Chem* **283:** 29-36

Tai AW, Benita Y, Peng LF, Kim SS, Sakamoto N, Xavier RJ, Chung RT (2009) A functional genomic screen identifies cellular cofactors of hepatitis C virus replication. *Cell Host Microbe* **5:** 298-307

Takahasi K, Yoneyama M, Nishihori T, Hirai R, Kumeta H, Narita R, Gale M, Jr., Inagaki F, Fujita T (2008) Nonself RNA-sensing mechanism of RIG-I helicase and activation of antiviral immune responses. *Mol Cell* **29:** 428-440

Taupin JL, Tian Q, Kedersha N, Robertson M, Anderson P (1995) The RNA-binding protein TIAR is translocated from the nucleus to the cytoplasm during Fas-mediated apoptotic cell death. *Proc Natl Acad Sci U S A* **92:** 1629-1633

Tian Q, Streuli M, Saito H, Schlossman SF, Anderson P (1991) A polyadenylate binding protein localized to the granules of cytolytic lymphocytes induces DNA fragmentation in target cells. *Cell* **67:** 629-639

Tourriere H, Chebli K, Zekri L, Courselaud B, Blanchard JM, Bertrand E, Tazi J (2003) The RasGAP-associated endoribonuclease G3BP assembles stress granules. *J Cell Biol* **160:** 823-831

Tourriere H, Gallouzi IE, Chebli K, Capony JP, Mouaikel J, van der Geer P, Tazi J (2001) RasGAP-associated endoribonuclease G3Bp: selective RNA degradation and phosphorylation-dependent localization. *Mol Cell Biol* **21:** 7747-7760

Tuschl T, Zamore PD, Lehmann R, Bartel DP, Sharp PA (1999) Targeted mRNA degradation by double-stranded RNA in vitro. *Genes Dev* **13:** 3191-3197

Uchil PD, Kumar AV, Satchidanandam V (2006) Nuclear localization of flavivirus RNA synthesis in infected cells. *J Virol* **80:** 5451-5464

Umareddy I, Chao A, Sampath A, Gu F, Vasudevan SG (2006) Dengue virus NS4B interacts with NS3 and dissociates it from single-stranded RNA. *J Gen Virol* **87:** 2605-2614

Venkataraman T, Valdes M, Elsby R, Kakuta S, Caceres G, Saijo S, Iwakura Y, Barber GN (2007) Loss of DExD/H box RNA helicase LGP2 manifests disparate antiviral responses. *J Immunol* **178:** 6444-6455

Wagner EJ, Garcia-Blanco MA (2001) Polypyrimidine tract binding protein antagonizes exon definition. *Mol Cell Biol* **21:** 3281-3288

Wang JP, Liu P, Latz E, Golenbock DT, Finberg RW, Libraty DH (2006) Flavivirus activation of plasmacytoid dendritic cells delineates key elements of TLR7 signaling beyond endosomal recognition. *J Immunol* **177:** 7114-7121

Wang SH, Syu WJ, Huang KJ, Lei HY, Yao CW, King CC, Hu ST (2002) Intracellular localization and determination of a nuclear localization signal of the core protein of dengue virus. *J Gen Virol* **83:** 3093-3102

Wang T, Town T, Alexopoulou L, Anderson JF, Fikrig E, Flavell RA (2004) Toll-like receptor 3 mediates West Nile virus entry into the brain causing lethal encephalitis. *Nat Med* **10:** 1366-1373

Ward AM, Bidet K, Yinglin A, Ler SG, Hogue K, Blackstock W, Gunaratne J, Garcia-Blanco MA (2011) Quantitative mass spectrometry of DENV-2 RNA-interacting proteins reveals that the DEAD-box RNA helicase DDX6 binds the DB1 and DB2 3' UTR structures. *RNA Biol* **8:** 1173-1186

Welsch S, Miller S, Romero-Brey I, Merz A, Bleck CK, Walther P, Fuller SD, Antony C, Krijnse-Locker J, Bartenschlager R (2009) Composition and three-dimensional architecture of the dengue virus replication and assembly sites. *Cell Host Microbe* **5:** 365-375

Wengler G (1993) The NS 3 nonstructural protein of flaviviruses contains an RNA triphosphatase activity. *Virology* **197:** 265-273

Wengler G, Gross HJ (1978) Studies on virus-specific nucleic acids synthesized in vertebrate and mosquito cells infected with flaviviruses. *Virology* **89:** 423-437

Werme K, Wigerius M, Johansson M (2008) Tick-borne encephalitis virus NS5 associates with membrane protein scribble and impairs interferon-stimulated JAK-STAT signalling. *Cell Microbiol* **10:** 696-712

Westaway EG (1987) Flavivirus replication strategy. *Adv Virus Res* **33:** 45-90

Westaway EG, Khromykh AA, Mackenzie JM (1999) Nascent flavivirus RNA colocalized in situ with double-stranded RNA in stable replication complexes. *Virology* **258:** 108-117

Westaway EG, Mackenzie JM, Kenney MT, Jones MK, Khromykh AA (1997) Ultrastructure of Kunjin virus-infected cells: colocalization of NS1 and NS3 with double-stranded RNA, and of NS2B with NS3, in virus-induced membrane structures. *J Virol* **71:** 6650-6661

White JP, Cardenas AM, Marissen WE, Lloyd RE (2007) Inhibition of cytoplasmic mRNA stress granule formation by a viral proteinase. *Cell Host Microbe* **2:** 295-305

White JP, Lloyd RE (2011) Poliovirus unlinks TIA1 aggregation and mRNA stress granule formation. *J Virol* **85:** 12442-12454

Williams BR (2001) Signal integration via PKR. *Sci STKE* **2001:** re2

Yamshchikov VF, Compans RW (1993) Regulation of the late events in flavivirus protein processing and maturation. *Virology* **192:** 38-51

Yamshchikov VF, Compans RW (1994) Processing of the intracellular form of the west Nile virus capsid protein by the viral NS2B-NS3 protease: an in vitro study. *J Virol* **68:** 5765-5771

Yoneyama M, Fujita T (2009) RNA recognition and signal transduction by RIG-I-like receptors. *Immunol Rev* **227:** 54-65

Yoneyama M, Kikuchi M, Matsumoto K, Imaizumi T, Miyagishi M, Taira K, Foy E, Loo YM, Gale M, Jr., Akira S, Yonehara S, Kato A, Fujita T (2005) Shared and unique functions of the DExD/H-box helicases RIG-I, MDA5, and LGP2 in antiviral innate immunity. *J Immunol* **175:** 2851-2858

Yoneyama M, Kikuchi M, Natsukawa T, Shinobu N, Imaizumi T, Miyagishi M, Taira K, Akira S, Fujita T (2004) The RNA helicase RIG-I has an essential function in double-stranded RNA-induced innate antiviral responses. *Nat Immunol* **5:** 730-737

Yu IM, Zhang W, Holdaway HA, Li L, Kostyuchenko VA, Chipman PR, Kuhn RJ, Rossmann MG, Chen J (2008) Structure of the immature dengue virus at low pH primes proteolytic maturation. *Science* **319:** 1834-1837

Zeng L, Falgout B, Markoff L (1998) Identification of specific nucleotide sequences within the conserved 3'-SL in the dengue type 2 virus genome required for replication. *J Virol* **72:** 7510-7522

Zhou Z, Licklider LJ, Gygi SP, Reed R (2002) Comprehensive proteomic analysis of the human spliceosome. *Nature* **419:** 182-185

Zuck P, Murray EM, Stec E, Grobler JA, Simon AJ, Strulovici B, Inglese J, Flores OA, Ferrer M (2004) A cell-based beta-lactamase reporter gene assay for the identification of inhibitors of hepatitis C virus replication. *Anal Biochem* **334:** 344-355